Deciphering the Ubiquitin CODE by chemical tools

Perez Berrocal, D.A.

Chapter 5

A Pro-Fluorescent Ubiquitin-Based Probe to Monitor Cysteine-Based E3 Ligase Activity

In memory of Prof. Dr. Huib Ovaa, his passion for science will always be an inspiration to us.

David A. Pérez Berrocal[1],*, Thimmalapura M. Vishwanatha[1], Daniel Horn-Ghetko[2], J. Josephine Botsch[2], Laura A. Hehl[2], Sebastian Kostrhon[2], Mohit Misra[3], Ivan Đikić[3], Paul P. Geurink[3], Hans van Dam[1], Brenda A. Schulman[2], Monique P.C. Mulder[1]

[1]. Cell and Chemical Biology, Leiden University Medical Centre, Leiden, The Netherlands
[2]. Department of Molecular Machines and Signaling, Max Planck Institute of Biochemistry, Martinsried, Germany
[3]. Institute of Biochemistry II, Faculty of Medicine, Goethe University, Frankfurt am Main, Germany

*First author

Adapted from :
Angew Chem Int Ed Engl. **2023** Aug 7;62(32)

Abstract.

Protein post-translational modification with ubiquitin (Ub) is a versatile signal regulating almost all aspects of cell biology, and an increasing range of diseases is associated with impaired Ub modification. In this light, the Ub system offers an attractive, yet underexplored route to the development of novel targeted treatments. A promising strategy for small molecule intervention is posed by the final components of the enzymatic ubiquitination cascade, E3 ligases, as they determine the specificity of the protein ubiquitination pathway. Here, we present UbSRhodol, an autoimmolative Ub-based probe, which upon E3 processing liberates the pro-fluorescent dye, amenable to profile the E3 transthiolation activity for recombinant and in cell-extract E3 ligases. UbSRhodol enabled detection of changes in transthiolation efficacy evoked by enzyme key point mutations or conformational changes, and offers an excellent assay reagent amenable to a high-throughput screening setup allowing the identification of small molecules modulating E3 activity.

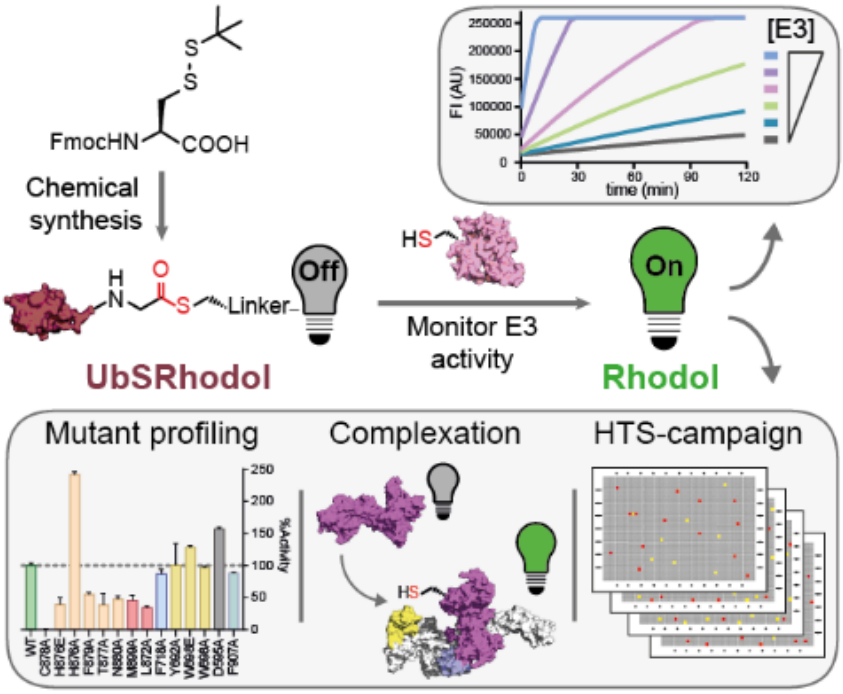

Introduction

Ubiquitination constitutes one of the most versatile and dynamic post-translational modification pathways in eukaryotes[1]. ATP-dependent reversible covalent attachment of ubiquitin (Ub), a 76 amino acid protein, to, in most cases, a lysine residue on protein substrates[1a, 2], yields a vast cellular signalling network pivotal in a myriad of biological processes[3]. A vast number of possible combinations of Ub patterns decorating a substrate protein can be formed, generating a complex and dynamic Ub code[1b]. The state of this code is controlled by both the writers (E1–E2–E3 enzymes) responsible for ubiquitination and the erasers (deubiquitinases (DUBs)) that reverse or modify it. The encoded message in the generated Ub chains serves as a beacon to exert a plethora of biological functions including protein homeostasis, cell cycle progression, and regulation of DNA integrity[1b]. The actions of writers and erasers are tightly coupled and the balance between ubiquitination and deubiquitination is a critical determinant of protein levels and activity. It is not surprising that aberrant functioning of this finely tuned system is implicated in numerous diseases, including neurodegeneration, cancer, autoimmune and metabolic diseases[4]. In this light, the Ub system offers an attractive, yet underexplored route to the development of novel targeted treatments and recent studies have shown the feasibility and complexity of targeting the Ub system for drug intervention[5].

Given the hierarchical nature of Ub signaling, E3 ligases are of particular interest as they determine the specificity of the ubiquitination system by recognizing, discriminating, and interacting with the proper protein substrate thereby regulating its stability and functioning[6]. Drugs targeting the activity of a particular E3 ligase are therefore expected to offer one of the most specific and powerful approaches for therapeutic intervention within the ubiquitination cascade[7]. Traditionally, E3 inhibitor screening relied on entire E1-E2-E3 cascade assays[8], due to the intrinsic multi-step nature of the system, which made the methodology not amenable for high-throughput formats[9]. Recently, however, simplified reconstitution systems have been reported, in which Ub is chemically activated as a thioester thereby allowing its reaction with the catalytic cysteine of E3 ligases in the absence of ATP, and E1 and E2 enzymes[10]. Here, we describe a sensitive high-throughput assay based on a synthetic pro-fluorescent Ub thioester (UbSRhodol) that allows quantitative analysis of changes in cysteine-based E3 ligase activity evoked by small molecules, biochemical mutations or conformational changes induced by protein-protein interactions.

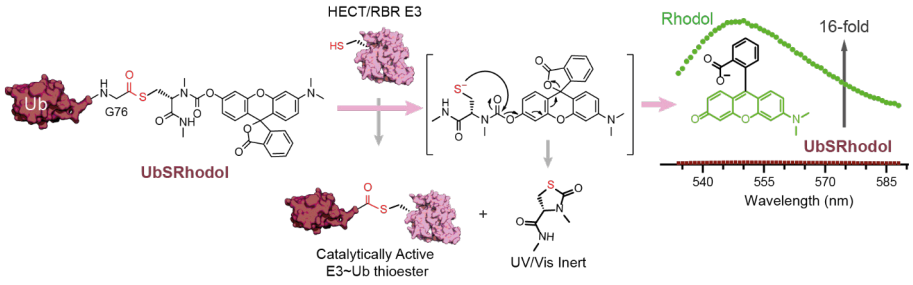

Figure 1. Mechanism of UbSRhodol. Ub equipped with a self-immolative fluorophore liberated after attack of the E3 ligase allows monitoring of the transthiolation reaction. Attack of the E3 ligase triggers an intramolecular cyclisation liberating an inert UV/

Vis thiolazolidine-2-one while rearranging the Rhodol dye in its fluorescent state giving rise to a 16-fold fluorescence intensity increase (DTT was used as reducing agent to determine the FI fold increase). (λex/em 515/548 nm).

UbSRhodol was synthesized by conjugating a glycine thioester bearing a pro-fluorescent molecule[11] via a carbamate-thiol linker (1) to the C-terminus of Ub(1-75). The carbamate modification on Ub forces the rhodol fluorophore into the lactone form, which has very low fluorescence. This self-immolative fluorophore is liberated after a direct transthiolation reaction with the catalytic cysteine of the E3 ligase, producing the catalytically active E3~Ub thioester. Enzymatic release of the pro-fluorescent molecule liberates a cysteine-based linker which cyclizes rapidly, intramolecularly attacking the carbamate bond, thereby releasing a free Rhodol dye and concomitantly triggering a strong fluorescence signal (Fig. 1). Importantly, where other assays such as fluorescence polarization (FP) readout is based on the ratio between bound and unbound fluorophore, requiring a large amount of substrate processed to have an acceptable window for the assay signal, our setup relies on unbound fluorophore only.

This setup allowed us to profile E3 ligase activities in real time, while the high sensitivity of the assay permits enzyme screening in the low nanomolar range, enabling screening of large libraries with minimal enzyme and reagent amounts. Thus far, we have profiled the activity of 9 HECTs and 5 RBR enzymes using this reagent, including assays for overexpressed ligases in total cell lysates, showing its ease of execution and facile translation from one E3 ligase to the next. Collectively, our UbSRhodol bypass system presents a potent screening platform for targeting and monitoring enzymatic activity, offering opportunities for drug discovery.

Results and Discussion

Chemical Synthesis of UbSRhodol

The synthesis of key building block **1** (Scheme 1) started from commercially available Fmoc-Cys(SStBu)-OH (**2**), which was converted to the corresponding oxazolidinone **3** by heating it to reflux in toluene with paraformaldehyde and catalytic amount of camphorsulfonic acid. Treatment of **3** with TFA:TES afforded Fmoc-MeCys(SStBu)-OH (4)[12], which was coupled with methyl amine hydrochloride under standard peptide coupling conditions giving rise to amide 5. Fmoc deprotection of **5** yielded the pro-autoimmolative linker **6**. Subsequently, Rhodol[13] (**7**) was treated with triphosgene in presence of triethylamine and the resulting carbamoyl chloride reacted with the amine of cysteine derivative **6**, affording compound **8**. By use of THPP (Tris(3-hydroxypropyl)phosphine) as a reducing agent[14] the reduction of the SStBu protecting group of derivative **8** was achieved within 20 min, after which the solution was acidified to pH 5.0, and followed by treatment with Boc-glycine acyl imidazole[15] to obtain the carbamate-thiol precursor **9**. A final Boc deprotection carried out in 4N HCl in dioxane, afforded key building block **1**.

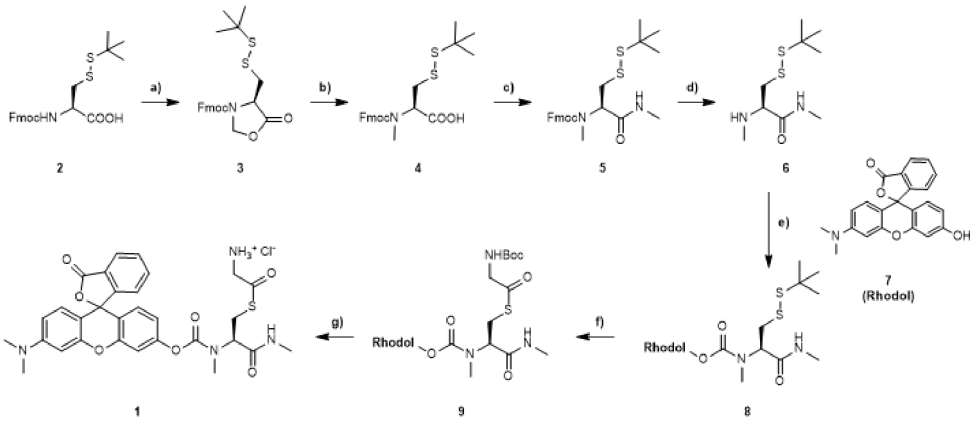

Scheme 1. Synthesis of building block 1. Reagents and conditions: a) (HCHO)n, CSA (cat), toluene, reflux, 18h, 92%; b) TFA, TES, CHCl3, rt, 24h, 85%; c) MeNH2. HCl, HBTU/HOBt, DIPEA, CH2Cl2, 0°C to rt, 12h, 90%; d) DEA, ACN, rt, 1h, 91%; e) i.) Triphosgene, TEA, THF, 0°C, 30 min; ii.) 6, THF, rt, 1h, 28%; f) i.) THPP, THF:H2O (9:2), rt, 30 min; ii.) Boc-Gly-Im, THF, rt, 1 h, 60%; g) 4N HCl/dioxane, rt, 30 min, 98%.

UbSRhodol was synthesized on a 20 µmol scale starting from Ub(1–75), using a previously reported linear Fmoc-based solid phase peptide synthesis (SPPS) of Ub[16], in which 1 was coupled to the C-terminal carboxyl group of protected Ub(1–75). Global deprotection with 90 % TFA and purification by HPLC gave the desired UbSRhodol in ~18 % overall yield. LC-MS analysis confirmed successful preparation of the compound in >95% purity (Supplementary Fig. 1) The thioester proved stable both during synthesis and storage.

Profiling Transthiolation Activity

With the UbSRhodol reagent in hand we set out to confirm the cyclization and spectral properties of the self-immolative fluorophore. Incubation of UbSRhodol with the reducing agent DTT (0.001-5 mM) followed over time yielded the hydrolysis of the thioester (Supplementary Fig. 2), releasing the cysteine-based linker which cyclizes intramolecularly by attacking the carbamate bond, triggering a strong fluorescence signal (Fig. 1). The formation of the liberated fluorophore was measured using a fluorescence photospectrometer (λex/em 515/548nm, Fig. 1 and Supplementary Fig. 3A-B), and a fluorescence intensity (FI) increase of 16-fold was observed. The Rhodol liberation and FI build-up can also be measured at the widely used rhodamine wavelength (λex/em 490/520nm) with a comparable FI increase fold (Supplementary Fig. 3C). Having successfully demonstrated the intramolecular cyclisation and release of the Rhodol in a general assay buffer at physiological pH (HEPES 50mM, 150mM NaCl, 1mM TCEP, pH 7.5), we started to test the ability of UbSRhodol to measure E3 transthiolation activity. Importantly, DTT has to be omitted in buffers for enzyme preparations as it affects thioester stability (Supplementary Fig. 2), instead TCEP can be used as reducing agent as it reduces oxidized sulfhydryls and disul-

fides but has no effect on thioester stability[17].

The ability of UbSRhodol to measure E3 transthiolation activity is dependent on the E3~Ub adduct formed and the easiness of its lysine-dependent discharge yielding a repertoire of Ub products with the bypass system (UbSR + E3) (Fig. 2A). In short, the E3 catalytic cysteine attacks UbSRhodol at its thioester bond forming a new E3~Ub thioester, which can then discharge Ub onto a lysine either from the probe (unanchored Ub chain elongation pattern (I)), the E3 ligase itself (autoubiquitination pattern (II); a common phenomenon for E3s in in vitro assays), or from a cognate substrate (substrate ubiquitination (III)). These Ub products can be confirmed employing chemically synthesized fluorescently labelled bypass probes in gel-based assays (Supplementary Fig. 4A). When the newly formed E3~Ub adduct is discharged the E3 ligase will undergo multiple cycles increasing the window of the assay and this will considerably reduce the amount of E3 needed for an acceptable assay window. Moreover, by simply modifying the ratio of enzyme over probe, reactions can be run under single turnover conditions (ST, from excess to equimolar amount of E3) to measure transthiolation rates, or under multi turnover conditions (MT, excess of probe) to observe the overall rate of Ub probe turnover and study both transthiolation and ligation steps. This fluorescence intensity read-out is highly sensitive and allows to profile E3 transthiolation activity in the low nanomolar range (Fig. 2C).

We measured the transthiolation profile of different cysteine-based E3 ligase members (Supplementary Fig. 5 and 6). In humans, the known thioester-forming E3s, which harbour a catalytic cysteine loaded with Ub by a mechanism analogous to the E1 and E2 enzymes, fall into the HECT[18] (28 human family members) and RBR[19] (13 human members) classes. Therefore, panels comprising different subfamilies within both the HECT class (9/28 E3s profiled, Supplementary Fig. 5) and RBR class (5/13 E3s profiled, Supplementary Fig. 6) were evaluated. For all enzymes a concentration and incubation time dependent processing of UbSRhodol was demonstrated.

As HECT E3 ligases are often very large, ranging from 700 amino acids to giant enzymes of more than 3000 residues (i.e UBR5[20], HUWE1 and HERC1, 2798, 4374 and 4861 residues respectively), it can be a challenge to study them in biochemical studies. Strikingly, the isolated C-terminal HECT domain of UBR5, was still able to process UbSRhodol in a catalytic transthiolation dependant manner (Supplementary Fig. 7A). Under similar conditions, gel-based experiments using chemically synthesized N-terminal rhodamine tagged Ub bypass probe (RhoUbSR) detects marginal thioester formation by fluorescent scanning (Supplementary Fig. 7B-C). Given the technical problems in reconstituting full-length HECT E3 enzymes of large HECT E3s, our sensitive readout opens the avenue of in-vitro activity profiling of low reactive E3 ligases constructs.

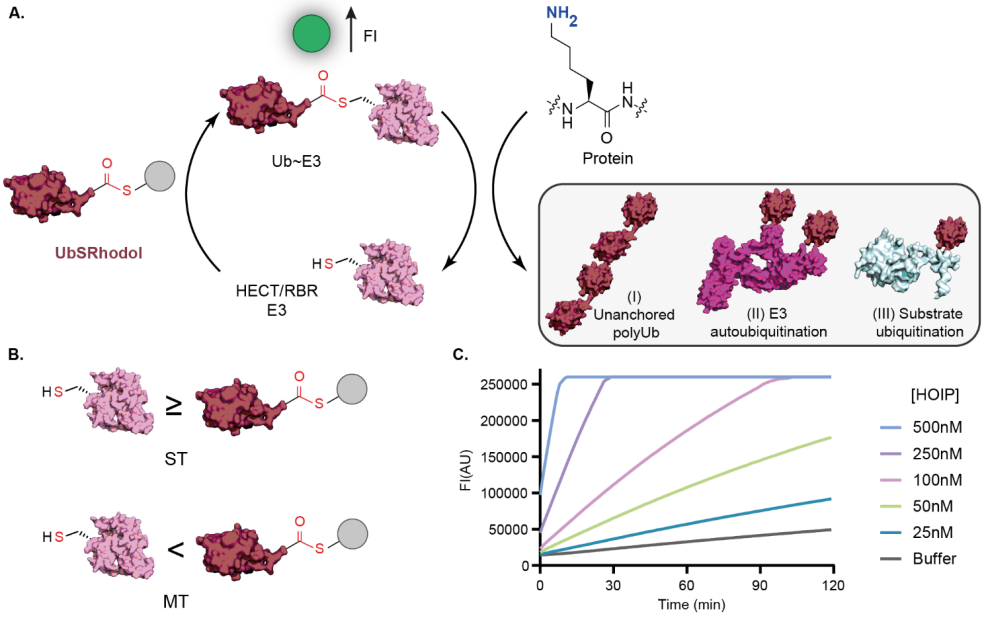

Figure 2. UbSRhodol assay set up. A. UbSRhodol is recognized by Ub-binding domains at the catalytic domain of HECT and RBR ligases, positioning the reactive thioester for transthiolation reaction and forming a Ub~E3 thioester adduct. Concomitantly, a molecule of Rhodol dye is liberated after rapid intramolecular cyclisation of the autoimmolative linker. If an acceptor lysine is present, and E3 favors ligation, different ubiquitination products can be generated: (I) Unanchored polyUb formation, (II) E3 autoubiquitination and (III) Substrate ubiquitination. **B**. Single turnover (ST) or Multi turnover (MT) conditions can be selected by altering the ratio of E3 over probe. In general, ST conditions are preferential to study transthiolation, while MT conditions are preferred to study both transthiolation and ligation. **C**. HOIP-dependent transthiolation of UbSRhodol in the low nanomolar range showcases sensitivity of the assay.

UbSRhodol profiling of E3 key point mutations

With this platform in hand, we evaluated the potential of our assay in measuring changes in ligase activity, caused by key point mutations. As the mode of action of HECT ligases is conserved through the different NEDD4 family members, with a high degree of homology in the HECT domain, a set of 14 representative mutants of the NEDD4L HECT domain were chosen. The point mutations can be sorted into different categories including the catalytic loop (H876A/E, T877A, F879A, N880A, C878A), the E2 binding site (Y692A and W698A/E), the C-lobe Ub binding site (L872A and M899A), the N-lobe Ub binding site (F718A), the -4F (F907A) and the

acidic loop (D595A). The mutants are based on previous studies determining the reaction mechanism of HECT E3 ligases[21]. All mutants were profiled using UbSRhodol to detect transthiolation and/or ligation defects (Fig. 3A, Supplementary Fig. 8). As expected, the catalytically dead C878A mutant was not able to form isopeptide linkages, as corroborated by bypass probe gel-based assays in the presence of β-mercapthoetanol (βME) (Supplementary Fig. 8). However, some residual activity was observed and therefore our UbSRhodol data was normalized against WT (100% activity) and C878A (0% activity) (Fig. 3).

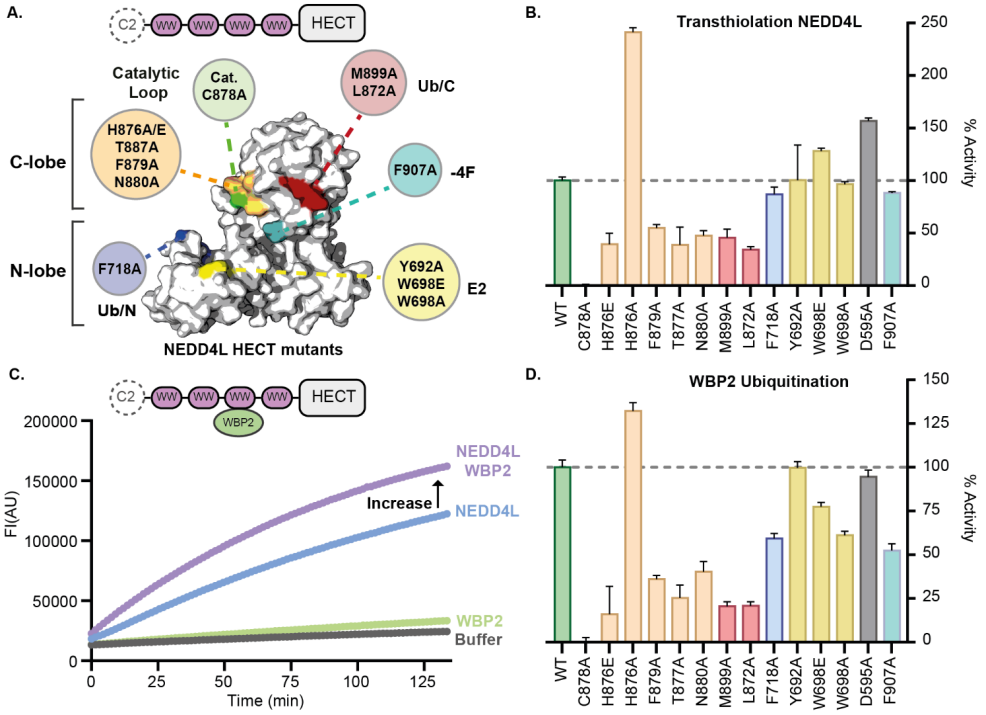

Figure 3. NEDD4L mutants and their effects on transthiolation and downstream cognate substrate ubiquitination profiled by UbSRhodol. A. Overview of ΔC2-NEDD4L HECT domain mutants derived from NEDD4L isoform 2 (PDB: Q96PU5-2). Mutations are clustered by region and depicted in green (catalytic site: C878A), orange (catalytic loop: H876A/E, T887A, F879A, N880A), blue (N-lobe Ub binding exosite: F718A), red (C-lobe Ub binding site: M899A, L872A, N880A), yellow (E2 binding site: Y692A, W698A/E), turquoise (-4F: F907A) and (not depicted) in grey (flexible linker: D595A) **B**. Transthiolation profile of NEDD4L. Mutants were screened against UbSRhodol under ST conditions (2.5μM NEDD4L vs 500 nM UbSRhodol) to measure transthiolation defects (stand. dev., n=4; 2 ST concentrations, 2.5uM and 1.25uM; normalized against WT (100%) and C878A (0%)). **C**. Ubiquitination of the model substrate WBP2 increases the assay window as WBP2 ligation results in discharge of the E3, which can then undergo multiple cycles. D) NEDD4L mediated ubiquitination of WBP2. Mutants were screened against UbSRhodol under ST conditions (2.5mM NEDD4L, 500nM of WBP2 vs 500 nM UbSRhodol) to

measure transthiolation defects (normalized against WT (100%) and C878A (0%), (stand. dev., n=4).

Importantly, as UbSRhodol bypasses E2 enzyme requirement, mutations in the N-terminal N-lobe responsible for binding parts of an E2 distal from the E2 catalytic cysteine, hardly show an effect in our assay. However, mutations in the C-terminal C-lobe, essential for the native transthiolation, are detrimental for ligase activity. A spike in activity was observed for mutant H876A, which seems to be an artefact of the bypass system as a similar observation was made by Krist et al.[10b] for a corresponding Rsp5 mutant. Next, we tested the ability of this set of mutants to discharge Ub from the catalytic C878 of Nedd4L by adding its cognate substrate WBP2[22]. Since reconstituted activity of NEDD4L in vitro yields the E3~Ub adduct and some autoubiquitination product, as corroborated by bypass probe gel-based assays in the presence or absence of βME (Supplementary Fig. 8), we observed that addition of WBP2 increased the assay window (Fig. 3B) and resulted in efficient cognate substrate ubiquitination (Supplementary Fig 9B). This set was compared to the in vitro ubiquitination of WBP2 by the native cascade using a E2~Ub discharge assay (Supplementary Fig. 9C). Fluorescence intensity read-outs of ubiquitination of WBP2 using UbSRhodol correlated with product formation observed by gel-based experiments (Supplementary Fig. 9). All mutants were defective except the ones with mutations targeting the E2 binding site (W698A/E and Y692A) or Ub binding site (F718A) in the N-lobe. Hyper ubiquitination of WBP2 by H876A mutant was observed, a bypass system-dependant phenomena, as discussed above. Although the H876A mutation has decreased reactivity in the native ubiquitination cascade (Supplementary Fig. 9C), this histidine in the catalytic loop is not needed in the bypass system and might even hinder the reaction slightly. Interestingly we observed that a mutation at asparagine 880 (N880) located at the catalytic loop, was still able to ubiquitinate WBP2 in the bypass system while none was observed in the native ubiquitination. Similar to the H876A mutation, a mutation of N880 could potentially change the positioning of the catalytic loop which decreases activity for Ub transfer with canonical E2s.

Together, our results show that UbSRhodol can be used to profile biochemical defects in transthiolation and substrate ubiquitination (ligation steps) of HECT E3s. As it utilizes an E2-independent transthiolation mechanism, caution should be taken when the mutations affect the E2 binding site. Here, the combined use with fluorescently labelled N-terminal Ub bypass probes for gel-based assays will complement the UbSRhodol readout as it facilitates discrimination between transthiolation and/or ubiquitination products.

UbSRhodol profiling of E3 allosteric activation

Subsequently, we investigated if UbSRhodol could recapitulate conformational changes induced by protein-protein interactions[6] and measure its downstream effect on ligase activity. Here we used ARIH1 and ARIH2 as these RBR E3 ligases possess complex autoinhibitory mechanisms[19]. Both enzymes have autoinhibitory Ariadne domains which mask the catalytic cysteine and impede its loading from the

E2~Ub. Upon complexation with neddylated Cullin-RING ligases, the ARIH Ariadne domain is sequestered and auto-inhibition concomitantly released. In this E3:E3 superassembly[23], the catalytic cysteine is accessible, allowing transthiolation from the E2~Ub. First, we focused on ARIH2 and investigated if we could recapitulate the activating effects of the E3:E3 superassembly[24] formation in our assay. We compared the activity of ARIH2 alone and in complex with neddylated CUL5-RBX2 against UbSRhodol (Fig. 4A). An enormous boost in ARIH2 transthiolation activity was observed when adding neddylated CUL5:RBX2 in equimolar amount. In contrast, active site mutated ARIH2 (C310A) did not show any transthiolation. These findings were corroborated by gel-based analysis using RhoUbSR (Supplementary Fig. 10), which showed that ARIH2 wild-type (WT) is only ubiquitinated upon addition of stochiometric amounts of neddylated CUL5:RBX2. (Fig 2A Panel I, II and III).

Next, we focussed on E3-E3 complex formation of ARIH1[25]. WT ARIH1 and relevant ligation defective mutants were assayed in the presence of neddylated CUL1-RBX1 and compared with the hyperactivated ARIH1OPEN mutant[23a]. In ARIH1OPEN, the intramolecular latch between the Rcat and Ariadne domain is released by introducing three mutations in the latter (F430A, E431A, E503A), mimicking the structural reconfiguration when bound to CUL1. The “OPEN” triple mutant was in fact more active than the E3-E3 complexed WT ARIH1 in the UbSRhodol assay (Fig. 3B), which was further corroborated by gel based experiments with the RhoUbSR bypass probe (Supplementary Fig. S11). Moreover, the assayed ligation defective mutants of ARIH1 showed reduced activity as recapitulated by both fluorescence intensity (Fig. 3B) and gel-based read-outs (Supplementary Fig. 11C), matching previous observations[23a]. Our data highlights that catalytic cysteine-to-alanine mutants (C357A) are preferred over cysteine-to-serine mutants (C357S) (Supplementary Fig. 11B), as the latter can still process UbSRhodol forming an oxyester intermediate[26].

Collectively, this shows that our platform can detect activity changes resulting from conformational changes induced by E3-E3 super-assemblies.

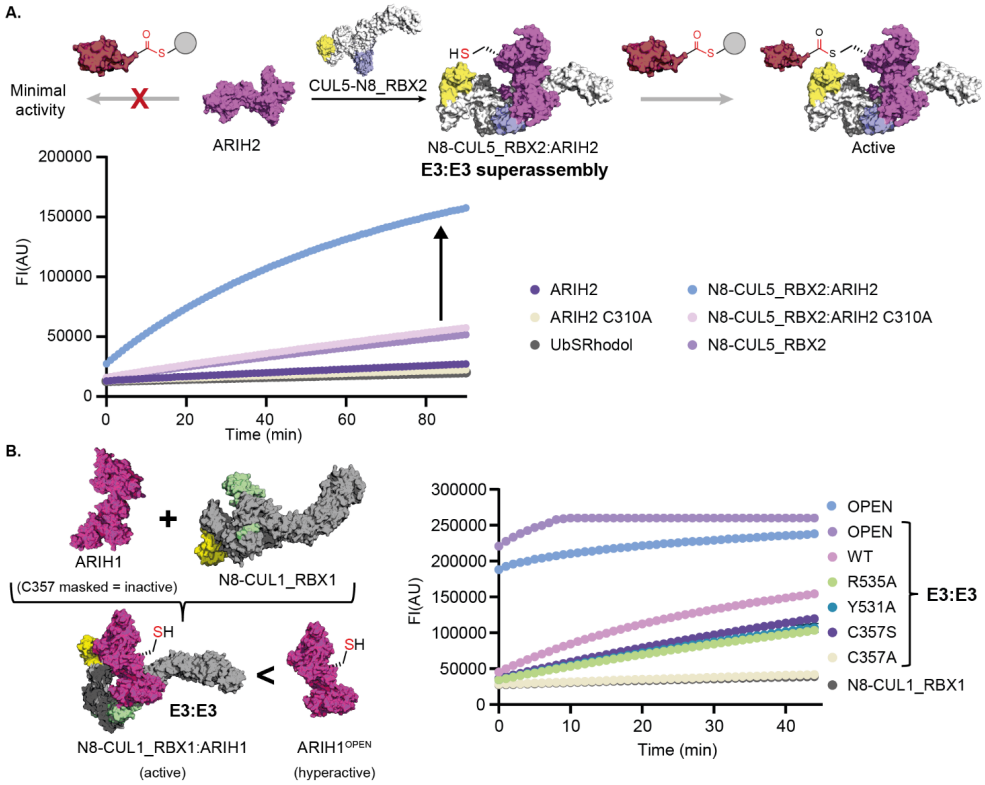

Figure 4. UbSRhodol can profile changes in activity level via E3:E3 superassembly formation of ARIH RBR ligases. A. E3:E3 superassembly of ARIH2 and neddylated CUL5:RBX2 enables transthiolation measurement overtime using UbSRhodol at ST conditions (500nM E3:E3 superassembly and 500nM UbSRhodol) in a plate reader. **B**. ARIH1 E3:E3 superassembly with neddylated CUL1:RBX1 enables profiling of different ARIH1 mutants under ST conditions (1:1:1, 500 nM). For full panel of mutants, see Supplementary Fig. 11. Note: the hyperactive mutant ARIH1OPEN upon complexation with N8-CUL1_RBX1 is so active that the signal is saturated (260k) after 10 minutes.

A Powerful Platform for HTS

Having validated the reactivity and high sensitivity of the UbSRhodol reagent in real time, we set out to test UbSRhodol for High-Throughput Screening (HTS) campaigns. As a proof of concept, we employed a fragment-based ligand discovery approach to identify transthiolation blockers for three E3 ligases, namely the homologous RBR E3 ligases HOIP and ARIH1OPEN and the HECT E3 ligase SMURF1, to investigate if a different subset of unique hits could be retrieved.

However, since a cysteine is targeted using electrophilic fragments and the mechanism of action of our pro-fluorescent probe is based on cyclization of the cysteine-based

linker, we first set out to investigate if commonly used positive controls in HTS, iodoacetamide (IAA) and N-ethylmaleimide (NEM) could block this cyclization progress by alkylating the thiol moiety. We titrated UbSRhodol with NEM or IAA and followed the inherent hydrolysis of the probe at pH 7.5 and pH 9 (Supplementary Fig. 12) as well as the effect of 1% DMSO. Only at high concentrations, > 1 mM of IAA and >0.5 mM of NEM, or alkaline pH the cyclization process was impaired (vs 500nM of UbSRhodol). We therefore selected 1% DMSO and 1 mM IAA as negative and positive controls respectively for our UbSRhodol screening campaigns. Here, an excess of probe over E3 ligase was chosen as MT conditions allowed screening with low E3 concentrations (Supplementary Fig. 11C, 13 and 14).The quality of our HTS assay was assessed by determining the screening window coefficient, the Z'-factor[27] (Z' >0.5 excellent). We inspected for the best balance between Z' values and amenable HTS timepoints having an acceptable assay window (Supplementary Fig. 15). In short, we decided to pick low nanomolar concentrations for HOIP (25nM, assay window: 2-2.5h, Z' > 0.65) and ARIH1OPEN (15nM, assay window 1-1.5h, Z'> 0.65) and a concentration of 150nM for SMURF1 (assay window >2h , Z'=0.7).

We then screened HOIP (H), ARIH1OPEN (A) and the HECT enzyme SMURF1 (S), lacking the C2 autoinhibitory domain, against a library of electrophilic fragments (7887 compounds, Enamine) with diverse covalent warheads and balanced reactivity (Supplementary Fig. 16) utilizing UbSRhodol. For each compound the percentage inhibition was determined from the fluorescence intensity by normalization of the measurement of the positive (iodoacetamide) and negative (DMSO) controls to 100% and 0% inhibition, respectively. Only compounds exhibiting an inhibition percentage of above 60%, were considered as hits. Next, selected hits were validated in triplicate and a different subset of unique hits was retrieved for each E3 ligase (Fig 4A and Supplementary Extended table S1). Here, HOIPIN-8, a known covalent inhibitor for HOIP[28] included as positive control, was retrieved in the subset of unique hits for HOIP (Fig. 5A).

Interestingly, a subset of compounds belonging to the family of carbonylimizadoles, a warhead typically reported to target serine residues[29], inhibited all three E3 ligases. Intrigued by their reactivity towards our ligases we tested their intrinsic reactivity in a thiol-reactivity assay. The fragments were incubated with Ellman's reagent (Supplementary Fig. 17) and no reactivity was observed towards the reagent. We next set out to assess target engagement in an orthogonal assay by measuring adduct formation by intact protein mass spectrometry (MS). Although multiple labelling was observed for ARIH1 and SMURF1 at 100 μM (Supplementary Fig. 18-19), in the case of HOIP we observed mainly one modification (Fig. 5B). Mutagenesis of catalytic cysteine 885 to alanine (C885A) confirmed the reactivity of these carbonylimidazoles towards cysteines (Fig. 4B and Supplementary Fig. S20) as further supported by a competition experiment with the irreversible suicide probe SulfoCy5UbVME (Supplementary Fig. 21). Here, we first incubate HOIP with the fragments after which the residual free active site cysteines are visualized by addition of SulfoCy5UbVME. A decrease in SulfoCy5Ub-VME-HOIP adduct, after incubation with the fragments, was observed (Supplementary Fig. 21B), corroborating our finding that these carbonylimidazoles target the catalytic cysteine of HOIP.

Although, this set of carbonylimidazole (covalent fragments X,Y and Z) require further optimization in medicinal chemistry campaigns to increase their potency and selectivity, we used them to showcase the ability of UbSRhodol to profile inhibitors. First, we assessed the IC_{50} values of fragments X,Y and Z against HOIP (Fig 5C and Supplementary Fig. 22). Second, as potency of these fragments increased with increasing incubation time their covalent nature was assessed by jump dilution assays (Fig 5C and Supplementary Fig. 23).). Second, as potency of these fragments increased with increasing incubation time their covalent nature was assessed by jump dilution assays (Fig 5C and Supplementary Fig. 23). Our jump dilution curves (300 to 3 µM) overlapped with the highest inhibitor concentration (300 µM) indicating an irreversible covalent mode of action for these carbonylimidazoles X, Y and Z.

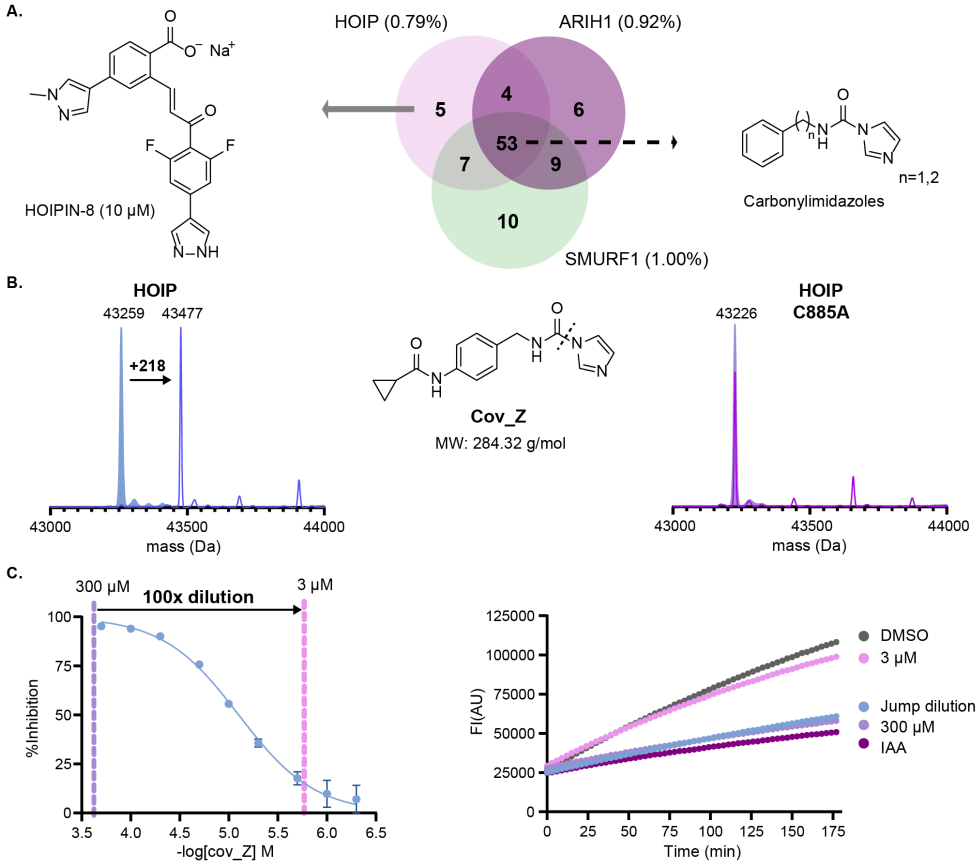

Figure 5. UbSRhodol in a fragment-based ligand HTS screening campaign. A. Venn diagram displaying the number of validated hits (>60% inhibition) obtained in the three screening campaigns with UbSRhodol. Percentage indicated represents the hit rate for each E3 ligase. For a deeper characterization of compounds see Supplementary Extended table S1. **B**. MS-adduct formation experiments with carbonyl imidazole Cov_Z showed specific targeting of cysteine 885 of HOIP as confirmed by mutagenesis experiments and **C**. Jump dilution assays (100X dilution) against HOIP showed an irreversible covalent mode of action (showed for Cov_Z, see Supplementary Fig. 22-23 for X and Y) (stand. dev., n=3).

Our UbSRhodol platform allows robust HTS screening campaigns which are characterized for the low amount of E3 and substrate used, permitting screening of large libraries and conduct follow up experiments with minimal reagent.

Visualizing E3 Transthiolation Activity in Cell-extract

Encouraged by the performance of UbSRhodol against recombinant proteins we set out to apply UbSRhodol in crude cell lysates. First, we explored if other members of the ubiquitination machinery could also process this thioester-based probe. For that we screened a panel of Ub enzymes of the conjugation (E1-E2-E3 (RING)) and deconjugation (DUBs and Ub-like (Ubl) proteases of SUMO and NEDD8) machinery. We observed a structural class E2[30] dependent processing of UbSRhodol with the tested conjugation enzymes (Supplementary Fig. 24). E2 Enzymes belonging to Class I (UBE2G1, UBE2D1, UBE2D2, UBE2D3) were hardly able to process UbSRhodol, whereas members of Class III (UBE2R1 and UBE2R2) could process UbSRhodol. Next, we tested a panel of Ub(l) proteases as they harbor highly reactive active site cysteine residues. First, we confirmed that the proteases were active by using a well-established reagent[31] for Ub(l) deconjugation enzymes based on Ub-Rho-morpholine (Supplementary Fig. 25). We then assessed potential cross-reactivity by incubating UbSRhodol with our panel of proteases (Supplementary Fig. 26). Whereas DUBs could process UbSRhodol, no cross-reactivity was observed for the Ubl proteases NEDP1 and SENP2 (Supplementary Fig. 26F,G).

Next, we overexpressed wild-type (WT) GFP-ARIH1 and different mutants WT-CS, OPEN and OPEN-CS in HEK293T cells and analysed their activity in the corresponding total cell lysates with the activity-based probe (ABP) SCy5UbVME. In line with the assays with recombinant enzymes shown above, GFP-ARIH1 UbVME labelling activity was only observed in the ARIH1OPEN expressed cell lysate (Supplementary Fig. 27). We next compared the reactivity of the activity-based probes SCy5UbVME[32] and SCy5UbPA[33] (with different reactive warheads) and the bypass probe (SCy5UbSR) in lysates of GFP-ARIH1OPEN or -ARIH1OPEN-CS expressing cells, and control cells. Labeling of GFP-ARIH1OPEN was observed for both the VME-warhead ABP and the bypass probe (SR), but not for the PA-warhead probe, whereas ARIH1OPEN-CS did not react at all (Fig. 6A). In addition, we added UbSRhodol as substrate to these cell lysates and measured ligase dependent liberation of free Rhodol. As shown in Fig. 6B (DMSO), the endogenous proteins in untransfected cells can process these type of thioester-based probes, but the activity in the lysate of GFP-ARIH1OPEN but not GFP-ARIH1OPEN-CS overexpressing cells was higher. Since UbSRhodol ligase recognition takes place through Ub binding domains at the catalytic domain of HECT or RBR ligases, we next included two different competitors of UbSRhodol interactions. Plain Ub76 was selected as non-covalent competitor and UbPA[33] as putative covalent competitor and pan-inhibitor for proteases in a cell-lysate context to reduce the background since no UbPA labelling of GFP-ARIH1OPEN was observed (Fig. 6A). As expected, reduced processing of UbSRhodol was observed in a concentration-dependent manner, and

UbPA inhibited more than Ub76 (Fig 5B and Supplementary figure FigS28). These results indicate that overexpression of active E3 ligases can offer opportunities for inhibitor profiling.

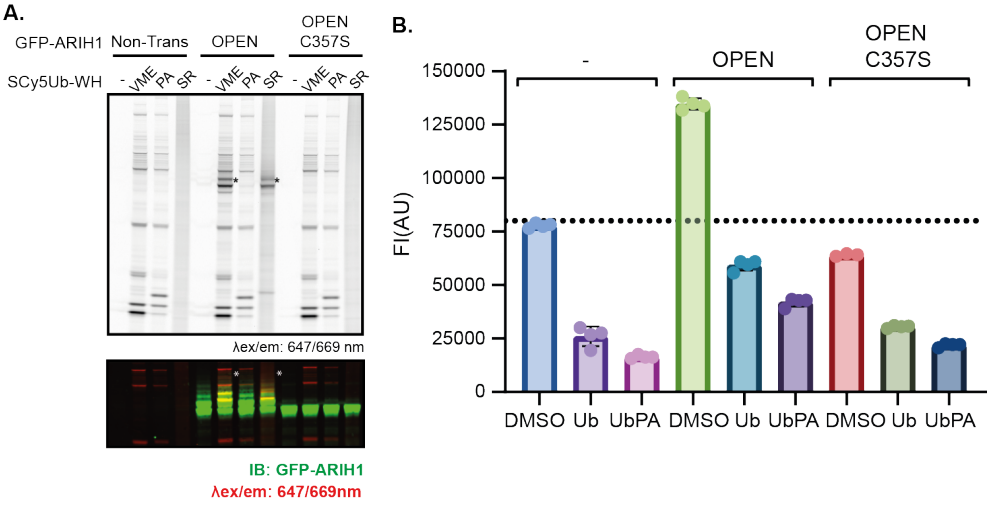

Figure 6. UbSRhodol and bypass probes to measure and visualize transthiolation activity of overexpressed E3 ligases (GFP-ARIH1). A. Reactivity of Ub based probes bearing a VME or PA electrophile warhead (WH) versus the bypass probe Ub-SR in lysates of control HEK293T cells (-) or cells overexpressing the indicated versions of GFP-ARIH1. Top: fluorescent scan after SDS-PAGE at 647/669nm. Only GFP-ARIH1OPEN containing cell lysate shows GFP-ARIH1 dependent activity with VME and SR probes (asterisk). Bottom: anti-GFP immunoblots (IB), and Cy5 fluorescent scans of the blot, corresponding to the GFP-ARIH1 containing part of the gel shown at the top. (See Supplementary Fig.29 for full gel higher exposure and Ponceau S staining of the blot validating equal loading). **B**. UbSRhodol dependent transthiolation in cell lysates of control HEK293T cells (-), HEK293T cells overexpressing GFP-ARIH1OPEN, or GFP-ARIH1OPEN-CS. Fluorescence intensity values at time point 120 min is depicted. Experiment performed in the absence or presence of bypass probe system competitors Ub and UbPA. (stand. dev., n=4).

Conclusion

The enzymatic activity of Ub E3 ligases, which accommodate chemical transthiolation to alter substrates, is critical for many biological processes and can go awry, causing disease[34]. Due to their regulatory role in cells and the recent emergence of targeted protein degradation concepts there is an increased interest in E3 ligases as drug targets[35]. Tools for this important target class are crucial for deepening our understanding of E3 ligase biology and the discovery of new ligands for E3 ligases. Here we presented a unique reagent, UbSRhodol, to monitor Ub ligase activity,

amenable to profile E3 transthiolation activity in real time. The key advantage of our methodology lies in its ability to bypass the need for E1 and E2 enzymes, its high sensitivity and ease of read-out.

Chemical synthesis of UbSRhodol, permitted us to stabilize the intrinsic reactivity of Ub-thioesters in both preparation as storage conditions. Endorsement of an autoimmolative linker onto the Ub C-terminus allowed us to profile E3 transthiolation activity by following the build-up of fluorescence intensity in real time. UbSRhodol processing by HECT/RBR E3 ligases proved catalytic cysteine-dependent at lower nanomolar concentrations among the different type and family members.

Our UbSRhodol platform provides ample possibilities for future therapeutic interventions as it allows quantitative analysis of changes in ligase activity. Not only evoked by biochemical mutations, but also by conformational changes and small molecules. Its ease of execution allows facile translation from one E3 ligase to the next, including assays for overexpressed ligases in total cell lysates, offering opportunities for E3 inhibitor screening platform in cell lysates. Moreover, its combined use with fluorescently labelled N-terminal Ub bypass probes and/or activity-based probes for gel-based assays, as demonstrated here, complements the UbSRhodol readout to study both transthiolation and ligation steps.

We demonstrated the robustness of our assay in an HTS setup, where we screened for small molecule modulators that block the transthiolation between our E3 enzyme and the activated Ub. In these screens we routinely achieved $Z' > 0.65$, while screening against low nanomolar E3 concentrations. Coupled to a fragment-based HTS[36] we identified hits from a relatively small library of less complex molecules that cover the larger part of the available chemical space, thereby providing structurally diverse starting points toward E3 inhibitors and potentially increasing the repertoire of scaffolds amenable to modulate E3 ligase activity.

To properly assess inhibitor potential one does need sufficient enzyme activity, and for physiological reasons many E3 enzymes, as demonstrated here for ARIH1 and ARIH2, are for a large part present in an inhibitory conformation, inactive state, and/or complex, regulated via inhibitory domains, co-factors and/or post-translational modifications. In addition, the technical problems in reconstituting full-length HECT E3 enzymes of large HECT E3s, have urged the need for sensitive readouts, opening the avenue of in-vitro activity profiling of low reactive E3 ligases constructs. As the readout of UbSRhodol relies on unbound fluorophore only, it provides a sensitive readout that translated to a sufficient assay window enabling the study of such low reactive E3 ligases constructs, as demonstrated here for UBR5 and ARIH2 (Supplementary Fig. 30).

We anticipate that our setup will attain a thorough understanding of diseases associated with altered E3 ligase activity. Here, HECT and RBR ligases are particularly attractive drug targets, due to their key roles in various diseases[37], small number compared with RING ligases and their diverse domain structures that could potentially facilitate specific manipulations. UbSRhodol can be applied as a general reagent to study E3-dependent molecular mechanisms, dissecting the

contribution of e.g. protein-induced allosteric activation and substrate recognition on E3 ligase activity. Moreover, screening endeavors to scout for protein activators or inhibitors of HECT or RBR E3 ligases will open new avenues for modulation of E3 ligases activity. Based on the platform presented here we envision different ways to inhibit their activity, namely: (i) by tackling the catalytic cysteine of the enzymes; (ii) by blocking the binding of protein-protein interactions as in the context of E3:E3 superassembly formation; and (iii) by impairing substrate recognition. Additionally, these modulators can open the route towards a wide variety of chemical tools ranging from E3 specific ABPs to targeted protein degradation tools (e.g. PROTACs) targeting an E3 ligase to selectively induce protein degradation[38].

Author contributions: D.A.P.B.: Conceptualization, Methodology, Investigation, Formal analysis, Validation, Visualization, Writing - Original Draft; T.M.V.: Investigation, Methodology, Visualization, Writing - Original Draft; D.H.G.: Resources, Validation, Writing - Review & Editing; J.J.B.: Resources, Validation, Writing - Review & Editing; L.A.H.: Resources, Validation, Writing - Review & Editing; S.K.: Resources, Writing - Review & Editing; M.M.: Resources, Writing - Review & Editing; I.D.: Resources, Writing - Review & Editing; P.P.G.: Formal analysis, Writing - Review & Editing; H.D.: Investigation, Methodology, Validation, Visualization, Writing - Original Draft, Writing - Review & Editing; B.A.S.: Resources, Validation, Supervision, Writing - Review & Editing; M.P.C.M.: Conceptualization, Methodology, Validation, Visualization, Project administration, Supervision, Writing - Original Draft, Writing - Review & Editing.

Acknowledgements

We thank Cami Talavera Ormeño for solid phase peptide synthesis, Bjorn van Doodewaerd for assistance with the ECHO screening platform. We would like to acknowledge Angeliki Moutsiopoulou and Robbert Kim from the LUMC Protein Facility for molecular cloning, expression and purification of the SMURF1 proteins. We would like to acknowledge Arno Alpi from Max Planck Institute Biochemistry for plasmids of ARIH1 for cell lysate experiments. This work was supported by the European Union's Horizon 2020 research and innovation programme under the Marie Skłodowska-Curie grant agreement No. 765445 to D.P.B, the EU/EFPIA/OICR/McGill/KTH/Diamond Innovative Medicines Initiative 2 Joint Undertaking (EUbOPEN grant no. 875510) and NWO (VIDI Grant VI. 213.110 to M.P.C.M.).

References:

[1] a) A. Hershko, A. Ciechanover, Annual review of biochemistry 1998, 67, 425-479; b) D. Komander, M. Rape, Annual review of biochemistry 2012, 81, 203-229.

[2] D. R. Squair, S. Virdee, Nature chemical biology 2022, 18, 802-811.

[3] a) Y. Liao, I. Sumara, E. Pangou, Communications biology 2022, 5, 114; b) C. Pohl, I. Dikic, Science (New York, N.Y.) 2019, 366, 818-822.

[4] D. Popovic, D. Vucic, I. Dikic, Nature Medicine 2014, 20, 1242-1253.

[5] I. E. Wertz, X. Wang, Cell Chemical Biology 2019, 26, 156-177.

[6] D. E. Spratt, H. Walden, G. S. Shaw, The Biochemical journal 2014, 458, 421-437.

[7] X. Huang, V. M. Dixit, Cell Research 2016, 26, 484-498.

[8] V. Landré, B. Rotblat, S. Melino, F. Bernassola, G. Melino, Oncotarget 2014, 5, 7988-8013.

[9] R. Macarrón, R. P. Hertzberg, Methods in molecular biology (Clifton, N.J.) 2009, 565, 1-32.

[10] a) S. Park, D. T. Krist, A. V. Statsyuk, Chemical Science 2015, 6, 1770-1779; b) D. T. Krist, S. Park, G. H. Boneh, S. E. Rice, A. V. Statsyuk, Chemical science 2016, 7, 5587-5595; c) S. Park, P. K. Foote, D. T. Krist, S. E. Rice, A. V. Statsyuk, Journal of Biological Chemistry 2017, 292, 16539-16553.

[11] R. S. Kathayat, P. D. Elvira, B. C. Dickinson, Nature chemical biology 2017, 13, 150-152.

[12] E. L. Ruggles, S. Flemer, Jr., R. J. Hondal, Biopolymers 2008, 90, 61-68.

[13] R. R. Sauers, S. N. Husain, A. P. Piechowski, G. R. Bird, Dyes and Pigments 1987, 8, 35-53.

[14] J. McNulty, V. Krishnamoorthy, D. Amoroso, M. Moser, Bioorg Med Chem Lett 2015, 25, 4114-4117.

[15] R. Raz, J. Rademann, Organic Letters 2011, 13, 1606-1609.

[16] F. El Oualid, R. Merkx, R. Ekkebus, D. S. Hameed, J. J. Smit, A. de Jong, H. Hilkmann, T. K. Sixma, H. Ovaa, Angewandte Chemie International Edition 2010, 49, 10149-10153.

[17] E. B. Getz, M. Xiao, T. Chakrabarty, R. Cooke, P. R. Selvin, Analytical bio-

chemistry 1999, 273, 73-80.

[18] J. Weber, S. Polo, E. Maspero, Frontiers in physiology 2019, 10, 370.

[19] a) H. Walden, K. Rittinger, Nature structural & molecular biology 2018, 25, 440-445; b) T. R. Cotton, B. C. Lechtenberg, Biochem Soc Trans 2020, 48, 1737-1750.

[20] a) F. Wang, Q. He, W. Zhan, Z. Yu, E. Finkin-Groner, X. Ma, G. Lin, H. Li, Structure 2023, 31, 541-552.e544; b) Z. Hodáková, I. Grishkovskaya, H. L. Brunner, D. L. Bolhuis, K. Belačić, A. Schleiffer, H. Kotisch, N. G. Brown, D. Haselbach, bioRxiv 2022, 2022.2011.2003.515015.

[21] a) H. B. Kamadurai, J. Souphron, D. C. Scott, D. M. Duda, D. J. Miller, D. Stringer, R. C. Piper, B. A. Schulman, Molecular Cell 2009, 36, 1095-1102; b) J. Sluimer, B. Distel, Cellular and Molecular Life Sciences 2018, 75, 3121-3141.

[22] H. Tabatabaeian, A. Rao, A. Ramos, T. Chu, M. Sudol, Y. P. Lim, Oncogene 2020, 39, 4621-4635.

[23] a) D. C. Scott, D. Y. Rhee, D. M. Duda, I. R. Kelsall, J. L. Olszewski, J. A. Paulo, A. de Jong, H. Ovaa, A. F. Alpi, J. W. Harper, B. A. Schulman, Cell 2016, 166, 1198-1214.e1124; b) I. R. Kelsall, D. M. Duda, J. L. Olszewski, K. Hofmann, A. Knebel, F. Langevin, N. Wood, M. Wightman, B. A. Schulman, A. F. Alpi, The EMBO Journal 2013, 32, 2848-2860.

[24] S. Kostrhon, J. R. Prabu, K. Baek, D. Horn-Ghetko, S. von Gronau, M. Klügel, J. Basquin, A. F. Alpi, B. A. Schulman, Nature chemical biology 2021, 17, 1075-1083.

[25] D. Horn-Ghetko, D. T. Krist, J. R. Prabu, K. Baek, M. P. C. Mulder, M. Klügel, D. C. Scott, H. Ovaa, G. Kleiger, B. A. Schulman, Nature 2021, 590, 671-676.

[26] C. Garcia-Barcena, N. Osinalde, J. Ramirez, U. Mayor, Frontiers in cell and developmental biology 2020, 8.

[27] J. H. Zhang, T. D. Chung, K. R. Oldenburg, Journal of biomolecular screening 1999, 4, 67-73.

[28] K. Katsuya, D. Oikawa, K. Iio, S. Obika, Y. Hori, T. Urashima, K. Ayukawa, F. Tokunaga, Biochemical and Biophysical Research Communications 2019, 509, 700-706.

[29] C. Jöst, C. Nitsche, T. Scholz, L. Roux, C. D. Klein, Journal of Medicinal Chemistry 2014, 57, 7590-7599.

[30] S. J. L. van Wijk, H. T. M. Timmers, The FASEB Journal 2010, 24, 981-993.

[31] R. Kooij, S. Liu, A. Sapmaz, B. T. Xin, G. M. C. Janssen, P. A. van Veelen, H. Ovaa, P. T. Dijke, P. P. Geurink, J Am Chem Soc 2020, 142, 16825-16841.

[32] A. de Jong, R. Merkx, I. Berlin, B. Rodenko, R. H. M. Wijdeven, D. El Atmioui, Z. Yalçin, C. N. Robson, J. J. Neefjes, H. Ovaa, ChemBioChem 2012, 13, 2251-2258.

[33] R. Ekkebus, S. I. van Kasteren, Y. Kulathu, A. Scholten, I. Berlin, P. P. Geurink, A. de Jong, S. Goerdayal, J. Neefjes, A. J. R. Heck, D. Komander, H. Ovaa, Journal of the American Chemical Society 2013, 135, 2867-2870.

[34] a) I. Dikic, B. A. Schulman, Nature reviews. Molecular cell biology 2022, 1-15; b) M. Rape, Nature reviews. Molecular cell biology 2018, 19, 59-70.

[35] I. N. Michaelides, G. W. Collie, Journal of Medicinal Chemistry 2023, 66, 3173-3194.

[36] S. Knight, D. Gianni, A. Hendricks, SLAS discovery : advancing life sciences R & D 2022, 27, 3-7.

[37] a) J. Weber, S. Polo, E. Maspero, Frontiers in Physiology 2019, 10; b) P. Wang, X. Dai, W. Jiang, Y. Li, W. Wei, Semin Cancer Biol 2020, 67, 131-144; c) Y. Wang, D. Argiles-Castillo, E. I. Kane, A. Zhou, D. E. Spratt, J Cell Sci 2020, 133.

[38] a) C. C. Ward, J. I. Kleinman, S. M. Brittain, P. S. Lee, C. Y. S. Chung, K. Kim, Y. Petri, J. R. Thomas, J. A. Tallarico, J. M. McKenna, M. Schirle, D. K. Nomura, ACS Chemical Biology 2019, 14, 2430-2440; b) T. Ishida, A. Ciulli, SLAS Discovery 2021, 26, 484-502.

Supplemental Chapter 5.

A Pro-Fluorescent Ubiquitin-Based Probe to Monitor Cysteine-Based E3 Ligase Activity

Table of Contents

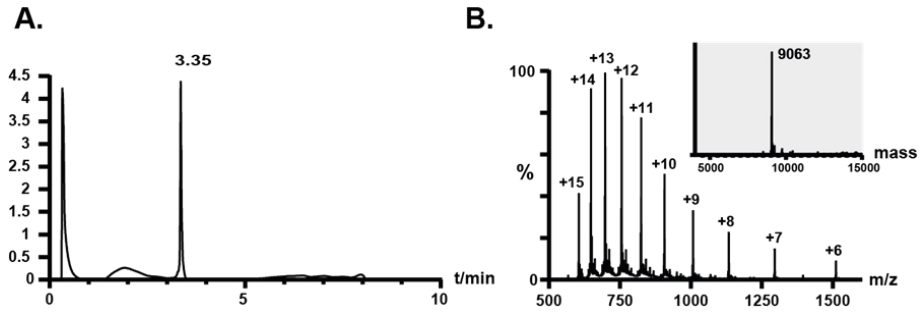

Supplementary Figure 1. LC-MS characterization of UbSRhodol. A) Liquid chromatography trace (3.35min, 107 scale) and B) Mass charge (m/z) envelope and deconvoluted mass spectra (ESI MS+ (amu) calcd: 9063, found 9063 (deconv.)).

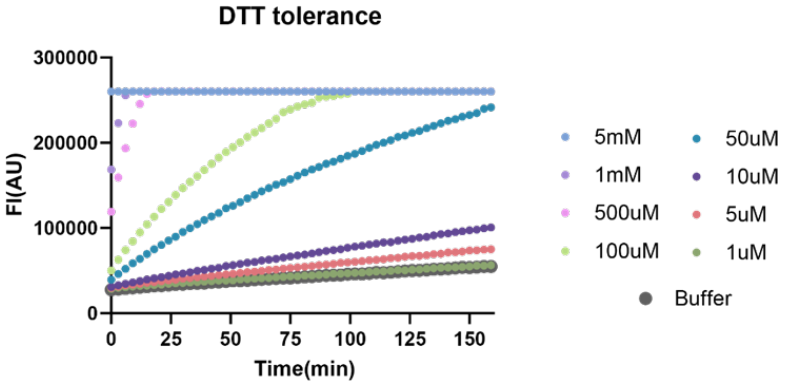

Supplementary Figure 2. DTT titration UbSRhodol. Incubation of UbSRhodol with the reducing agent DTT (5-0.001 mM) shows hydrolysis of the thioester of the probe over time.

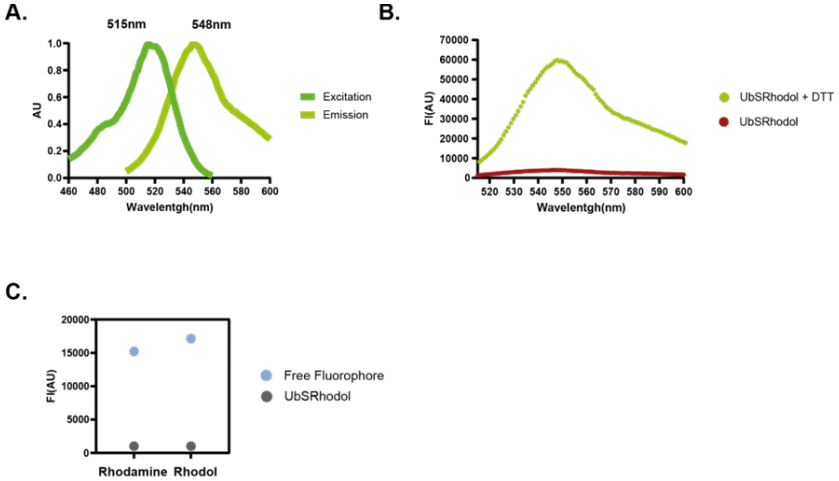

Supplementary Figure 3. Spectroscopic characterization of Rhodol and

UbSRhodol upon DTT transthiolation. A) Spectral scan of excitation and emission of the Rhodol dye B) Fluorescence intensity (FI) increase of 16 fold after DTT (5Mm) processing of UbSRhodol C) FI increase of UbSRhodol after DTT processing at Rhodamine and Rhodol channel (Rhodamine (λex/em): 490/520nm; Rhodol(λex/em): 515/548nm). FI fold increase is comparable for both wavelengths (17/15.2 FI fold, Rhodol/Rhodamine).

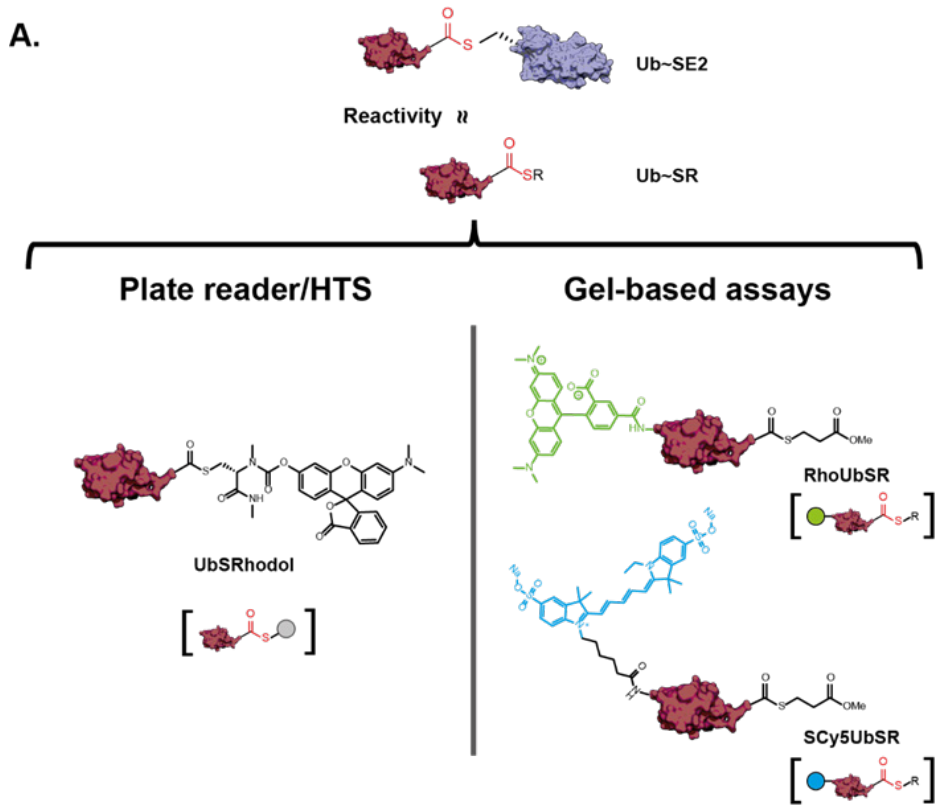

Supplementary Figure 4. Bypass probes for plate reader versus gel-based assays UbSRhodol facilitates plate reader based assays, whereas N-terminal labeled fluorophore based probes (RhoUbSR and SCy5UbSR) will ease gel-based analysis.

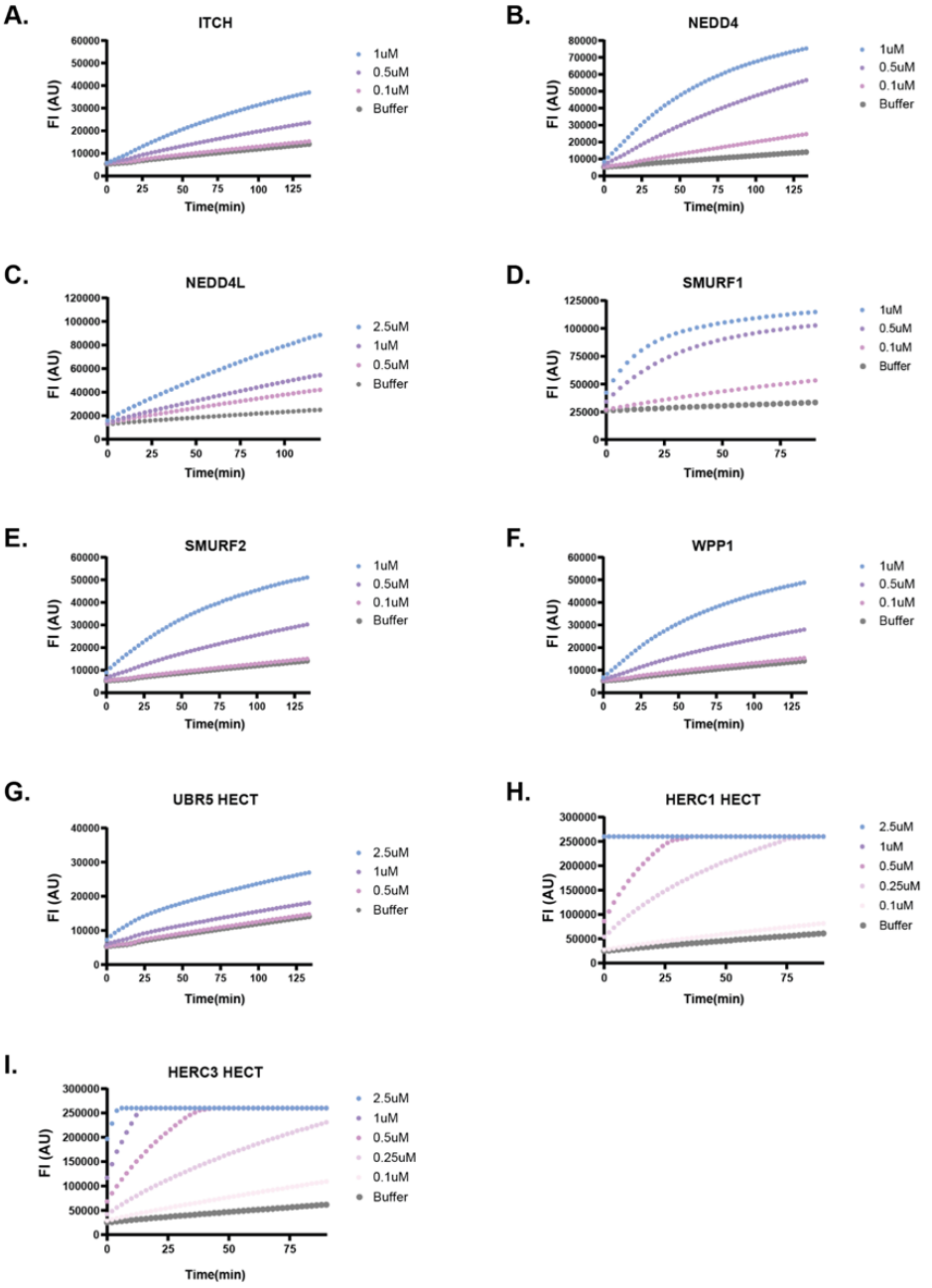

Supplementary Figure 5. Transthiolation profile of HECT E3 ligases panel profiled by UbSRhodol. HECT NEDD4 family ligases: A. ITCH; B. NEDD4; C. NEDD4L; D. SMURF1; E. SMURF2 and F. WPP1. Other HECTs: G.: UBR5 (HECT domain only) and HERC family ligases: H. HERC1 and I. HERC3 (HECT domain only)

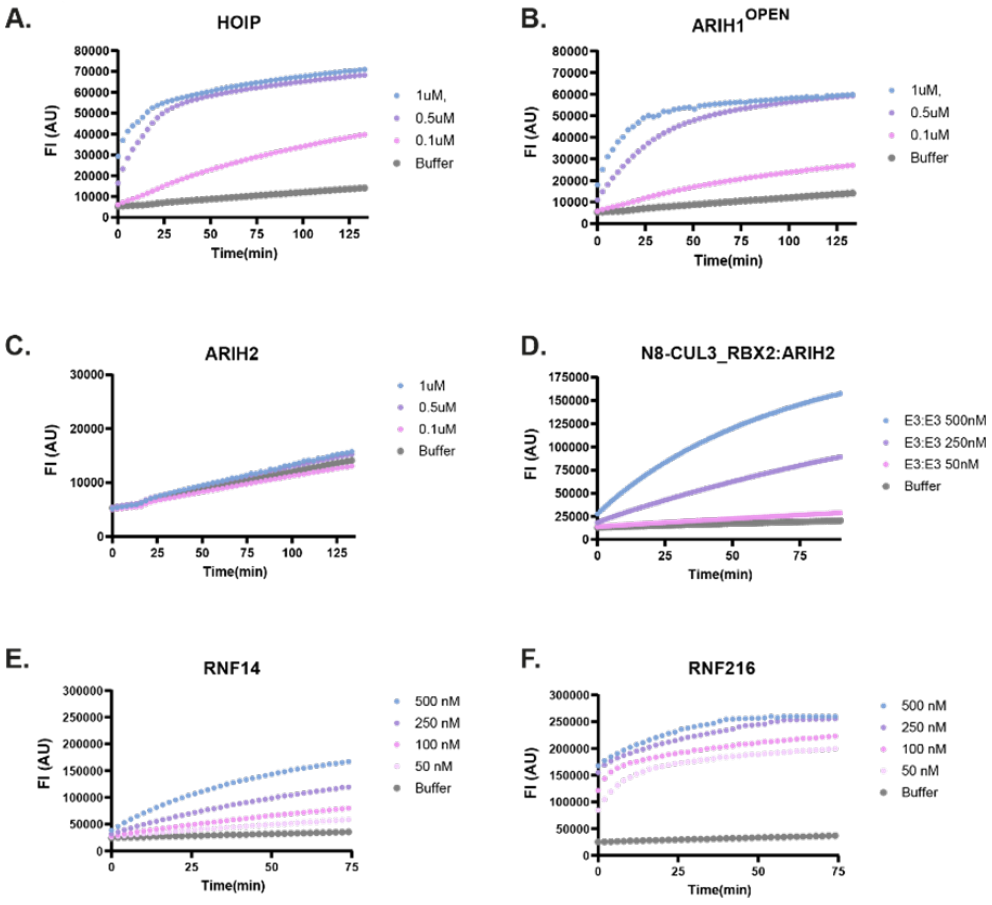

Supplementary Figure 6. Transthiolation profile of RBR E3 ligases panel profiled by UbSRhodol. A. HOIP; B. ARIH1OPEN; C. ARIH2 (not active) versus D. ARIH2 in a E3:E3 super assembly with Neddylated CUL3-RBX2 (active); E. RNF14; F. RNF216; were profiled.

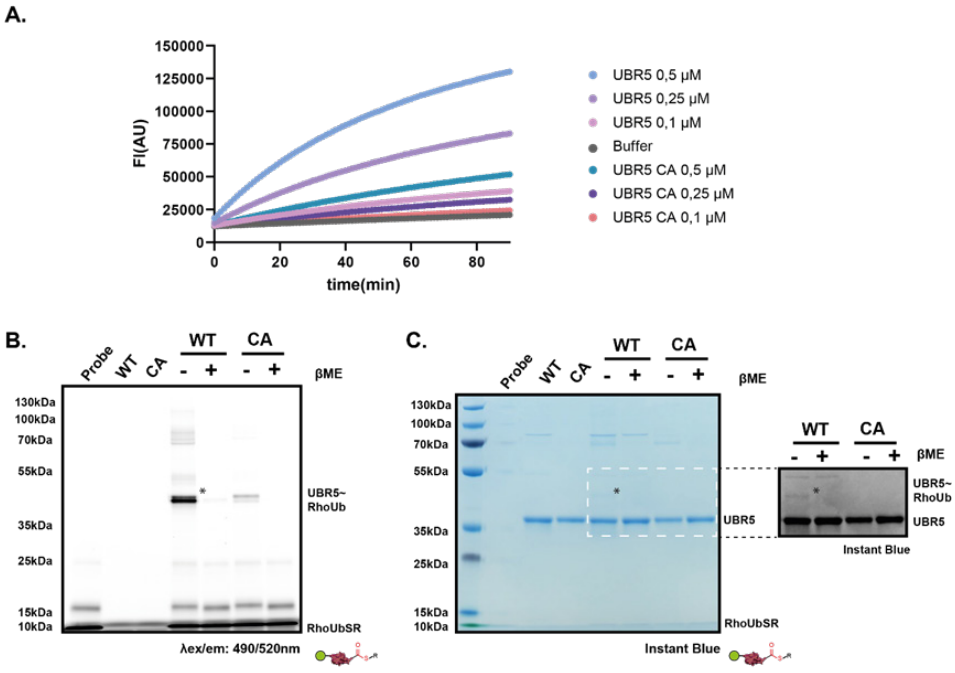

Supplementary Figure 7. UBR5 HECT dependent transthiolation and product formation with bypass probes. A) Transthiolation graph of UBR5 HECT domain wild type (WT) and catalytic cysteine 2768 mutated to alanine (CA) mutant using UbSRhodol (500nM). B) Alternatively, RhoUbSR harboring a fluorophore on its N-terminus, was used to evaluate product formation by gel-based assays. Samples were untreated or boiled under the presence of βME to assess thioester formation (marked with asterisk, *). C) Instant blue stain of gel and higher exposure of the square area to observe minimal thioester formation.

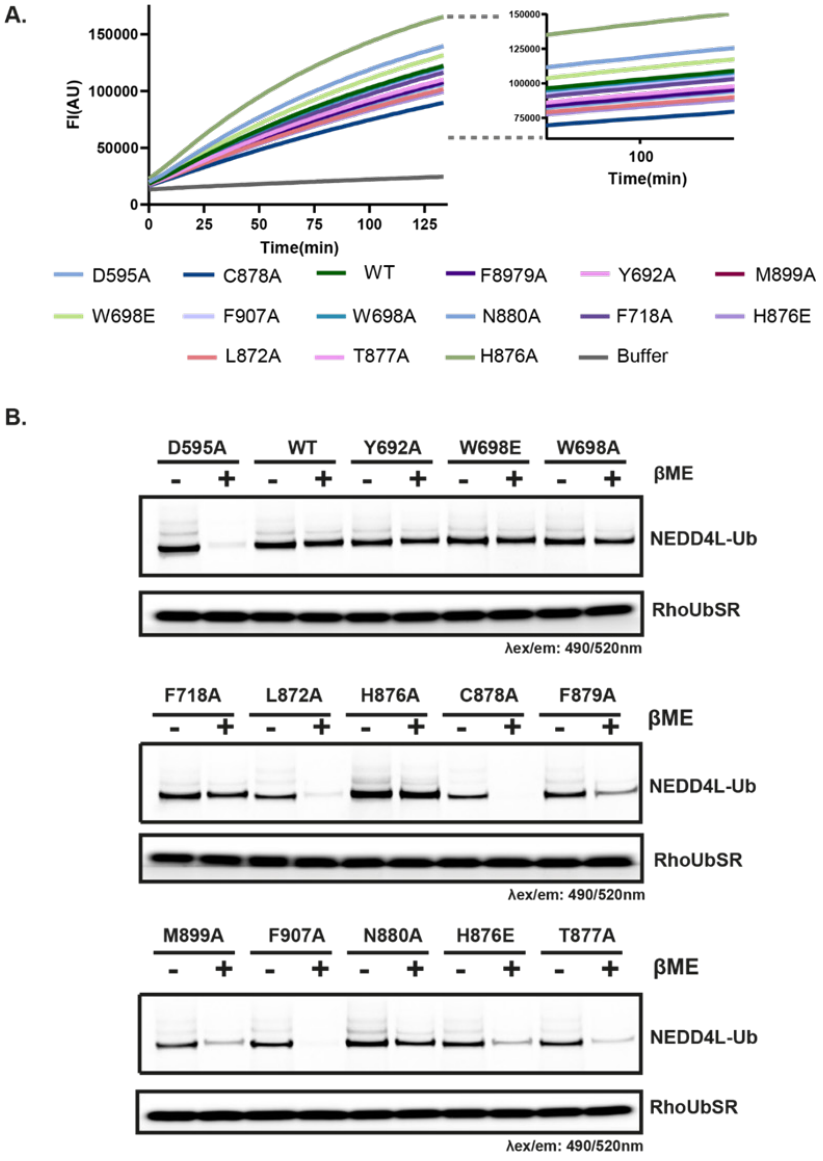

Supplementary Figure 8. Transthiolation profile of (ΔC2)NEDD4L isoform 2 mutants with UbSRhodol under ST conditions (2.5 μm E3 vs 500 nM UbSRhodol). A) (ΔC2)NEDD4L mutant-dependent fluorescence intensity build-up over time with UbSRhodol under ST conditions (2.5 μM E3 vs 500 nM UbSRhodol). Zoom in around 100 minutes time point used for the standardization of the mutants WT(100%) and C878A(0%). B) RhoUbSR was used under the same conditions to evaluate thioester and product formation by gel-based assays measuring at the rhodamine channel. Samples were untreated or boiled in the presence of βME to assess thioester formation. (See Supplementary Fig. 30 for full gel).

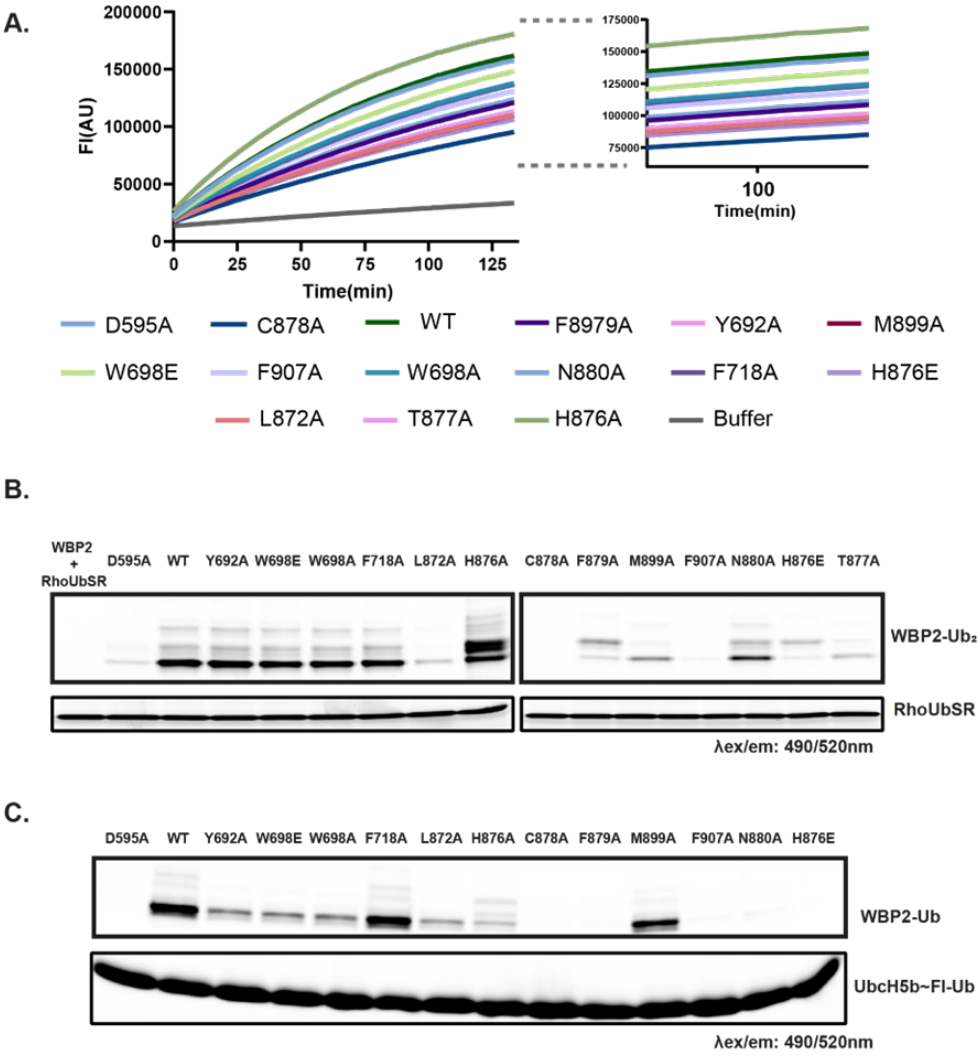

Supplementary Figure 9. WBP2 ubiquitination profile of all (ΔC2)NEDD4L isoform 2 mutants with UbSRhodol under ST conditions (2.5μM E3 vs 500nM UbSRhodol) and native ubiquitination cascade. A.) (ΔC2)NEDD4L mutant-dependent fluorescence intensity build-up over time with UbSRhodol under ST conditions (2.5 μM E3, 500 nM WBP2 vs 500 nM UbSRhodol). Zoom in around 100 minutes time point used for the standardization of the mutants WT(100%) and C878A(0%). B.) RhoUbSR was used under the same conditions to evaluate WBP2 ubiquitination by gel-based assays measuring at the rhodamine channel. Samples were βME treated and boiled. C.)Pulse-chase assay of Ubch7 loaded fluorescein ubiquitin as thioester (Ubch5b~Fl-Ub, ~ for thioester) (ΔC2)NEDD4L and ubiquitination of WBP2 with native cascade 0.5 μM UbcH5b~ubiquitin, 0.2 μM NEDD4L and 10 μM WBP2. Reactions were quenched after 5 minutes. (See Supplementary Fig. 31 for full gel).

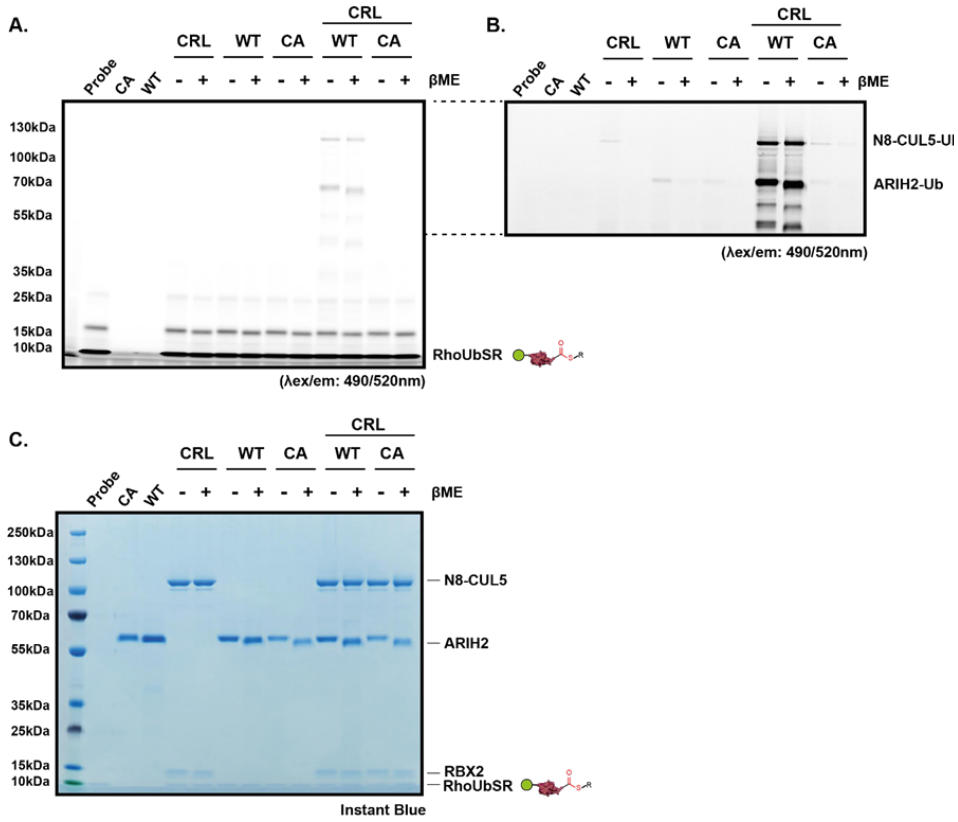

Supplementary Figure 10. Gel-based analysis of ARIH2 E3:E3 super assembly formation. RhoUbSR was incubated at the same UbSRhodol conditions (500 nM of E3 or E3:E3 and 500 nM of probe) with ARIH2 and CA mutant both alone or in complex with another E3 CRL (N8-CUL5-RBX2). Samples were untreated or boiled in the presence of βME. A) Fluorescence scan, B) Higher exposed fluorescence scan and C) Instant Blue stain.

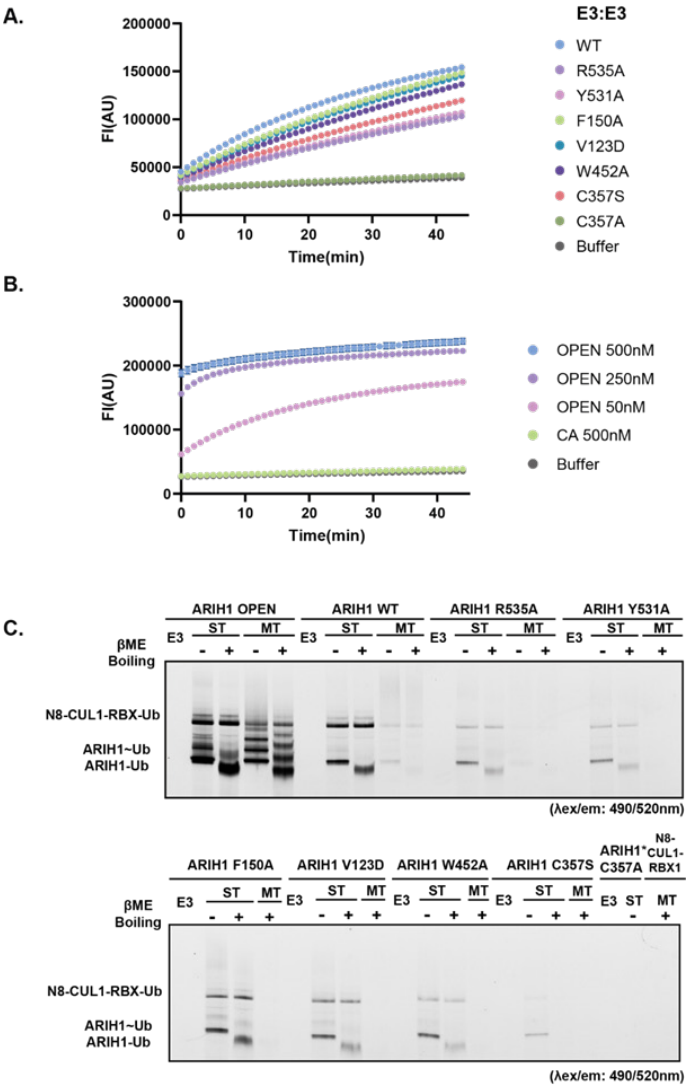

Supplementary Figure 11. Profiling ARIH1 and mutants in E3:E3 superassembly formation. A) E3:E3 super-assembly transthiolation profile of defective ligation mutants of ARIH1 (500 nM) with UbSRhodol (500 nM) under Single Turnover conditions (ST). B) ARIH1OPEN concentration dependent transthiolation profile with UbSRhodol (500 nM) C) RhoUbSR was incubated at the same UbSRhodol conditions (E3:E3 and probe 500nM) with N8-CUL1-RBX1:ARIH1 mutants to evaluate product formation by gel-based assays under ST (500nM E3, 1:1 E3 vs probe) or MT (50nM E3, 1:10 E3 vs probe) conditions. Hyperactivated ARIH1OPEN showed product formation (autoubiquitination) under MT conditions while the other mutants showed diminished ligation activity as compared with ARIH1 WT.

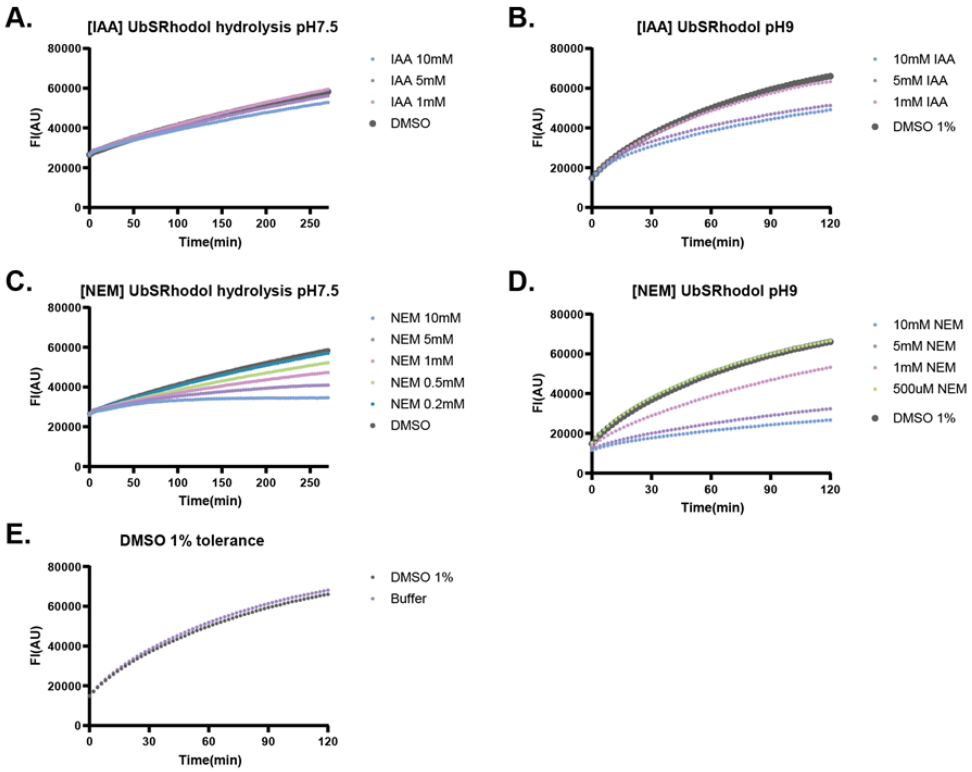

Supplementary Figure 12. Examining effect of positive controls (IAA and NEM) and DMSO on intramolecular cyclization of UbSRhodol. A) IAA titration against UbSRhodol hydrolysis at pH7.5 or B) pH 9 C.) NEM titration against UbSRhodol hydrolysis at pH7.5 or D) pH 9 to select concentrations of positive control E) Effect of 1% DMSO on cyclisation.

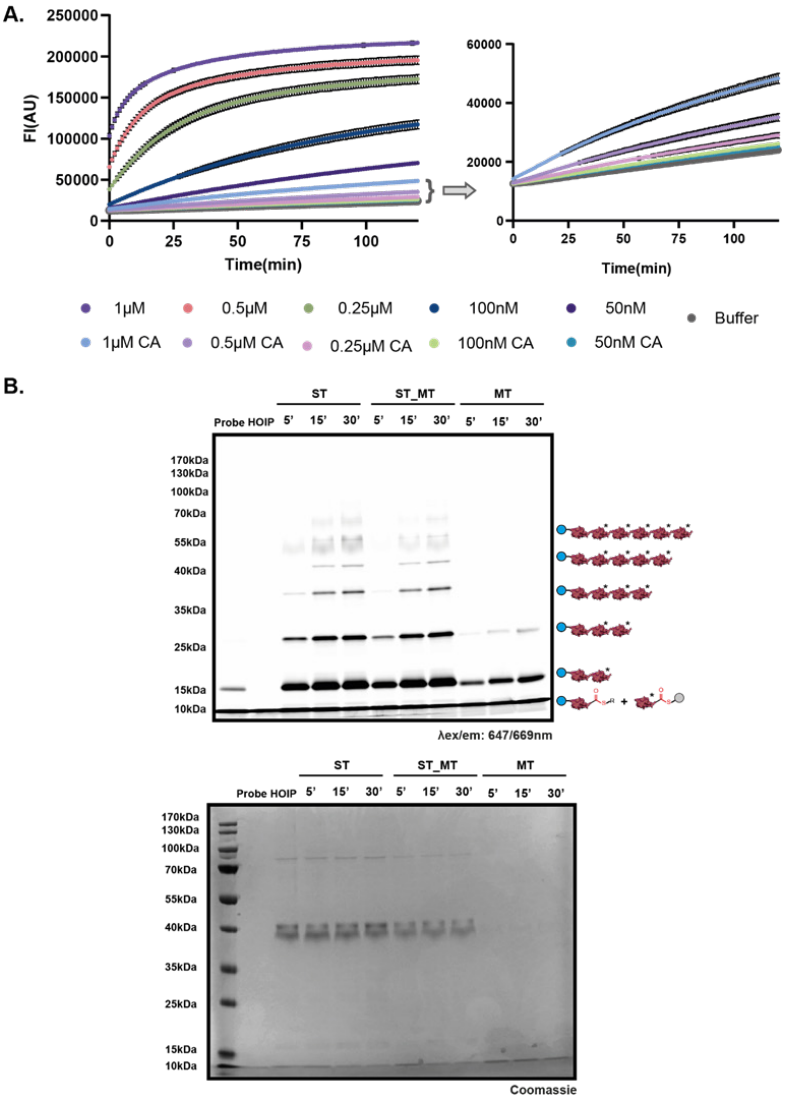

Supplementary Figure 13. HOIP bypass system and product formation. A) Activity profile of HOIP using UbSRhodol (1μM). UbSRhodol transthiolation of HOIP is exclusive of catalytic cysteine 885 at low concentrations (0.5μM to 50nM) as observed with the C885A mutant. B) UbSRhodol (500nM) and SCy5UbSR (500nM) were incubated at different ST and MT conditions (ST: 1:1, ST_MT: 0.25 fold or MT 0.05 fold E3 over total probe (1 μM) to evaluate product formation by gel-based assays. Samples were collected at different timepoints and boiled under the presence of βME.A clear anchored linear ubiquitin chain build-up was observed over time. Note: Combination of bypass probes was required to observe chain building as SCy5UbSR has a blocked N-terminus.

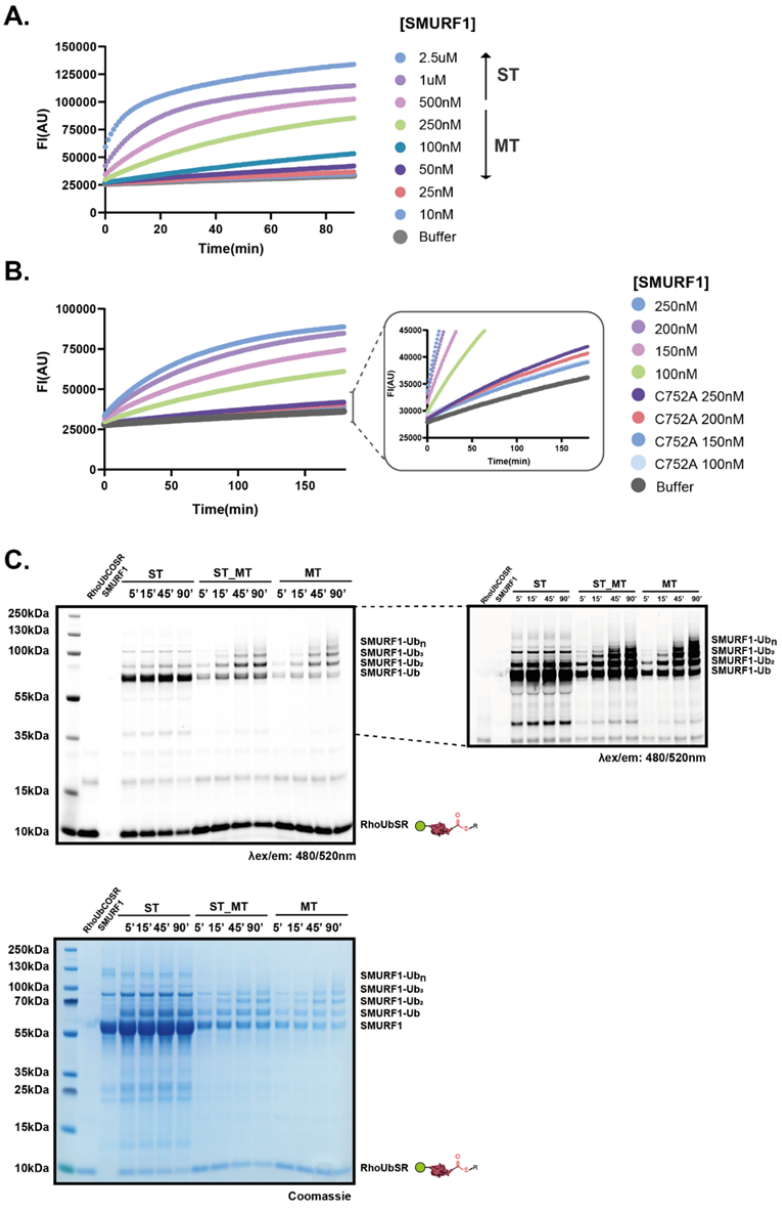

Supplementary Figure 14. SMURF1 bypass system and product formation. A) Activity profile of (ΔC2)SMURF1 using UbSRhodol (500nM). B) UbSRhodol transthiolation (ΔC2)SMURF1 is exclusive of catalytic cysteine 752 as observed with the C752A mutant. C) RhoUbSR was incubated different ST and MT conditions (ST: 5 fold, ST_MT: 0.5 fold or MT 0.2 fold E3 over probe (500nM) to evaluate product formation by gel-based assays. Samples were collected at different timepoints and boiled under the presence of βME.

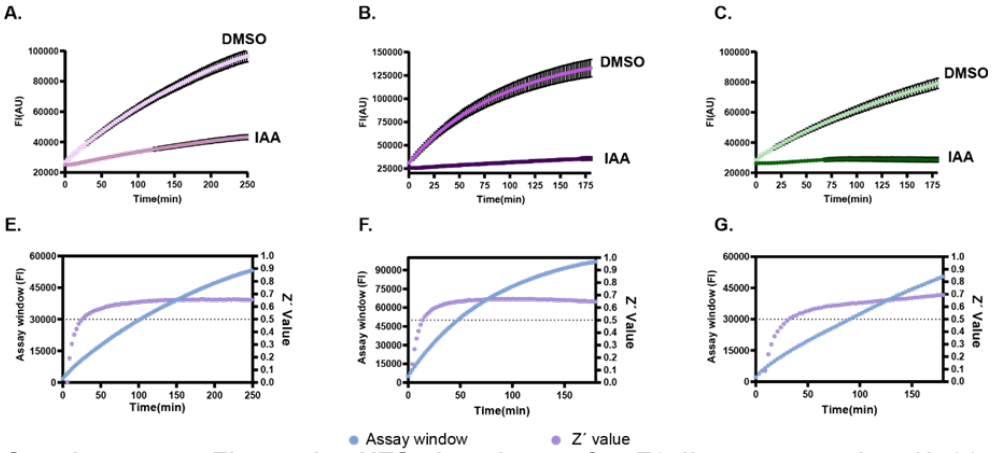

Supplementary Figure 15. HTS descriptors for E3 ligase screening (1536-well plate). UbSRhodol E3 transthiolation profile using positive and negative controls (1mM IAA and 1% DMSO, npos=nneg=128) of A) HOIP 25nM; B) ARIH1OPEN 15nM; C) SMURF1 150nM. Z' values (purple) and assay window in (AU)(blue) relationship with time for E) HOIP; F) ARIH1OPEN ; G) SMURF1.

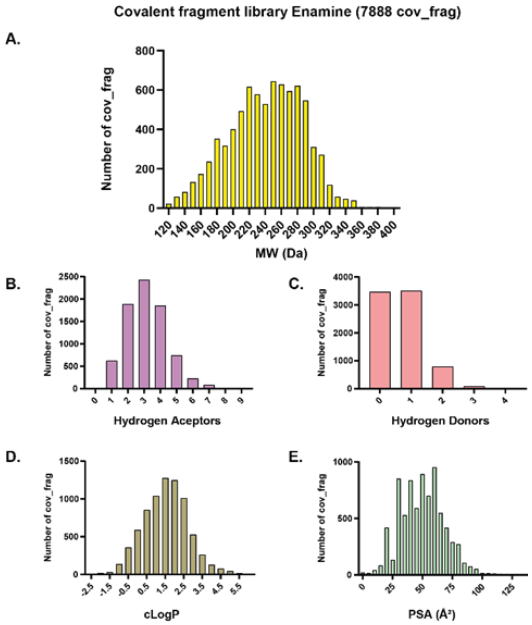

Supplementary Figure 16. Enamine covalent library descriptors. A.) Distribution of molecular weight (Da) of covalent fragment library. B.) Distribution of hydrogen acceptors of covalent fragment library. C.) Distribution of hydrogen donors of covalent fragment library. D.) Distribution of partition coefficient (clogP) of covalent fragment library E.) Distribution of Polar surface area (PSA) of covalent fragment library. Descriptors were calculated using CHEMDRAW software 20.0.0.41 with the SMILE codes.

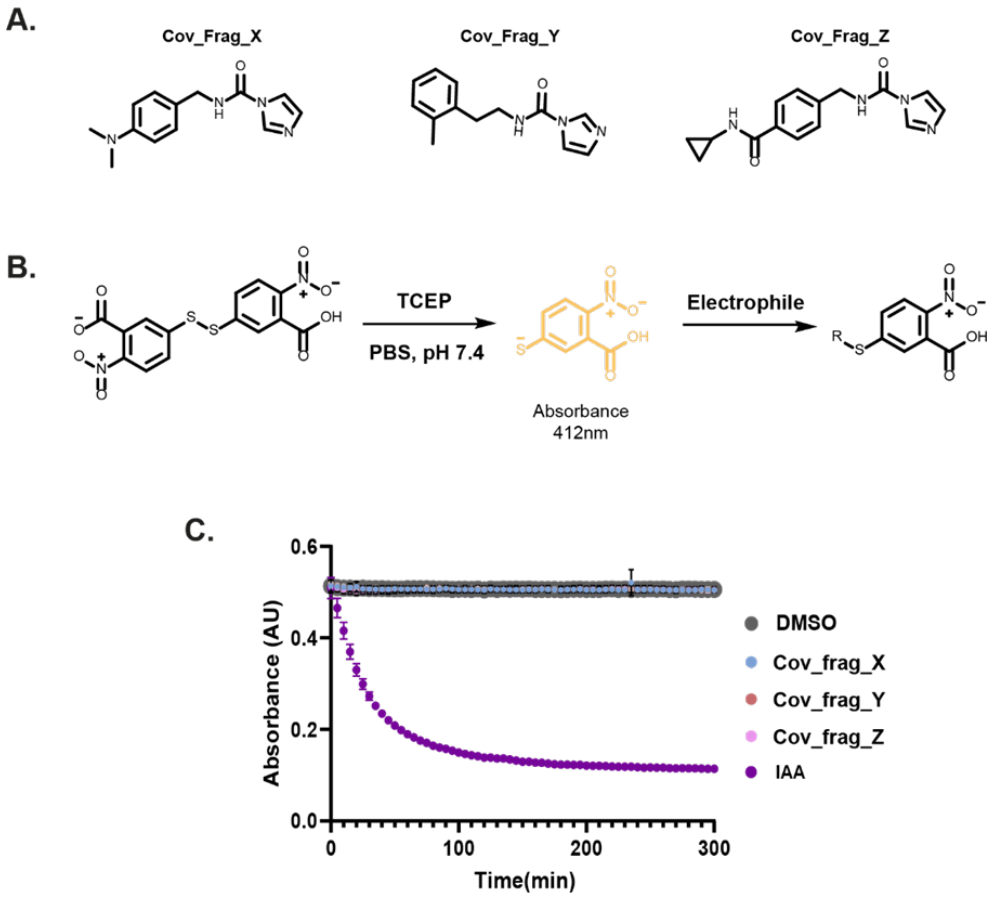

Supplementary Figure 17. Elmann's reagent experiment to access intrinsic reactivity of carbonylimidazole serie fragment X,Y,Z. A) Chemical structures of fragments X,Y and Z. B) Scheme of Elmann's reactionMechanism of reactivity assay using Elmann's reagent. Absorbance at 412nM is measured overtime after adding an electrophile. If the electrophile is reactive it will attack the nucleophilic sulfur of the reagent, thereby reducing its absorbance C) Fragments X,Y and Z are incubated with the elmann's reagent and the reaction is measured overtime at 412nM.

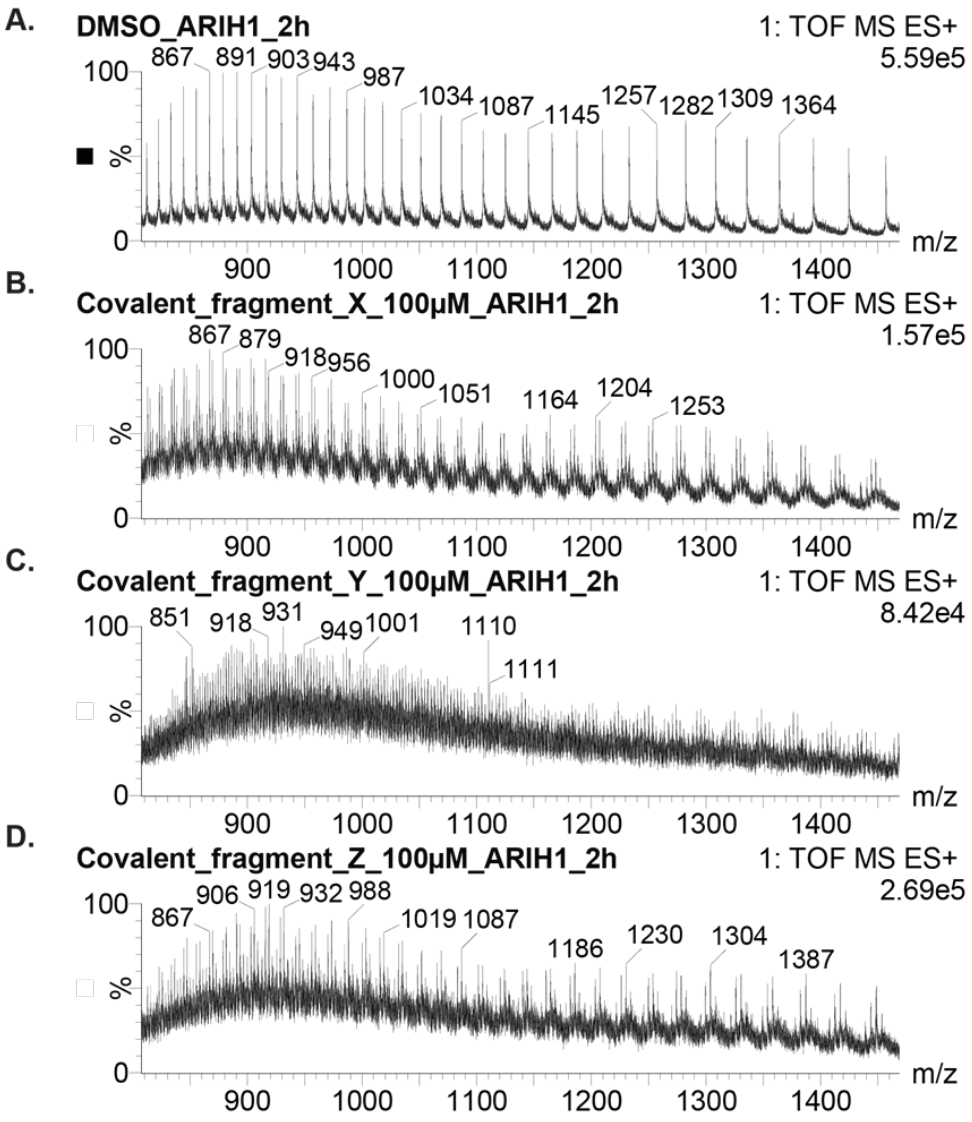

Supplementary Figure 18. MS adduct formation experiments of fragments X,Y and Z with ARIH1. Mass charge envelopes of ARIH1 (1 µM) incubated for 2 hours at room temperature with 100µM of covalent fragment or DMSO. Multiple labelling of at least 4 molecules was observed. A) DMSO B) Covalent fragment X C) Covalent fragment Y and D) Covalent fragment Z

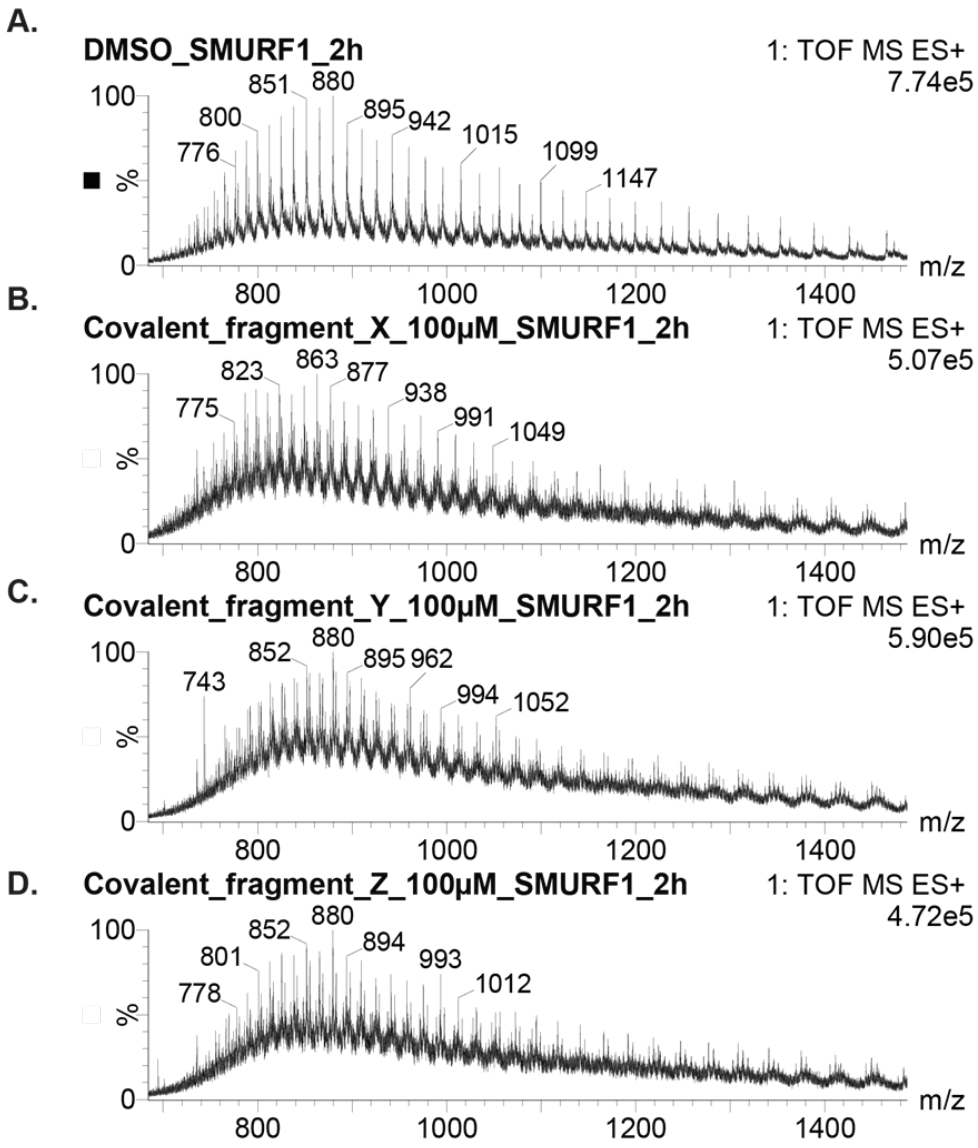

Supplementary Figure 19. MS adduct formation experiments of fragments X,Y and Z with SMURF1. Mass charge envelopes of SMURF1 (1 µM) incubated for 2 hours at room temperature with 100µM of covalent fragment or DMSO. Multiple labelling of at least 4 molecules was observed. A) DMSO B) Covalent fragment X C) Covalent fragment Y and D) Covalent fragment Z

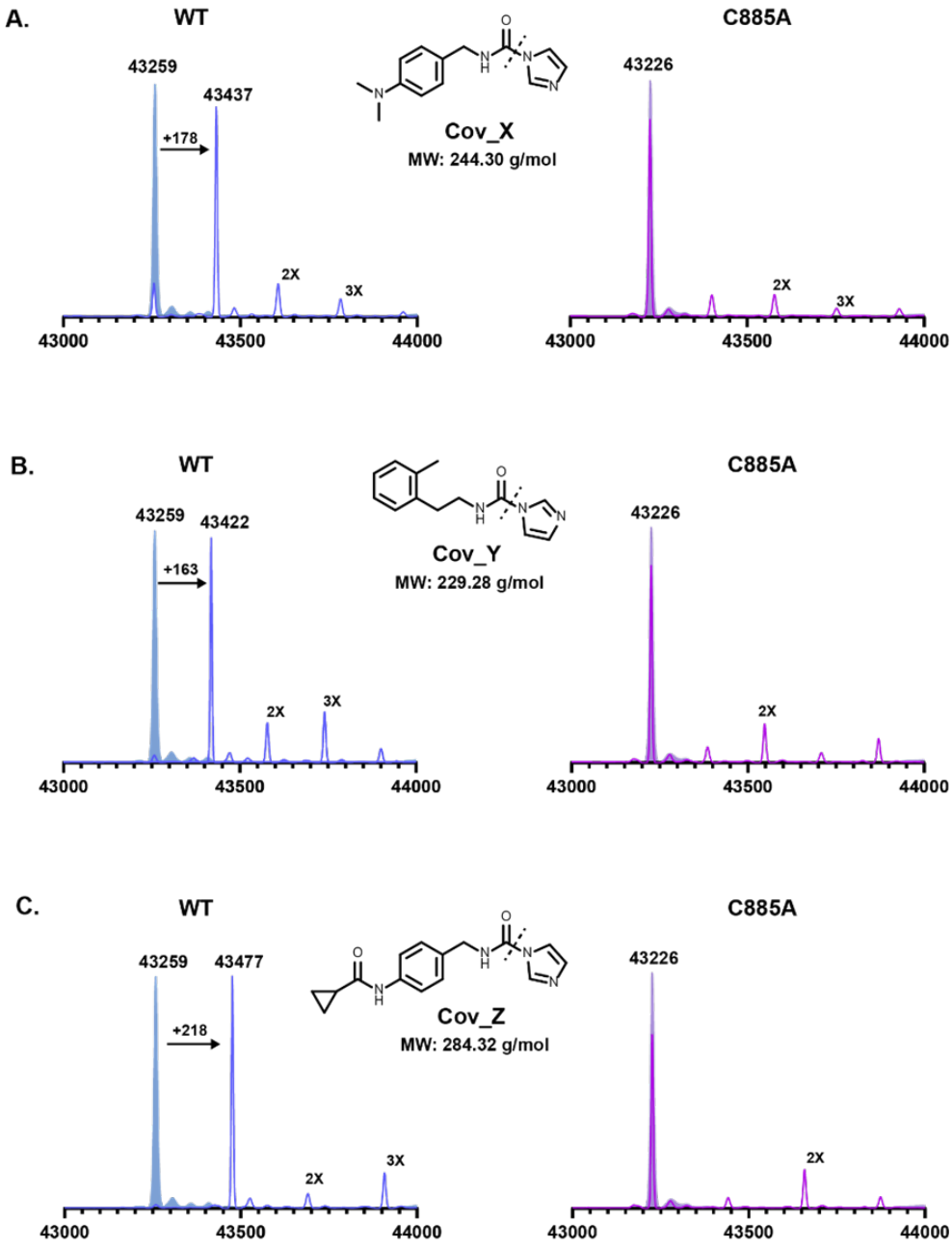

Supplementary Figure 20. MS adduct formation experiments of series of fragments X,Y and Z against HOIP and catalytically dead HOIP C885A. Deconvoluted mass of HOIP and HOIP C885A (1 µM) incubated for 24 hours at 4°C with 100 µM of covalent fragment.

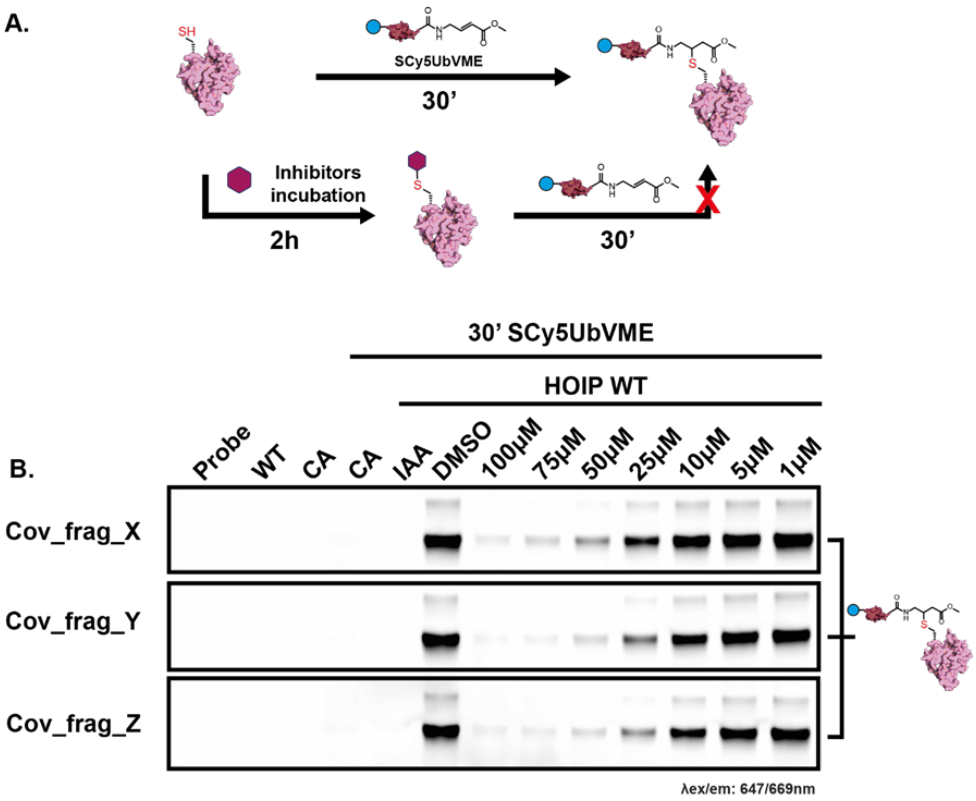

Supplementary Figure 21. HOIP competition experiment with SCy5UbVME of fragments X, Y and Z. A) Schematic of competition assay. The catalytic cysteine of HOIP will be labelled by the suicide probe SCy5UbVME unless any small molecule impedes its labelling (purple hexagon) by blocking the active site of HOIP. B.) Concentration range of covalent fragments X, Y and Z in competition with SCy5UbVME (10μM) to label HOIP (1μM). HOIP C885A mutant and IAA (1 mM) are taken along as negative controls.

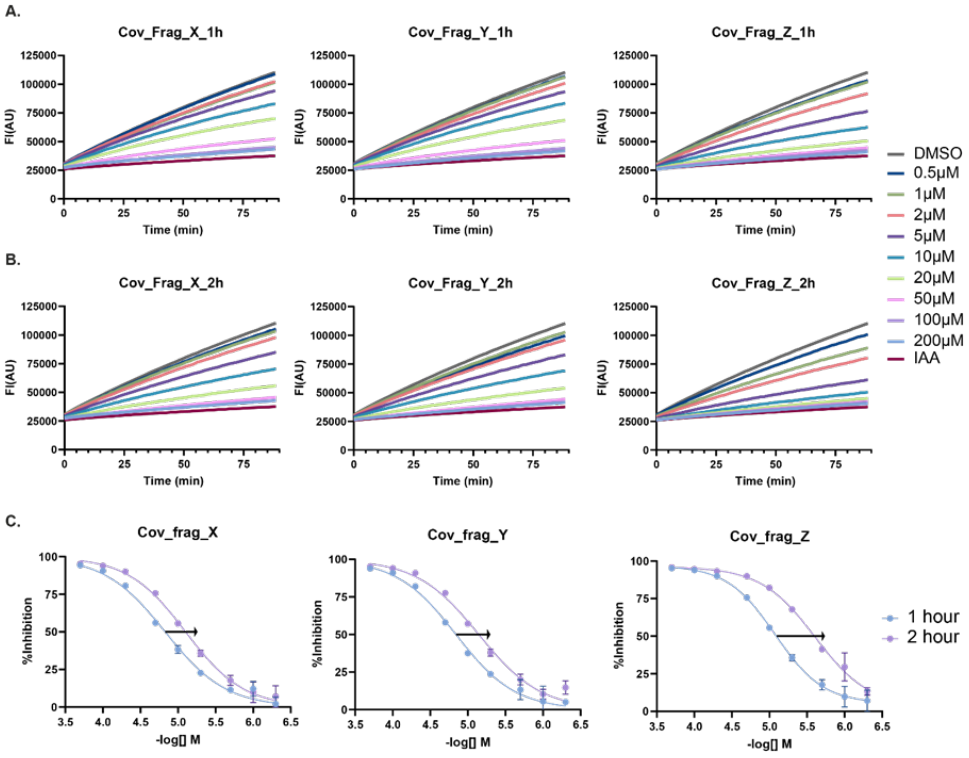

Supplementary Figure 22. HOIP IC50 determination of fragments X,Y and Z. A) HOIP-dependent fluorescence intensity increase over time measured with UbSRhodol of depicted cov_frag concentrations after 1h incubation and B) after 2h incubation of depicted cov_frag concentrations. C) IC50 determination of cov_frag. An incubation time-dependent IC50 shift (arrow 1h to 2h) is observed indicating a covalent mode of action. (IC50 : Cov_frag_X 1h: 14.84 µM, 2h: 7.92 µM; Cov_frag_Y 1h: 14.42 µM, 2h: 7.16 µM; Cov_frag_Z 1h: 7.92 µM, 2h: 2.57 µM).

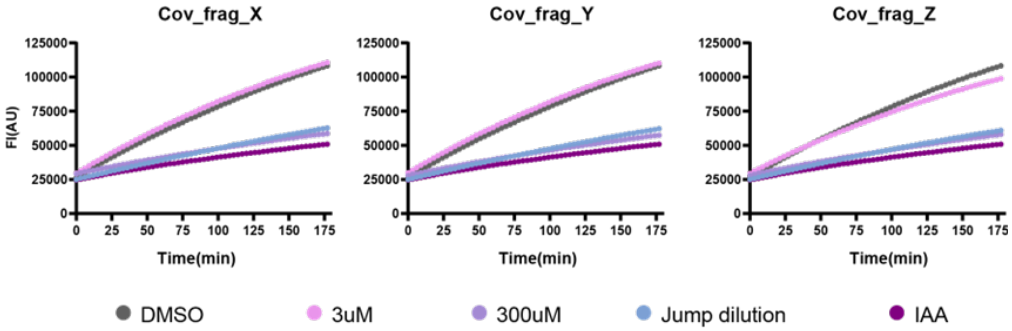

Supplementary Figure 23. Jump dilution assays of fragments X, Y and Z with HOIP. (100x dilution) Jump dilution curves overlaps with highest concentration inhibitor (300µM).

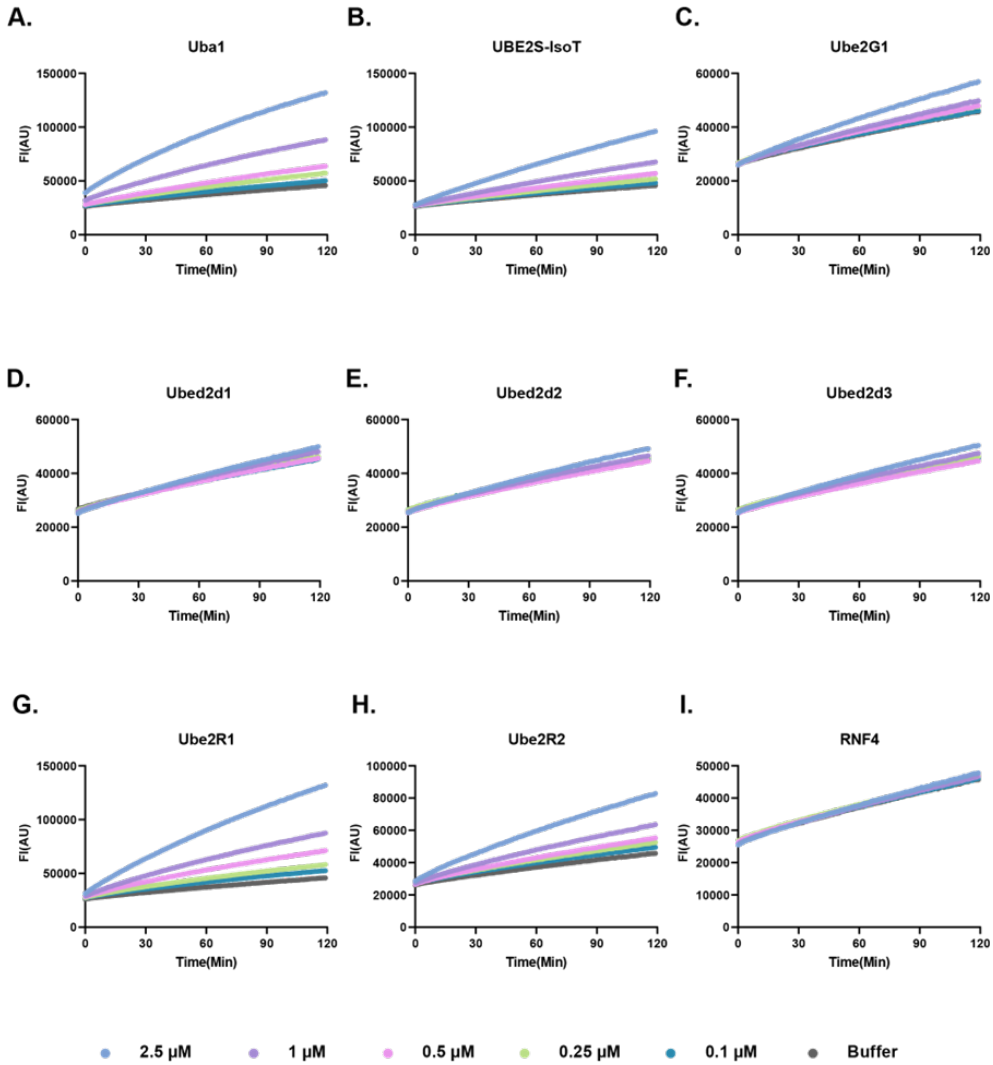

Supplementary Figure 24. UbSRhodol transthiolation profile of Ub cascade enzymes. A) Uba1 (E1) B) UBE2S-IsoT C) Ube2G1 D) Ubed2d1 E) Ubed2d2 F) Ubed2d3 G) Ube2R1 H) Ube2R2 I) RNF4 (RING E3).

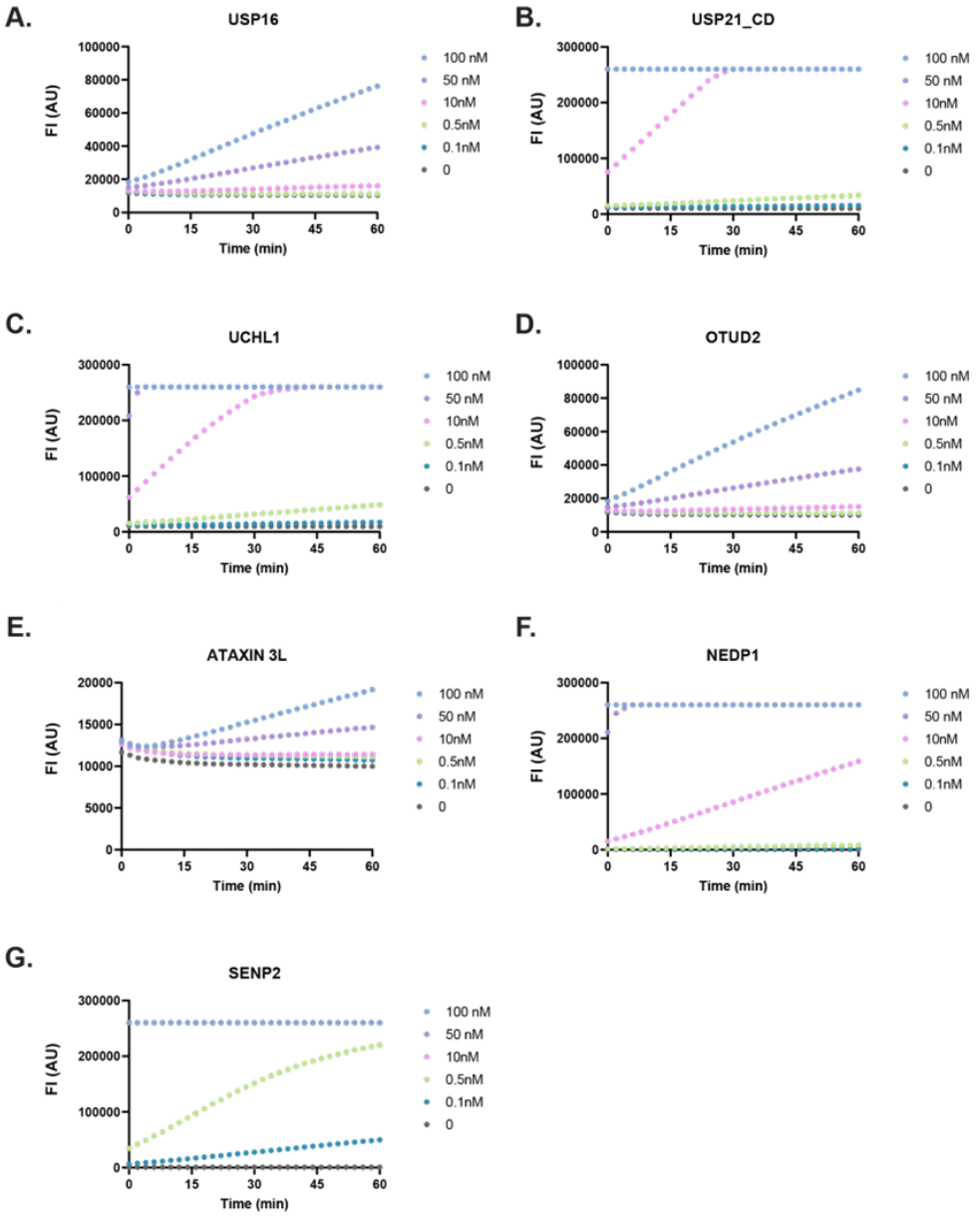

Supplementary Figure 25. Activity assay of protease panel by amide cleavage assay using fluorogenic substrates. Enzyme activity was checked by cleavage of a C' terminal amide releasing rhodamine morpholine of each cognate substrate (Ub, Nedd8 or SUMO2) A) USP16 B) USP21_CD C) UCHL1 D) OTUD2 E) ATAXIN 3L F) NEDP1 G) SENP2

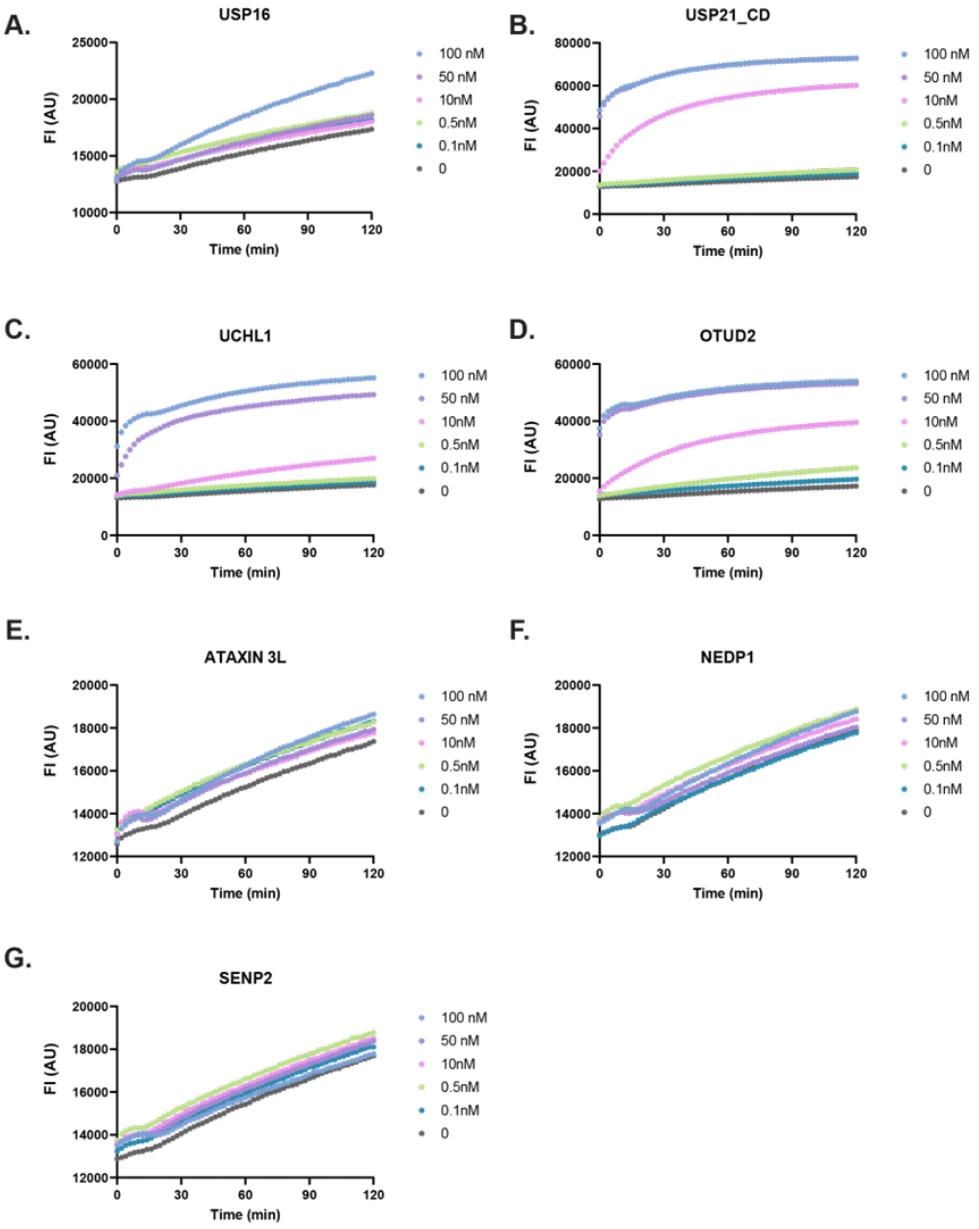

Supplementary Figure 26. UbSRhodol transthiolation profile of protease panel.
A) USP16 B) USP21_CD C) UCHL1 D) OTUD2 E) ATAXIN 3L F) NEDP1 G) SENP2

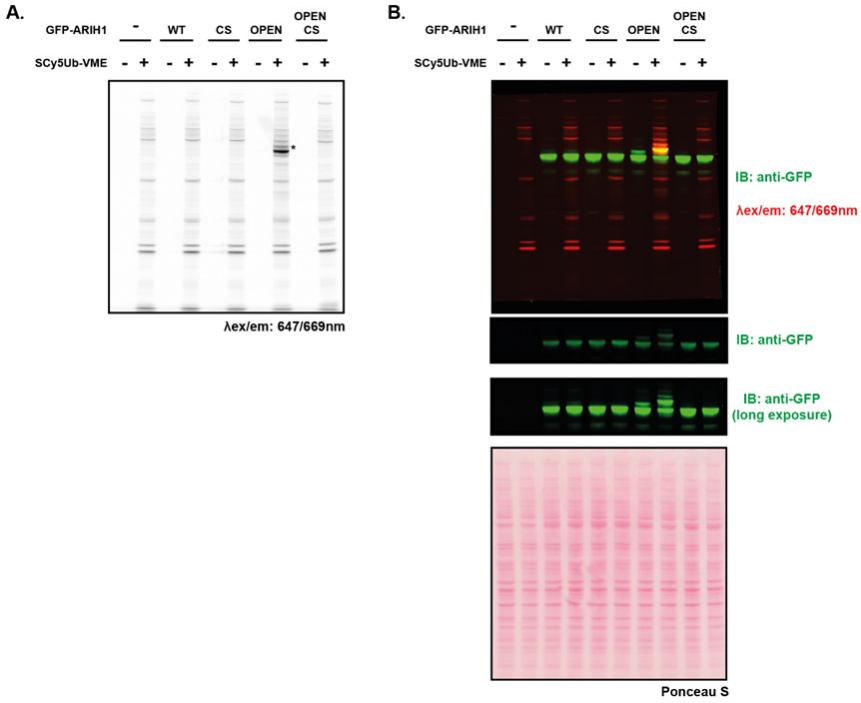

Supplementary Figure 27. SCyUbVME probe labelling in total cell lysates of HEK293T cells overexpressing GFP-ARIH1 WT, CS, OPEN and OPEN-CS. A) Fluorescent scan after SDS-PAGE at 647/669 nM. Activity of control HEK293T cells (-) or cells overexpressing the indicated versions of GFP-ARIH was tested with the suicide probe SCy5UbVME. Only GFP-ARIH1 OPEN showed activity versus the VME probe (*) B) Top: Anti-GFP immunoblot (IB) blot and fluorescent scan at the Cy5 wavelength shows labelling of only ARIH1 OPEN. Middle: Anti-GFP signal only. Bottom: Ponceau S staining of the blot validating equal loading.

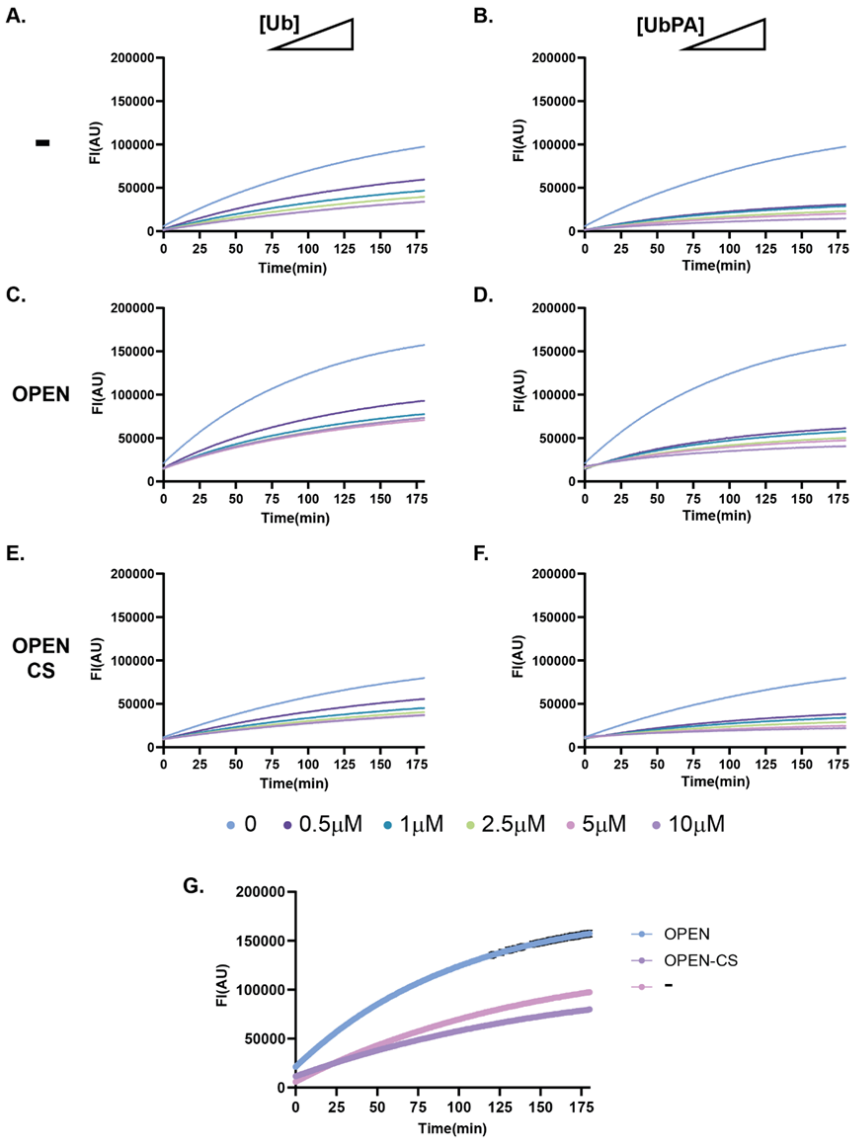

Supplementary Figure 28. UbSRhodol mediated transthiolation in cell lysates of control HEK293T cells (-) , HEK293T cells overexpressing GFP-ARIH1 OPEN, or GFP-ARIH1 OPEN-CS. Experiment performed in the absence or presence of different concentrations of bypass probe system competitors Ub and UbPA. A) Untransfected Ub titration B) Untransfected UbPA titration C) ARIH1OPEN Ub titration D) ARIH1OPEN UbPA titration E) ARIH1OPEN-CS Ub titration F) ARIH1OPEN-CS UbPA titration G) DMSO control (concentration 0 competitors) all cell lysates.

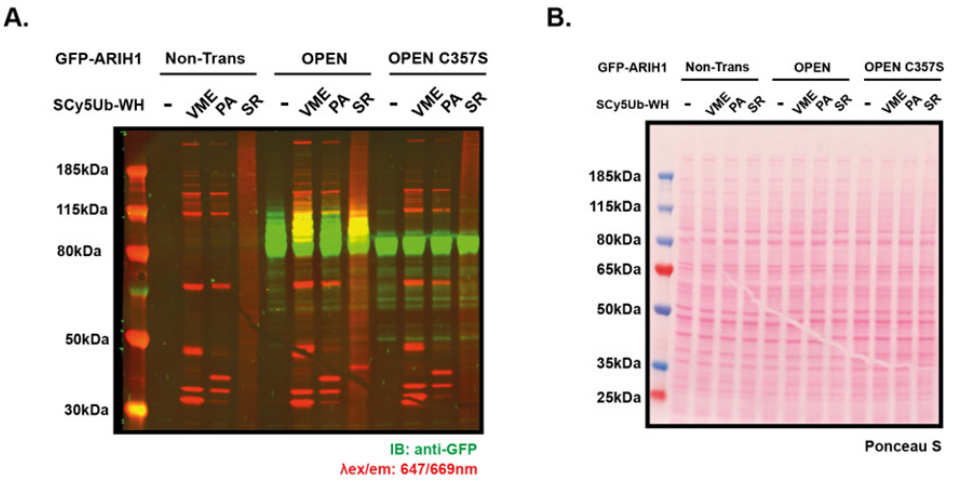

Supplementary Figure 29. Comparison of labelling profile for suicide ubiquitin-based probes (PA and VME) and bypass probe SCy5UbSR of overexpressed E3 ligase (GFP-ARIH1). A) Western blot high exposure B) Ponceau S staining.

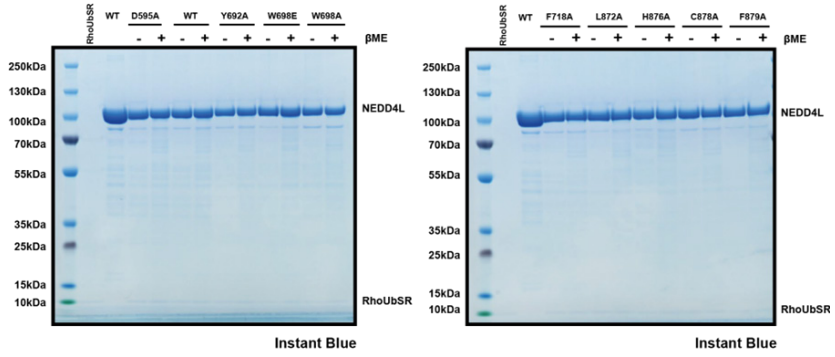

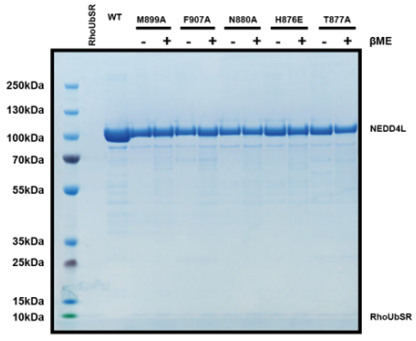

Supplementary Figure 30. Instant Blue staining of (ΔC2)NEDD4L mutants with bypass probe RhoUbSR. (corresponding to Supplementary Figure 8)

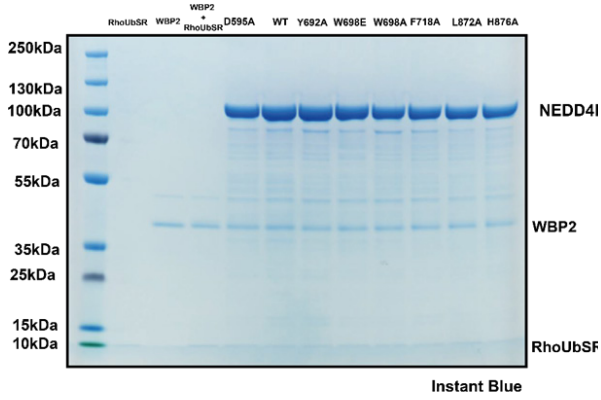

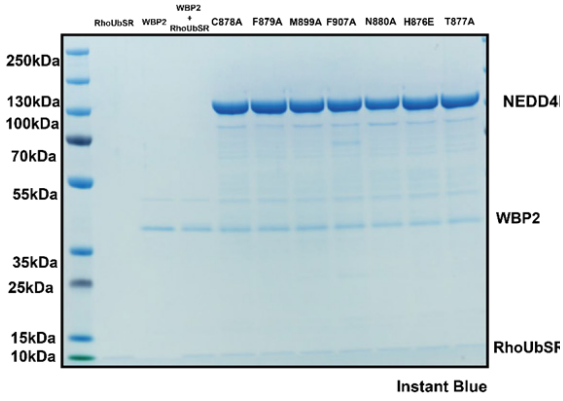

Supplementary Figure 31. Instant Blue staining of (ΔC2) NEDD4L mutant WBP2-ubiquitination with bypass probe RhoUbSR. (corresponding to Supplementary Figure 9)

Chemical synthesis

General. All commercially available reagents and solvents were used as purchased. Reported yields are given after the purification. Nuclear magnetic resonance (NMR) spectra were recorded on a Bruker Avance 300 (300 MHz for 1H, 75.00 MHz for 13C) using the residual solvent as internal standard (1H: 7.26 ppm for CDCl3, 2.50 ppm for DMSO-d6 and 3.31 ppm for MeOD. 13C: 77.16 ppm for CDCl3, 39.52 ppm for DMSO-d6 and 49.00 ppm for MeOD). Chemical shifts (δ) are given in ppm and coupling constants (J) are quoted in hertz (Hz). Resonances are described as s (singlet), d (doublet), t (triplet), q (quartet), p (quintet), b (broad) and m (multiplet) or combinations thereof. Thin Layer Chromatography (TLC) was performed using TLC plates from Merck (SiO2, Kieselgel 60 F254 neutral, on aluminum with fluorescence indicator) and compounds were visualized by UV, KMnO4 or ninhydrin staining. Flash Column Chromatography (FCC) purifications were performed using Grace Davisil Silica Gel (particle size 40–63 μm, pore diameter 60 Å) and the indicated eluent.

Synthesis of building block 1

Synthesis of (9H-fluoren-9-yl)methyl (R)-4-((tert-butyldisulfaneyl)methyl)-5-oxooxazolidine-3-carboxylate 3

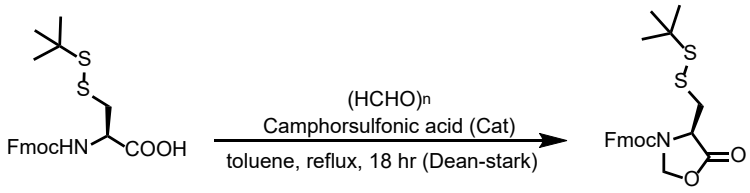

2 **3**

To a room temperature solution of Fmoc-Cys(StBu)-OH (2 g, 4.63 mmol, 1.0 eq.) in 46 mL toluene was added para-formaldehyde (0.715 mg, 23.8 mmol, 5.1 eq.) and camphorsulfonic acid (107 mg, 0.463 mmol, 0.1 eq.). The reaction was heated to reflux (oil-bath 100 C°) in a Dean-Stark apparatus and stirred for 18 hr. The reaction was concentrated to provide clear oil. After impregnation onto flash silica, the oxazolidinone 3 was purified via flash-chromatography (Silica gel; 0 – 50% Heptane:EtOAc) to provide 3 as a white amorphous solid. Yield: 94% (1.9 g). TLC (Rf): 0.42 (Heptane/EtOAc, 70:30).

HRMS (ESI-TOF) m/z: [M + H]+ calculated for C23H25NO4S2 444.1303; found 444.1309

1H NMR (300 MHz, CDCl3) δ 7.84 – 7.76 (m, 2H), 7.63 – 7.52 (m, 2H), 7.50 – 7.30 (m, 4H), 5.55 – 5.21 (br, m's, 2H), 4.68 – 4.55 (br, m's, 2H), 4.28 (t, J = 5.9 Hz, 1H), 4.07 (br, s, 1H), 3.56 (br, s, 0.5H), 3.23 (br, s, 0.5H), 3.01 (br, s, 0.5H), 2.72 (br, s, 0.5H), 1.30 (s, 9H).

13C NMR (75 MHz, CDCl3) δ 170.8, 152.1, 143.4, 141.3, 128.0, 127.2, 124.8, 120.1, 78.4, 67.9, 67.4, 55.4, 48.4, 47.0, 29.6.

Synthesis of N-(((9H-fluoren-9-yl)methoxy)carbonyl)-S-(tert-butylthio)-N-methyl-L-cysteine 4

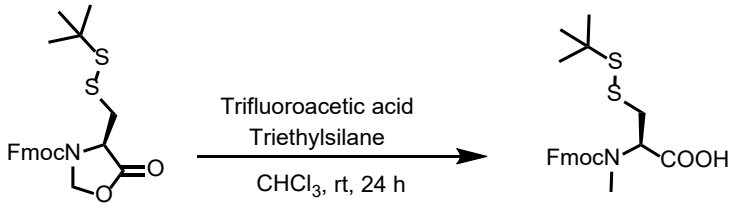

3 4

T

o a stirring solution of 3 (1.5 g, 3.38 mmol, 1.0 eq.) in 20 mL of CHCl3 under room temperature was added triethylsilane (TES, 5.4 mL, 45.1 mmol, 10.0 eq.) followed by the rapid addition of trifluoroacetic acid (TFA, 10.3 mL, 135.2 mmol, 40.0 eq.). The reaction was stirred at room temperature for 16 h and then concentrated. The oil was co-evaporated several times with dichloromethane to complete removal of TFA. The crude product was further purified through flash-chromatography (Silica gel; 0 – 5% CH2Cl2:MeOH) was provided 4 as white solid1. Yield: 92% (1.39 g). TLC (Rf): 0.30 (CH2Cl2/MeOH, 95:5).

HRMS (ESI-TOF) m/z: [M + H]+ calculated for C23H27NO4S2 446.1460; found 446.1462

1H NMR (300 MHz, CDCl3, mixture of rotamers) δ 10.91 (s, 1H), 7.84 – 7.75 (m, 3H), 7.69 – 7.61 (m, 3H), 7.44 (td, J = 7.4, 1.3 Hz, 3H), 7.40 – 7.30 (m, 4H), 4.80 (ddd, J = 18.3, 10.3, 4.5 Hz, 2H), 4.65 – 4.52 (m, 1H), 4.52 – 4.42 (m, 2H), 4.31 (dt, J = 15.2, 6.5 Hz, 2H), 3.41 (dd, J = 14.0, 4.5 Hz, 1H), 3.33 – 3.12 (m, 2H), 3.09 (s, 3H), 3.00 (s, 2H), 1.39 (s, 9H), 1.37 (s, 5H).

13C NMR (75 MHz, CDCl3, mixture of rotamers) δ 175.4, 175.3, 156.6, 156.1, 143.8, 143.8, 143.7, 143.6, 141.3, 141.2, 127.8, 127.6, 127.7, 127.63, 127.1, 127.0, 125.1, 125.0, 124.8, 124.7, 119.9, 68.0, 67.8, 59.8, 58.7, 48.2, 47.0, 39.1, 38.9, 33.8, 33.0, 29.8.

Synthesis of (9H-fluoren-9-yl)methyl (R)-(3-(tert-butyldisulfaneyl)-1-(methylamino)-1-oxopropan-2-yl)(methyl)carbamate 5

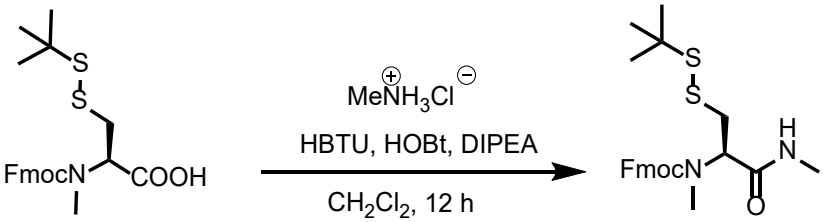

4 **5**

To an ice cooled solution of 4 (1.2 g, 2.7 mmol, 1.0 eq) in CH2Cl2 (25 mL), HBTU (1.1 g, 3.0 mmol, 1.1 eq.), HOBt (400 mg, 3.0 mg, 1.1 eq.), methylamine hydrochloride (272 mg, 4.05 mmol, 1.5 eq.) and DIPEA (1.2 mL, 6.75 mmol, 2.5 eq.) were added sequentially. The reaction mixture was allowed to warm to room temperature and stirred for 12 hr. The reaction mixture was then diluted with 30 mL of CH2Cl2 and washed with H2O. The aqueous layer was washed again with 20 mL CH2Cl2 and the combined organic layers were washed with 1N HCl (2 X 10 mL), saturated NaHCO3 (2 X 10 mL) and finally with water and brine. The organic layer collected dried with Na2SO4, filtered, evaporated to give a crude product, and purified by flash column chromatography (Silica gel; 0 – 100% Heptane:EtOAc) to give 5 as white solid. Yield: 97% (1.2 g). TLC (Rf): 0.42 (Heptane/EtOAc, 50:50)

HRMS (ESI-TOF) m/z: [M + H]+ calculated for C24H30N2O3S2 459.1776; found 459.1790

1H NMR (300 MHz, CDCl3, mixture of rotamers) δ 7.79 (d, J = 7.3 Hz, 3H), 7.62 (d, J = 7.4 Hz, 3H), 7.49 – 7.28 (m, 7H), 6.22 (d, J = 5.7 Hz, 1H), 4.90 (dd, J = 9.7, 5.8 Hz, 1H), 4.68 (d, J = 5.1 Hz, 1H), 4.62 – 4.40 (m, 2H), 4.40 – 4.22 (m, 2H), 3.31 (dd, J = 13.9, 5.8 Hz, 1H), 3.15 (dd, J = 13.9, 6.0 Hz, 1H), 3.01 (dd, J = 13.9, 9.8 Hz, 1H), 2.84 (s, 3H), 2.82 (s, 3H), 2.81 – 2.78 (m, 2H), 2.62 (d, J = 4.8 Hz, 1H), 1.35 (s, 9H), 1.31 (s, 5H).

13C NMR (75 MHz, CDCl3, mixture of rotamers) δ 170.0, 169.4, 157.1, 155.8, 143.9, 143.9, 143.6, 141.5, 141.4, 141.3, 141.1, 127.9, 127.8, 127.7, 127.4, 127.2, 127.1, 127.0, 125.0, 124.6, 120.1, 120.0, 120.0, 67.8, 67.1, 58.5, 58.3, 48.0, 48.0, 47.3, 47.2, 38.9, 38.6, 30.7, 29.9, 26.4, 26.3.

*Synthesis of (R)-3-(tert-butyldisulfaneyl)-N-methyl-2-(methylamino)propenamide **6**.*

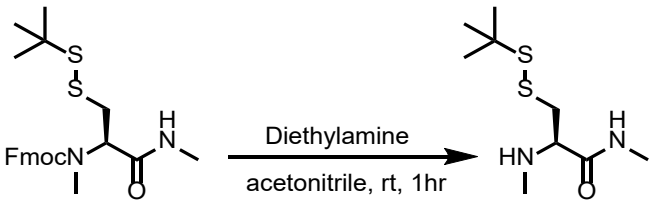

5 **6**

A solution of 5 (1 g, 2.18 mmol, 1.0 eq.) in 10 mL of acetonitrile was treated with diethylamine (5.64 mL, 54.5 mmol, 25 eq.) and the reaction mixture was stirred at room temperature under nitrogen for 1 hr (TLC analysis). The solvent and volatiles were removed by rotatory evaporation. The crude product

was then purified by column chromatography (Silica gel; 0 – 5% CH2Cl2:MeOH) to afford 6. Yield: 98% (505 g). TLC (Rf): 0.35 (CH2Cl2/MeOH, 97:3).

HRMS (ESI-TOF) m/z: [M + H]+ calculated for C9H20N2OS2 237.1095; found 237.1103

1H NMR (300 MHz, CDCl3) δ 7.32 (br, s, 1H), 3.23 – 3.05 (m, 2H), 2.73 (d, J = 5.0 Hz, 3H), 2.64 (dd, J = 13.1, 9.1 Hz, 1H), 2.30 (s, 3H), 1.94 (br, s, 1H), 1.24 (s, 9H).

13C NMR (75 MHz, CDCl3) δ 172.8, 63.4, 48.2, 43.1, 35.1, 29.8, 25.8.

*Synthesis of 3'-(dimethylamino)-6'-hydroxy-3H-spiro[isobenzofuran-1,9'-xanthen]-3-one **7***

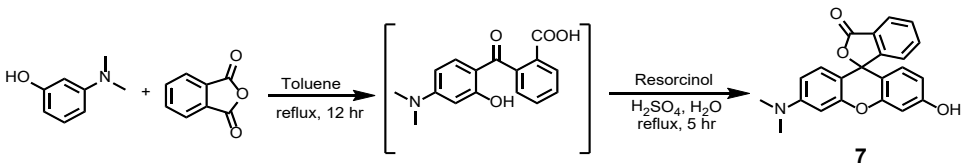

7

A mixture of m-dimethylaminophenol (6.0 g, 43.7 mmol) and phthalic anhydride (6.48 g, 43.7 mmol, 1.0 eq.) in 50 ml of toluene was refluxed for 6 h. The toluene was evaporated under vacuum and dried. To the crude intermediate 50 ml of 50% H2SO4, resorcinol (7.22 g, 65.6 mmol, 1.5 eq.) was added and the crude reaction mixture was heated to 120-130°C for 5 hr. Further, the reaction mixture was cooled to 0 °C and the pale orange precipitate obtained was filtered and washed with ice-cold water, dried and crystalized in chloroform. The bisulfate salt obtained was further treated with 5% Na2CO3 (50 mL) and filtered, the resulting solid product

was neutralized with 1N HCl, washed with water and crystalized with methanol to yield desired product 7 as pale brown solid which was used directly without further purification2. Yield: 60% (9.43 g). TLC (Rf): 0.35 (CH2Cl2/MeOH, 90:10).

HRMS (ESI-TOF) m/z: [M + H]+ calculated for C22H17NO4 360.1236; found 360.1244

1H NMR (300 MHz, DMSO-d6) δ 10.12 (s, br, 1H), 8.04 – 7.94 (m, 1H), 7.75 (dtd, J = 23.6, 7.4, 1.2 Hz, 2H), 7.24 (dt, J = 7.6, 1.0 Hz, 1H), 6.68 (t, J = 1.4 Hz, 1H), 6.53 (dd, J = 4.0, 1.5 Hz, 3H), 6.50 (d, J = 1.6 Hz, 2H), 2.94 (s, 6H).

13C NMR (75 MHz, DMSO) δ 169.2, 159.8, 152.9, 152.5, 152.3, 152.3, 135.9, 130.4, 129.4, 128.7, 126.8, 124.9, 124.4, 112.8, 110.3, 109.6, 106.1, 102.6, 98.4, 84.2, 40.2.

Synthesis of 3'-(dimethylamino)-3-oxo-3H-spiro[isobenzofuran-1,9'-xanthen]-6'-yl ((R)-3-(tert-butyldisulfaneyl)-1-(methylamino)-1-oxopropan-2-yl)(methyl)carbamate ***8***

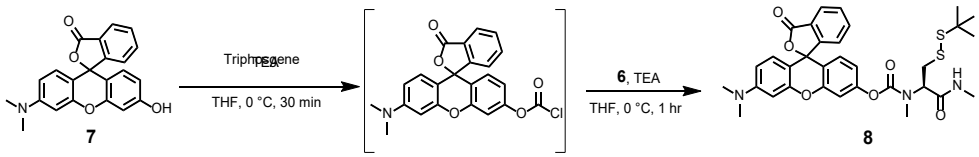

To a solution of triphosgene (165 mg, 0.55 mmol, 0.4 eq.) in dry THF (10 mL) at 0 °C, a solution of 7 (500 mg, 1.39 mmol, 1.0 eq.) with triethylamine (193 µL, 1.39 mmol, 1.0 eq.) in THF (10 mL) was added dropwise over 20 min. The reaction was stirred at room temperature for 30 min to generate the intermediate chloroformate. To this intermediate THF solution of Rhodol 7 (330 mg, 1.39 mmol, 1.0 eq.), followed by triethylamine (193 µL, 1.39 mmol, 1.0 eq.) were added. The reaction mixture was stirred at room temperature for another 1 hr at room temperature then the solvent was evaporated and the solid reaction mixture was directly loaded onto a flash chromatography and purified (Silica gel; 0 – 100% Heptane:EtOAc) to give 8 as pale yellow solid3. Yield: 48% (415 mg). TLC (Rf): 0.36 (Heptane/EtOAc, 20:80).

HRMS (ESI-TOF) m/z: [M + H]+ calculated for C32H35N3O6S2 622.2045; found 622.2051

1H NMR (300 MHz, CDCl3, mixture of rotamers) δ 7.93 (t, J = 1.2 Hz, 1H), 7.91 – 7.88 (m, 1H), 7.57 (t, J = 1.5 Hz, 0.3H), 7.54 (dt, J = 2.2, 1.3 Hz, 1.8H), 7.51 (t, J = 1.0 Hz, 1H), 7.09 (s, 0.5H), 7.08 – 7.01 (m, 4H), 6.78 – 6.70 (m, 2H), 6.70 – 6.67

(m, 1.6H), 6.65 (d, J = 3.7 Hz, 0.6H), 6.56 – 6.46 (m, 4H), 6.41 (d, J = 2.5 Hz, 2H), 6.35 (d, J = 2.5 Hz, 1H), 6.32 (d, J = 2.6 Hz, 1H), 5.01 – 4.89 (m, 0.8H), 4.82 (ddd, J = 9.8, 5.8, 1.4 Hz, 1H), 3.03 – 2.97 (m, 1H), 2.97 – 2.95 (m, 4H), 2.89 (s, 11H), 2.83 (s, 2H), 2.76 (d, J = 2.7 Hz, 1H), 2.70 (dd, J = 4.8, 3.4 Hz, 3H), 2.66 – 2.65 (m, 2H), 2.65 – 2.63 (m, 2H), 1.26 (s, 9H), 1.25 (s, 6H).

13C NMR (75 MHz, CDCl3, mixture of rotamers) δ 171.1, 169.6, 169.4, 169.4, 155.2, 154.3, 153.0, 153.0, 152.9, 152.4, 152.3, 152.3, 152.2, 152.1, 152.1, 152.0, 134.9, 129.7, 128.9, 128.9, 128.8, 128.6, 126.8, 124.9, 124.1, 124.0, 117.2, 117.1, 116.8, 116.7, 110.3, 110.3, 110.2, 109.2, 105.9, 98.5, 83.7, 59.6, 59.5, 48.3, 48.1, 40.2, 39.0, 38.7, 31.4, 31.4, 29.9, 29.9, 26.4, 26.3.

Synthesis of S-((2R)-2-((((3'-(dimethylamino)-3-oxo-3H-spiro[isobenzofuran-1,9'-xanthen]-6'-yl)oxy)-carbonyl)(methyl)amino)-3-(methylamino)-3-oxopropyl) 2-((tert-butoxycarbonyl)amino)ethanethioate ***9***

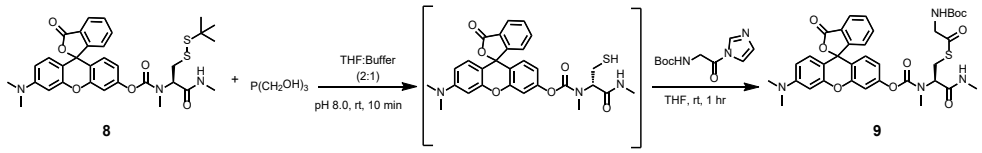

To a round bottom flask were charged Tris(3-hydroxypropyl)phosphine (THPP) (92 mg, 0.44 mmol, 1.10 eq.) and the basic buffer solution [tris-(hydroxymethyl)-aminomethane-CaCl2 based buffer; pH 8.00; 0.5 mL]. The reaction mixture was stirred at room temperature for about 5 min and then to this homogenous solution was charged the solution of 5 (250 mg, 0.4 mmol, 1.00 eq.) in 1 mL of THF. This homogeneous aqueous reaction mixture was stirred for 10 mins at room temperature (until TLC showed complete disappearance of the starting material). To this solution, a preformed tert-butyl (2-(1H-imidazol-1-yl)-2-oxoethyl)carbamate4 (4.5 g, 20 mmol, 50 eq.) was added and the reaction mixture was stirred for 1 hr at room temperature under nitrogen atmosphere. The crude reaction mixture extracted with ethyl acetate (2 X 20 mL). The organic layer collected dried with Na2SO4, filtered, evaporated to give a crude product, and purified by flash column chromatography (Silica gel; 0 – 100% Heptane:EtOAc) to give 9 as pale brown solid which is stored under inert atmosphere. Yield: 60% (165 mg). TLC (Rf): 0.41 (Heptane/EtOAc, 30:70).

HRMS (ESI-TOF) m/z: [M + H]+ calculated for C35H38N4O9S 691.2438; found 691.2471

1H NMR (300 MHz, CDCl3, mixture of rotamers) δ 8.02 (d, J = 1.7 Hz, 1H), 8.00

(d, J = 1.5 Hz, 1H), 7.73 – 7.56 (m, 4H), 7.14 (qd, J = 8.5, 7.6, 3.9 Hz, 4H), 6.87 – 6.70 (m, 4H), 6.62 (d, J = 8.8 Hz, 2H), 6.55 – 6.40 (m, 5H), 5.31 (s, 1H), 4.73 (dd, J = 9.2, 6.2 Hz, 2H), 4.07 – 3.95 (m, 3H), 3.52 (ddd, J = 21.1, 14.1, 6.1 Hz, 2H), 3.32 (dd, J = 14.1, 9.1 Hz, 2H), 3.04 (s, 4H), 2.99 (s, 11H), 2.94 (s, 2H), 2.83 (s, 3H), 2.76 (d, J = 4.6 Hz, 4H), 1.45 (s, 6H), 1.44 (s, 9H).

13C NMR (75 MHz, CDCl3, mixture of rotamers) δ 198.3, 198.0, 171.2, 169.5, 169.1, 168.9, 155.5, 155.19, 153.7, 152.8, 152.4, 152.3, 152.1, 152.0, 134.9, 129.7, 128.9, 128.9, 128.7, 126.8, 126.8, 125.0, 124.2, 124.0, 117.1, 117.1, 116.8, 110.2, 109.4, 106.3, 103.8, 98.7, 80.4, 66.9, 66.2, 60.4, 58.3, 50.3, 40.4, 31.8, 31.0, 28.3, 27.0, 26.4, 26.3.

Synthesis of 2-(((2R)-2-((((3'-(dimethylamino)-3-oxo-3H-spiro[isobenzofuran-1,9'-xanthen]-6'-yl)oxy)carbonyl)(methyl)amino)-3-(methylamino)-3-oxopropyl)thio)-2-oxoethan-1-aminium chloride ***BB-1.***

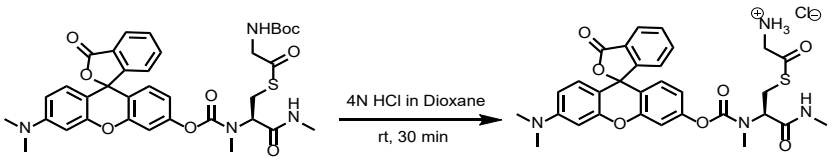

9 **BB-1**

A solution of HCl/dioxane (4 mL, 4M) in a 25-mL round-bottom flask equipped with a magnetic stir-bar was cooled by an ice-water bath under argon. Compound 10 (100 mg, 0.15 mmol) was added in one portion with stirring. The ice-bath was removed and the mixture was kept stirred. After 30 min, TLC indicated that the reaction was completed. The reaction mixture was condensed by rotary evaporation under high vacuum at room temperature. The residue was then washed with dry ethyl ether and collected by filtration. The solid product 1 obtained was further lyophilized and stored under argon atmosphere. Yield: 99% (89 mg). TLC (Rf): 0.5 (CH2Cl2:MeOH:AcOH, 80:18:2).

HRMS (ESI-TOF) m/z: [M + H]+ calculated for C30H30N4O7S 591.1913; found 591.1932

1H NMR (300 MHz, DMSO-d6) δ 8.75 1(br, m, 2H), 8.11 (d, J = 7.4 Hz, 2H), 7.81 (dt, J = 21.9, 7.3 Hz, 2H), 7.48 (d, J = 12.4 Hz, 1H), 7.37 (d, J = 7.4 Hz, 1H), 7.11 (t, J = 8.8 Hz, 1H), 6.99 (d, J = 9.4 Hz, 3H), 6.83 (d, J = 8.9 Hz, 1H), 4.63 (td, J = 11.4, 10.6, 5.6 Hz, 1H), 4.09 – 4.02 (br, m, 2H), 3.68 (dd, J = 8.6, 4.2 Hz, 1H), 3.62 (s, 3H), 3.47 (dd, J = 7.6, 3.8 Hz, 1H), 2.95 (s, 6H), 2.58 (d, J = 4.3 Hz, 3H).

13C NMR (75 MHz, DMSO) δ 193.4, 172.4, 168.3, 156.9, 156.3, 154.1, 153.2, 152.3, 151.5, 135.3, 133.6, 130.9, 130.3, 129.5, 128.5, 127.0, 124.4, 119.5, 117.4, 110.7, 110.6, 100.0, 72.5, 70.9, 53.2, 41.7, 32.3, 28.1, 26.3.

Synthesis of UbSRhodol.

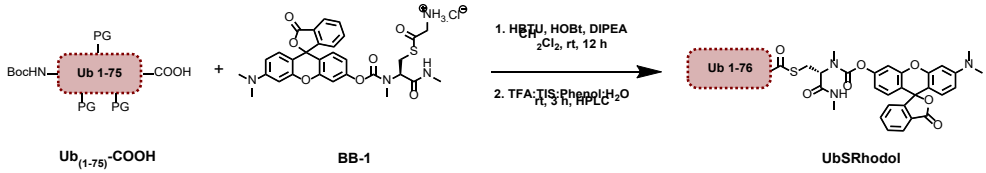

$Ub_{(1-75)}$-COOH BB-1 UbSRhodol

To a solution of protected Ub(1-75)-COOH (20 μmol)5 in DCM (20 mL), HBTU/HOBt (39.7mg/17mg, 100μmol, 5.eq.) and DIPEA (35μL, 200 μmol, 10 eq.) were added followed by BB-1 (15 mg, 24.5 μmol, 3.5 eq.). The reaction was allowed to stir overnight at room temperature and monitored by LC-MS. After confirmation of the desired product formation, the solvent was evaporated under vacuum and the crude peptide was further treated with TFA/TIS/H2O/Phenol (92.5/2.5/2.5/2.5, 5mL) for 3 hours at room temperature and then the peptide was further precipitated it in cold diethylether/pentane (1:1, 30 mL) and wash it several times with diethylether with centrifugation to yield crude solid material. Pure UbSRhodol was obtained by HPLC purification* and different fractions containing the desired product were pool together and lyophilized yielding 21mg of pure UbSRhodol (yield= 11.6%).

UbSRhodol: NleLIKVKTLTGKEIEIDIEPTDKVERIKERVEEKEGIPPQQQRLIYSG KQNleNDEKTAADYKILGGSVLHLVLALRGG~SRhodol (MWexp: 9062; MWobs: 9063 [UbSRhodol-H+)

Please note: Nle stands for Nor-Leucine, well known methionine isostere.

*(HPLC purification: samples were run on a Waters 2535 HPLC equipped with a Waters 2489 UV/Vis detector, Waters fraction collector III and Waters XBridge prep C18 OBD (30 mm × 150 mm, 5 μm). UbSRhodol crude mixture was dissolved in DMSO containing 2.5% TFA (5% total volume) and added to a vessel containing 0.1% formic acid in MQ, to a concentration of 5mg/ml.

Flowrate = 37.5 mL min−1. Eluents: A = H2O, B = CH3CN and D = 1% TFA in H2O. Gradient: 0–5 min: 90% A, 5% B, 5% C; 5–7 min: 90% A → 75% A, 5% B → 20% B, 5% C; 7–23 min: 75% A → 50% A, 20% B → 45% B, 5% C; 23–23.5 min: 50% A → 0% A, 45% B → 95% B, 5% C; 23.5–26.5 min: 0% A, 95% B, 5% C; 26.5–26.6 min: 0% A → 90% A, 95% B → 5% B, 5% C; 26.6–30 min: 90% A, 5% B, 5% C.

Synthesis bypass probes Rho/Cy5UbSR for gel based readout.

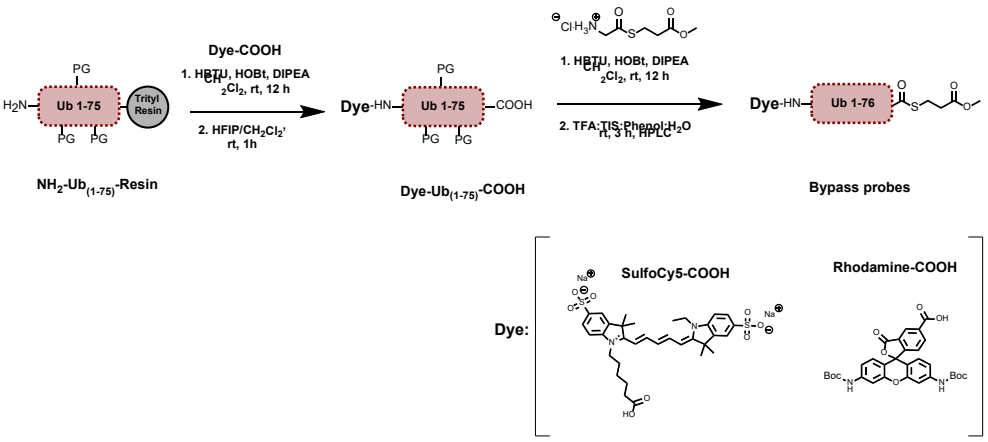

The N-terminus of Ub(1-75) was modified on resin by Rhodamine or SulfoCy5. To a solution of protected Ub(1-75)-COOH (20 µmol) in DCM (20 mL), HBTU/HOBt (39.7mg/17mg, 100µmol, 5.eq.) and DIPEA (35µL, 200 µmol, 10 eq.) were added followed by Rhodamine-COOH or SulfoCy5-COOH (3 equiv), respectively. Reactions were allowed to stir at room temperature overnight. Finally, the resin was washed with NMP, DCM and Et2O and the C-terminus modified as following. The resin was treated with 5 mL of DCM/HFIP (4:1 v/v) for 30 min and filtered. The resin was rinsed with DCM (3x5 mL) and the combined filtrates were concentrated. The partially protected peptide residue (1 equiv) was redissolved in DCM(1umol/ml) and HBTU/HOBt (39.7mg/17mg, 100µmol, 5.eq.) and DIPEA (35µL, 200 µmol, 10 eq.) were added followed by methyl methyl 3-(glycylthio)propanoate (42.4 mg,10 equiv). The reaction mixture was stirred overnight at room temperature. The solvent was removed in vacuo and the residue treated with TFA/H2O/phenol/iPr3SiH (90/5/2.5/2.5 v/v/v/v) for 3 h followed by precipitation with cold Et2O/pentane (1:1 v/v). Purification by HPLC following UbSRhodol protocol gave RhoUb(1-75)SR as a pink powder (27mg, yield= 15%) or Cy5Ub(1-75)SR as a blue powder (18mg, yield= 10%).

RhoUbSR: Rhodamine_NleLIKVKTLTGKEIEIDIEPTDKVERIKERVEEKEGIP-PQQQRLIYSGKQNleNDEKTAADYKILGGSVLHLVLALRGG~SR (MWexp: 9004; MWobs: 9005 [RhoUbSR-H+)

SCy5UbSR: SulfoCy5_NleLIKVKTLTGKEIEIDIEPTDKVERIKERVEEKEGIP-PQQQRLIYSGKQNleNDEKTAADYKILGGSVLHLVLALRGG~SR (MWexp: 9286; MWobs: 9287 [SCy5UbSR-H+)

Please note: Nle stands for Nor-Leucine, and R for methylmalonate.

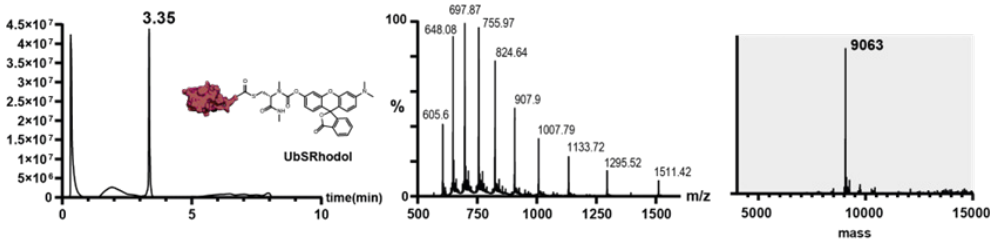

Supplementary Figure 32. LC-MS characterization of UbSRhodol. UV/Vis Chromatogram, charge/mass envelope and deconvoluted mass

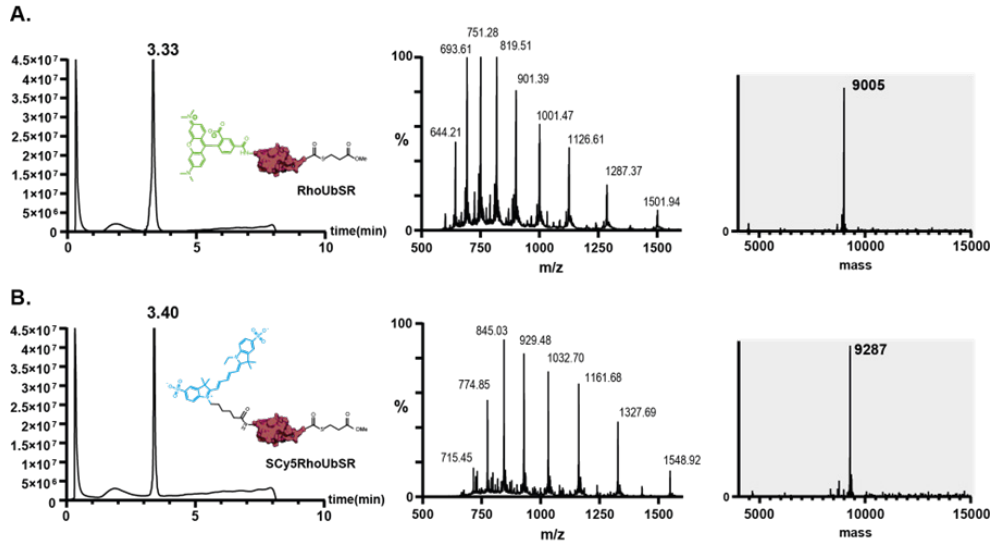

Supplementary Figure 33. LC-MS characterization of bypass probes: A) RhoUbSR and B) SCy5UbSRUbSRhodol. UV/Vis Chromatogram, charge/mass envelope and deconvoluted mass .

Materials and Methods

Expression of proteins

UBR5 HECT DOMAIN

Plasmids

Recombinant DNA: pRSF 6xHis-UBR5_HECT (2499-2799) and pRSF 6xHis-UBR5_HECT C2768A (2499-2799) were used.

Expression and purification

The C-terminal fraction of the wildtype HECT-domain of UBR5 (2499-2799) or the catalytic cysteine mutant C2768A respectively, were expressed with a N-terminal 6xHis-tag using BL21-CodonPlus (DE3)-RIL cells in Terrific Broth medium. Protein expression was induced with 0.6 mM IPTG with subsequent shaking overnight at 18°C. The cell pellet was resuspended in lysis buffer consisting of 25 mM Tris-HCl, pH 8.0, 200 mM NaCl, 5 mM β-Mercaptoethanole, 2.5 mM PMSF, and protease inhibitor. Lysis was performed using sonication followed by pre-clearance of the lysate using centrifugation for 40 min at 51.000 x g at 4°C. The protein was isolated by performing a gravity flow affinity purification with His-Select Nickel Affinity gel (SIGMA), subsequent anion exchange chromatography and lastly, size exclusion chromatography with the final buffer consisting of 25 mM HEPES. pH 7.5, 150 mM NaCl, 1 mM DTT. The protein was aliquoted and flash-frozen in liquid nitrogen until usage.

HERC proteins

Expression and purification

His tagged constructs of HERC1 and HERC3 HECT domains were expressed in E. coli BL21 RIL cells. Briefly, the cells were induced with 0.4 mM IPTG at 0.8 O.D. and were allowed to grow overnight at 18 degrees. After 16 hours of induction cells were harvested and resuspended in 50 mM Tris-HCl pH-7.5, 500 mM NaCl, 25 mM Imidazole and 5% glycerol (lysis buffer). The cells were lysed with sonication and insoluble fraction was pelleted down at 15000 rpm. Soluble fraction was allowed to bind to Talon beads which were preequilibrated with the lysis buffer. After binding, the beads were washed with the lysis buffer and the protein was eluted with 50 mM Tris-HCl pH-7.5, 500 mM NaCl, 250 mM Imidazole and 5% glycerol. The eluted protein was concentrated down to 1 ml and applied to Superdex 16/600 75 pg size exclusion column which was preequilibrated with 25 mM Tris-HCl pH-7.5, 200 mM NaCl and 1 mM TCEP. Following gel filtration, the protein was concentrated with the help of Centricon with 30 kDa molecular weight cut-off filter. After concentration the protein was flash frozen in liquid nitrogen and stored at -80 degrees.

NEDD4L

Plasmids and cloning

All NEDD4L constructs are listed in Supplementary Table S1. NEDD4L WT (full-length and ΔC2) and 14 HECT domain mutants (ΔC2) were cloned into pGEX-4T1 bearing an N-terminal GST-tag followed by a Tobacco Etch Virus (TEV) cleavage site. All NEDD4L constructs were derived from NEDD4L isoform 2. Full-length WBP2 was cloned into pBTD15 containing an N-terminal His-MBP-tag followed by a TEV cleavage site. All constructs were cloned using Gibson assembly.

Expression and purification

All proteins were expressed in E. coli BL21 (DE3) Gold. Cells were grown to an OD600 of 0.8 and expression was induced with 0.2 mM IPTG. After induction, the protein was expressed at 18°C overnight. E. coli cells were harvested and the cell pellet was resuspended in 1x PBS supplemented with 2.5 mM PMSF, 5 mM DTT and 0.001 mg/ml benzonase. The cells were lysed by sonication and insoluble material was separated by centrifugation at 50,000 x g for 30 min. For NEDD4L proteins, the supernatant was incubated with Glutathione Sepharose beads (Cytiva) for 1 h. After extensive washing of the beads with buffer A (30 mM Tris pH 7.5, 200 mM NaCl, 5 mM DTT) the bound protein was eluted by incubating the beads with buffer A supplemented with 0.02 mg/ml TEV protease at 4°C overnight. The next day, the protein was concentrated using an Amicon 30 kDa MWCO centrifugal filter and loaded on a Superdex 200 10/300 Increase SEC column (GE Healthcare) with buffer B (20 mM HEPES pH 7.5, 100 mM NaCl, 1 mM TCEP) as a final polishing step. Peak fractions containing NEDD4L protein were pooled, concentrated to 70-150 µM, shock frozen in liquid nitrogen and stored at -80°C. The WBP2 containing supernatant was incubated with His-Select Nickel Affinity gel (Sigma-Aldrich) at 4°C for 30 min. After washing the beads with buffer A, the protein was eluted with buffer A supplemented with 250 mM imidazole. Protein containing fractions were concentrated and loaded on a Superdex 200 10/300 Increase SEC column (GE Healthcare) with buffer B. Peak fractions of WBP2 were pooled, concentrated to 290 µM, shock frozen in liquid nitrogen and stored at -80°C.

Supplementary Table S1

Construct	mutation	residue function
GST-TEV-NEDD4L-ΔC2-D595A	D595A	acidic loop
GST-TEV-NEDD4L-ΔC2	WT	
GST-TEV-NEDD4L-ΔC2-Y692A	Y692A	E2 binding site
GST-TEV-NEDD4L-ΔC2-W698A	W698E	E2 binding site
GST-TEV-NEDD4L-ΔC2-W698E	W698A	E2 binding site
GST-TEV-NEDD4L-ΔC2-F718A	F718A	N-lobe/ubiquitin
GST-TEV-NEDD4L-ΔC2-L827A	L872A	C-lobe/ubiquitin
GST-TEV-NEDD4L-ΔC2-H876A	H876A	cat. loop
GST-TEV-NEDD4L-ΔC2-C878A	C878A	cat. Cys
GST-TEV-NEDD4L-ΔC2-F879A	F879A	cat. loop
GST-TEV-NEDD4L-ΔC2-M899A	M899A	C-lobe/ubiquitin
GST-TEV-NEDD4L-ΔC2-F907A	F907A	-4 F mutant
GST-TEV-NEDD4L-ΔC2-N880A	N880A	cat. loop
GST-TEV-NEDD4L-ΔC2-H876E	H876E	cat. loop
GST-TEV-NEDD4L-ΔC2-T877A	T877A	cat. loop
GST-TEV-NEDD4L	Full-length	
His-MBP-TEV-WBP2	model substrate – WBP2	

SMURF1

Plasmids and cloning

The expression plasmid (pET28a-LIC_SMURF1-W-HECT) for the W-HECT domain of SMURF1 (UNIPROT: Q9HCE7; a.a. 306-757) was a kind gift from Masoud Vedadi from the Structural Genomics Consortium Toronto. Catalytic point mutation (C725A) was performed using IVA cloning6 with primers listed in Supplementary table S2. All clones were sequence verified

Expression and purification

Wild-type and mutant SMURF1 plasmids were transformed into E. coli BL21(DE3) and

grown in LB supplemented with 50 µg L-1 kanamycin. Cultures were grown at 37°C until OD600 reached 1.0, upon which the temperature was lowered to 18°C and overnight expression was induced using 0.4 mM isopropyl-d-1-thiogalactopyranoside (IPTG). Next day, cells were pelleted by centrifugation for 20 min at 4000 G and subsequently resuspended in buffer A (20 mM Tris pH8.0, 300 mM NaCl and 20 mM Imidazole).

All purification steps were carried out at 4°C. Cells of 2L expression culture were lysed using sonification and debris was spun down for 40 min at 30000 G. The supernatant was applied to 2 mL of nickel-charged NTA beads and incubated for 30 min. Beads were washed extensively using buffer A, before elution using buffer B (buffer A with 200 mM Imidazole). The eluate was concentrated and applied to an equilibrated (in 20 mM Tris pH8.0, 150 mM NaCl, 1mM DTT) S75 16/60 (GE Healthcare) size-exclusion column using a Bio-rad NGC. Fractions were analysed using SDS-PAGE and SMURF1-containing ones were pooled and concentrated before aliquoting and flash freezing in liquid nitrogen for storage at -80°C.

Supplementary table S2

SMURF1-C725A-fw

CCATACCgcCTTTAACCGGATCGACATTCCACCATATGAGTCC

SMURF1-C725A-rv

GGTTAAAGgcGGTATGGGCCTTCGGAAGGTTGTCTGTG

RBR proteins ARIH1, ARIH2 and HOIP

Plasmids and cloning

Coding sequences for all proteins are of human origin, were obtained from Max Planck Institute of Biochemistry core facility cDNA libraries and cloned into expression vectors via Gibson assembly cloning. Mutant versions of ARIH1, ARIH2 and HOIP were generated using Quikchange system (Agilent).

Expression and purification

Neddylated versions of CUL1-RBX1 and CUL5-RBX2 were obtained as previously described7,8. ARIH1, ARIH2 and mutant versions were expressed as GST-TEV fusion proteins in E. coli Rosetta 2 (DE3) and induced with IPTG (0.1 mM) at an OD of 0.6-0.8 in Terrific Broth medium containing 0.1 mM ZnCl2. After induction, temperature was reduced to 18˚C and expression continued overnight. Cell lysis was performed by sonication and followed by centrifugation. Fusion protein-containing supernatant was subjected to incubation with Glutathione Sepharose® beads, washed several times with wash buffer (50 mM Tris pH 7.5, 200 mM NaCl and 1 mM DTT) and incubated with TEV protease overnight on beads. Target protein was eluted with two bead volumes of wash buffer and anion exchange and size-exclusion

chromatography (25 mM HEPES pH 7.5, 150 mM NaCl, 0.5 mM TCEP) were carried out. HOIP (696-1072) and its C885A mutant were expressed as His-SUMO fusion protein in E. coli Rosetta 2 (DE3) and cells consequently treated as for ARIH1/2. After incubation with Ni-NTA beads, beads were washed with five bead volumes of wash buffer (50mM Tris pH 8, 200 mM NaCl, 1 mM ß-Mercaptoethanol) and eluted with another five volumes of elution buffer (50 mM Tris pH 8, 200 mM NaCl, 300 mM Imidazole and 1 mM ß-Mercaptoethanol). Fusion protein was digested with SENP2 protease overnight and anion exchange and size-exclusion chromatography (25 mM HEPES pH 7.5, 150 mM NaCl, 0.5 mM TCEP) were performed the following day.

GST-TEV-RNF14 and STREP-3C-RNF216 were expressed in Trichoplusia Ni Hi-5™ insect cells in 0.1 mM ZnSO4-containing medium. After lysis, fusion proteins were subjected to either Glutathione Sepharose® or Streptavidin Sepharose® beads, washed several times with wash buffer and eluted with either Glutathione or Desthiobiotin-containing elution buffer. Overnight cleavage was performed with either TEV or 3C protease and target proteins further purified anion exchange and size-exclusion chromatography.

E3 activity measurements with UbSRhodol (384well plate) and product formation.

Assays were performed in non-binding-surface, flat-bottom, low-flange, black 384-well plates (Corning3820) at room temperature in a buffer containing 50 mM HEPES, 150 mM NaCl at pH 7.5, 1.0 mM TCEP, 0.5 mg/mL 3-[(3-cholamidopropyl) dimethylammonio]propanesulfonic acid (CHAPS) in quadruplets. UbSRhodol solution was prepared by pipetting gently 1.25µl of a 2mM DMSO (2.5%TFA) stock into 1mL of buffer to yield a 1.25µM solution (2.5X). Serial dilutions of proteins (2.5 µM/1µM/0.5µM (ST conditions) and 250/100/50/25/0 nM (MT conditions)) were prepared as a 1.66X stock and 9µL were added to the assay plate. Then, 6 µL of UbSRhodol (2.5X, 500nM final concentration or 1µM in the case of HOIP) were dispensed on a Biotek MultiFlowFX dispenser, plate was centrifuged (1000 rpm, 1min) and the E3-mediated release of Rhodol was measured at the emission wavelength of 520 nm (±10 nm) after excitation at 485 nm (±10 nm) in a Pherastar plate reader (BMG LABTECH GmbH, Germany) in continuous mode for several timepoints. Gain (5 /10%) was set at the probe only well.

Product formation assays (HOIP and SMURF1)

The assays were conducted in a buffer containing 50 mM HEPES, 150 mM NaCl at pH 7.5 and 1.0 mM TCEP. RhoUbSR/SCy5UbSR solution were prepared by pipetting gently the appropriate volume of a 2mM DMSO (2.5%TFA) stock

into the appropriate volume to yield a 2.5X solution of probe: 1.25μM for SMURF1 (500nM total concentration) or 2.5μM solution for HOIP (combination of 1.25μM UbSRhodol and 1.25μM SCy5UbSR) (1μM total concentration)

45μl of E3 stocks (see experimental 3. E3 activity measurements (1.66X, E3)) were combined with 30uL RhoUbSR/SCy5UbSR at a final concentration of 500nM or 1μM for HOIP(2.5X). Reactions were stopped at the selected timepoint by adding loading buffer with or without 5% βME to assess thioester formation. Samples containing 5% βME were boiled at 95°C for 5 minutes, cool down and centrifuge. Samples were resolved by SDS-PAGE using a 4–12% Bis-Tris gel (Invitrogen, NuPAGE) with MES or MOPS SDS running buffer (Novex, NuPAGE) for 45 min at 190 V. Gels were scanned for fluorescence on a GE Typhoon FLA 9500 using a green channel (λex/em 473/530 nm) and a red channel (λex/em 647/669 nm), followed by staining with InstantBlue Coomassie protein stain (Expedeon), after which the gel was scanned on a GE Amersham Imager 600.

NEDD4L-dependent transthiolation measurements and product formation

The assay was conducted in a buffer containing 50 mM HEPES, 150 mM NaCl at pH 7.5 and 1.0 mM TCEP , 0.5 mg/mL 3-[(3-cholamidopropyl)dimethylammonio] propanesulfonic acid (CHAPS) in quadruplets. UbSRhodol solution was prepared by pipetting gently the appropriate volume of a 2mM DMSO(2.5%TFA) stock into the appropriate volume to yield a 1.25μM solution (2.5X). Different dilutions of NEDD4L (2.5μM and 1μM) and NEDD4L(2.5μM and 1μM) containing 500nM of WBP2 were prepared as a 1.66X stock and 9μL were added to the assay plate. Then, 6 μL of UbSRhodol (2.5X, 500nM final concentration) were dispensed on a Biotek MultiFlowFX dispenser, plate was centrifuged (1000 rpm, 1min) and the E3-mediated release of Rhodol was measured at the emission wavelength of 520 nm (±10 nm) after excitation at 485 nm (±10 nm) in a Pherastar plate reader (BMG LABTECH GmbH, Germany) in continuous mode for several timepoints. Gain (5 /10%) was set at the probe only well. 100 minutes timepoint was selected for all the different mutants to quantify their percentage of activity by standardization between the WT (100%) and C878A(0%) and plotted in GraphPad Prism 9.3.1.

Using the E3 1.66X stocks (2.5μM) (see experimental 3. E3 activity measurements) the product formation assays were performed (Transthiolation and Cognate substrate ubiquitination model). 45μL of E3 were combined with 30μL of RhoUbSR (2.5X, 500nM final concentration). All the samples were incubated for 100 minutes at room temperature and stopped by adding loading buffer with or without 5% βME to asses thioester formation. Samples containing 5% βME were boiled at 95°C for 5 minutes, cool down and centrifuge. Samples were resolved by SDS-PAGE using a 4–12% Bis-Tris gel (Invitrogen, NuPAGE) with MOPS SDS running buffer (Novex, NuPAGE) for 45 min at 190 V. Gels were scanned for fluorescence on a GE Typhoon FLA 9500 using the green channel (λex/

em 473/530 nm), followed by staining with InstantBlue Coomassie protein stain (Expedeon), after which the gel was scanned on a GE Amersham Imager 600.

For native ubiquitination assays of WBP2 pulse-chase assays were performed to observe the efficiency of ubiquitin to NEDD4L and subsequently to WBP2 for different NEDD4L mutants. For ubiquitin loading, 10 µM UbcH5b were incubated with 0.2 µM E1, 0.04 mg/ml ovalbumin and 20 µM fluorescent ubiquitin for 30 min. The reaction was quenched with 2 µM apyrase. Afterwards, NEDD4L (WT and mutants) and WBP2 were added to the mixture to a final concentration of 0.5 µM UbcH5b~ubiqutin, 0.2 µM NEDD4L and 10 µM WBP2. The reaction was carried out at 4°C and 0.5 min, 2 min and 5 min time points were quenched with SDS loading dye.

E3:E3 superassembly mutant profiling and product formation (ARIH1 and ARIH2).

UbSRhodol assay: The assay was conducted in a buffer containing 50 mM HEPES, 150 mM NaCl at pH 7.5 and 1.0 mM TCEP , 0.5 mg/mL 3-[(3-cholamidopropyl) dimethylammonio]propanesulfonic acid (CHAPS) in quadruplets. UbSRhodol solution was prepared by pipetting gently the appropriate volume of a 2mM DMSO(2.5%TFA) stock into the appropriate volume to yield a 1.25µM solution(2.5X). RBR alone or an equimolar solution of RBR (ARIH1 or ARIH2) and neddylated cullin (N8-CUL1:RBX1 or N8-CUL5:RBX2) were prepared as a 1.66X stock (500nM final concentration) and 9µL were added to the assay plate. Then, 6µL of UbSRhodol (2.5X, 500nM final concentration) were dispensed on a Biotek MultiFlowFX dispenser, plate was centrifuged (1000 rpm, 1min) and the E3-mediated release of Rhodol was measured at the emission wavelength of 520 nm (±10 nm) after excitation at 485 nm (±10 nm) in a Pherastar plate reader (BMG LABTECH GmbH, Germany) in continuous mode for several timepoints. Gain (5 /10%) was set at the probe only well.

RhoUbSR gel-based assay: The same stocks were used for product formation assays with N' fluorescently labelled bypass probe (RhoUbSR, 500nM final concentration). 45µL of E3 were combined with 30µL of RhoUbSR (2.5X, 500nM final concentration). All the samples were incubated for 30 minutes at room temperature and stopped by adding loading buffer with or without 5% βME to assess thioester formation. Samples containing 5% βME were boiled at 95°C for 5 minutes, cool down and centrifuge. Samples were resolved by SDS-PAGE using a 4–12% Bis-Tris gel (Invitrogen, NuPAGE) with MOPS SDS running buffer (Novex, NuPAGE) for 45 min at 190 V. Gels were scanned for fluorescence on a GE Typhoon FLA 9500 using the green channel (λex/em 473/530 nm), followed by staining with InstantBlue Coomassie protein stain (Expedeon), after which the gel was scanned on a GE Amersham Imager 600.

Determination of positive control concentration for HTS screening

Assays were performed in non-binding-surface, flat-bottom, low-flange, black 384-well plates (Corning3820) at room temperature in a buffer containing 50 mM HEPES,

150 mM NaCl at pH 7.5 or pH 9.0 , 1.0 mM TCEP, 0.5 mg/mL 3-[(3-cholamidopropyl) dimethylammonio]propanesulfonic acid (CHAPS) in quadruplets. Iodoacetamide and NEM were transferred from freshly prepared stocks to the empty plate using a Labcyte Echo550 acoustic dispenser and accompanying dose–response software z obtain a 5-point serial dilution (4 replicates) of 10/5/1/0.5/0.2/0 mM. A DMSO backfill was performed to obtain equal volumes of DMSO (150 nL) in each well. Then, 9μL of buffer only at different pH (7.5 or 9.0) were added to the assay plate and 6 μL of UbSRhodol (2.5X, 500nM final concentration) were dispensed on a Biotek MultiFlowFX dispenser, plate was centrifuged (1000 rpm, 1min) and the release of Rhodol was measured at the emission wavelength of 520 nm (±10 nm) after excitation at 485 nm (±10 nm) in a Pherastar plate reader (BMG LABTECH GmbH, Germany) in continuous mode for several timepoints. Gain (5 /10%) was set at the probe only well (DMSO).

Z' value calculation (1536 well plate) for HTS

Calculations of were performed in non-binding-surface, flat-bottom, low-flange, black 1536-well plates (Corning3724) at room temperature in a buffer containing 50 mM HEPES, 150 mM NaCl at pH 7.5, 1.0 mM TCEP, 0.5 mg/mL 3-[(3-cholamidopropyl) dimethylammonio]propanesulfonic acid (CHAPS). Iodoacetamide (IAA, 1 mM) was used a positive control (100% inhibition), and DMSO was used as a negative control (0% inhibition), both were transferred from DMSO stocks (80nL per well) to the empty plate using a Labcyte Echo550 acoustic dispenser. 128 positive and negative controls were placed out in the columns covering the great area of the plate to minimize variability within the plate. Buffered solutions were dispensed using a Biotek MultiFlowFX dispenser. First, E3 enzyme buffer (6 μl, 1.33X enzyme stock, final concentration HOIP: 25nM, ARIH1: 15nM and SMURF1: 150nM) was dispensed, plate was shook gently for 10 seconds, centrifuged (1000rpm, 1min) and allowed to incubated for 2 hours at room temperature. Buffered UbSRhodol solution was prepared by pipetting gently the appropriate volume of a 2mM DMSO(2.5%TFA) UbSRhodol stock into the appropriate volume to yield a 2μM solution (4X UbSRhodol stock) 5 minutes prior the end of the E3-inhibitor incubation time. Then, 2 μl of this solution was dispensed, the plate was centrifuged and the E3-mediated release of Rhodol was measured at the emission wavelength of 520 nm (±10 nm) after excitation at 485 nm (±10 nm) in a Pherastar plate reader (BMG LABTECH GmbH, Germany) for 180 minutes each 3 minutes. Gain (10%) was set at the IAA control well. Z' values were calculated for each time point following Zhang's equation and plotted against time in GraphPad Prism 9.3.1 software.

$$(1) \quad Z^{\wedge\prime} = 1 - (3(\sigma_{pos} + \sigma_{neg}))/|\mu_{pos} - \mu_{neg}|$$

μpos and σpos average and standard deviation of 128 positive controls, respectively

μneg and σneg average and standard deviation of 128 positive controls, respectively

High-Throughput Screening of Enamine covalent fragment library (1536 well plate)

High-throughput screenings were performed in non-binding-surface, flat-bottom, low-flange, black 1536-well plates (Corning3724) at room temperature in a buffer containing 50 mM HEPES, 150 mM NaCl at pH 7.5, 1.0 mM TCEP, 0.5 mg/mL 3-[(3-cholamidopropyl)dimethylammonio]propanesulfonic acid (CHAPS). Iodoacetamide (IAA, 1 mM) was used a positive control (100% inhibition), and DMSO was used as a negative control (0% inhibition), both were transferred from DMSO stocks (80nL per well) to the empty plate using a Labcyte Echo550 acoustic dispenser. Buffered solutions were dispensed using a Biotek MultiFlowFX dispenser. First, E3 enzyme buffer (6 µl, 1.33X enzyme stock, 80ml) was dispensed, plate was shook gently for 10 seconds, centrifuged (1000rpm, 1min) and allowed to incubated for 2 hours at room temperature. Buffered UbSRhodol solution was prepared by pipetting gently 30µl of a 2mM DMSO(2.5%TFA) UbSRhodol stock into 30ml of buffer to yield a 2µM solution (4X UbSRhodol stock, ca. 550µg UbSRhodol per HTS) 5 minutes prior the end of the E3-inhibitor incubation time. Then, 2 µl of this solution was dispensed, the plate was centrifuged and the E3-mediated release of Rhodol was measured at the emission wavelength of 520 nm (±10 nm) after excitation at 485 nm (±10 nm) in a Pherastar plate reader (BMG LABTECH GmbH, Germany) in a single time point. Gain (10%) was set at the IAA control well. Data was then standardized to obtain the % of inhibition and a set of hits (60% cut-off) was selected for validation by triplicates. Validated hits by triplicates to discard possible dispensing errors was conducted for each ligase to generate the venn3 diagram. For HOIP 69 hits were retrieved (0.79% hit rate), for ARIH1 72 hits were retrieved (0.92% hit rate) and 79 for SMURF1 (1.00% hit rate).

Elmann's reagent reactivity assay against fragments X, Y and Z

A 100 µM sample of DTNB was incubated with 400 µM TCEP in 20 mM sodium phosphate buffer pH 7.4 and 150 mM NaCl for 5 min at room temperature, in order to obtain TNB2–. A same volume solution of carbonyl imidazoles X, Y and Z (400 µM) in the same buffer was mixed with the previous TNB2– solution, to yield a final solution of 200µM of compounds and 100µM of TNB2–. Compounds without DTNB were plated aswell to extract their absorbance at 412 nm at 37 °C were performed. The absorbances were acquired every 5 min for 7 h. The assay was performed in a 96-well plate (Costar) using a Clariostar plate reader(BMG LABTECH GmbH, Germany. Compounds were measured in triplicate and their absorbances were plotted in GraphPad Prism 9.3.1 software.

MS full intact protein inhibitor engagement for series X,Y and Z

The assay was conducted in a buffer containing 50 mM HEPES, 150 mM NaCl at pH 7.5 and 1.0 mM TCEP. Equal volumes of HOIP/ARIH1/SMURF1 (2µM, 50µL,

2X) and covalent fragment inhibitors (covfrag) (200μM, 50μL, 2X) were pooled together to yield a solution of 1μM HOIP/ARIH1/SMURF1 and 100 μM covfrag and incubated for 2 hours at room temperature or at 4°C overnight in the case of HOIP. Samples were then diluted 5-fold with water containing 0.1% formic acid and analyzed by mass spectrometry by injecting 5 μL into a Waters XEVO-G2 XS Q-TOF mass spectrometer equipped with an electrospray ion source in positive mode (capillary voltage 1.2 kV, desolvation gas flow 900 L/h, T = 60 °C) with a resolution of R = 26 000. Samples were run using two mobile phases: (A) 0.1% formic acid in water and (B) 0.1% formic acid in CH3CN on a Waters Acquity UPLC protein BEH C4 column [300 Å, 1.7 μm (2.1 × 50 mm2), flow rate = 0.5 mL/min, run time = 14.00 min, column T = 60 °C, and mass detection 200–2500 Da]. Gradient: 2–100% B. Data processing was performed using Waters MassLynx mass spectrometry software 4.2, and ion peaks were deconvoluted using the built-in MaxEnt1 function. Peak annotation was plotted using GraphPad Prism 9.3.1 software

SulfoCy5UbVME competition assays for series X,Y and Z

The assay was conducted in a buffer containing 50 mM HEPES, 150 mM NaCl at pH 7.5 and 1.0 mM TCEP. Equal amounts of HOIP (2μM, 50μL, 2X) and covalent fragment inhibitors (covfrag) (200/150/100/50/20/10/2μM, 50μL, 2X) were pooled together to yield a solution of 1μM HOIP and 100/75/50/25/10/5/1 μM covfrag and incubated for 2 hours at room temperature. Then 5μL of SulfoCy5-UbVME in buffer (200μM, 20X) was added and the solution was pipet up and down gently. All the samples were incubated for 30 minutes at room temperature and stopped by addition of loading buffer containing βME. Samples were resolved by SDS-PAGE using a 4–12% Bis-Tris gel (Invitrogen, NuPAGE) with MOPS SDS running buffer (Novex, NuPAGE) for 45 min at 190 V. Gels were scanned for fluorescence on a GE Typhoon FLA 9500 using the red channel (λex/em 532/570 nm), followed by staining with InstantBlue Coomassie protein stain (Expedeon), after which the gel was scanned on a GE Amersham Imager 600.

IC50 determination for series X,Y and Z

IC50 determination assays were performed in non-binding-surface, flat-bottom, low-flange, black 384-well plates (Corning3820) at room temperature in a buffer containing 50 mM HEPES, 150 mM NaCl at pH 7.5, 1.0 mM TCEP, 0.5 mg/mL 3-[(3-cholamidopropyl)dimethylammonio]propanesulfonic acid (CHAPS) in triplicate. Each well had a final volume of 15 μL. All dispensing steps involving buffered solutions were performed on a Biotek MultiFlowFX dispenser. The compounds were dissolved in DMSO as 10, 1, and 0.1 mM stock solutions, and appropriate volumes were transferred from these stocks to the empty plate using a Labcyte Echo550 acoustic dispenser and accompanying dose–response software to obtain a 9-point serial dilution (3 replicates) of 0.05 to 200 μM. A DMSO backfill was performed to obtain equal volumes of DMSO (150 nL) in each well. Iodoacetamide (IAA, 1 mM) was used a positive control (100% inhibition), and DMSO was used as a negative

control (0% inhibition). Enzyme (9 µL, 1.66X stock) was added, and the plate was vigorously shaken for 10 seconds and incubated either for 1h or 2h. Then, 6 µL of UbSRhodol of 2.5X stock (final concentration 500 nM) were dispensed and the plate was centrifuged and the rhodol-dependant increase in fluorescence intensity over time was recorded using a BMG Labtech CLARIOstar or PHERAstar plate reader (excitation 490 nm, emission 520 nm). The initial enzyme velocities were calculated from the slopes, normalized to the positive and negative controls, and plotted against the inhibitor concentrations (in M) using the built-in equation "[inhibitor] vs response – variable slope (four parameters), least-squares fit" with constraints "Bottom = 0" and "Top = 100" in GraphPad Prism 9.3.1 software to obtain the IC50 values.

Jump dilution assays determination for series X,Y and Z

Jump dilution assays were performed at room temperature in a buffer containing 50 mM HEPES, 150 mM NaCl at pH 7.5, 1.0 mM TCEP, 0.5 mg/mL 3-[(3-cholamidopropyl) dimethylammonio]propanesulfonic acid (CHAPS) in quadruplets. The final concentrations used were 30 nM HOIP, 1 µM UbSRhodol, and 300 µM or 3µM or a jump dilution of 300 µM to 3 µM of inhibitors. Samples of 20 µL containing 3 µM HOIP and 300 µM inhibitor (1% DMSO), 1% DMSO, or 1 mM Iodoacetamide (IAA) were incubated for 1 hour at room temperature. Each sample (5 µL) was then diluted into a 500 µL solution containing 1µM UbSRhodol. After a gentle mixing, 15 µL of each of these solutions was quickly transferred to a non-binding-surface, flat-bottom, low-flange, black 384-well plate (Corning3820) and the increase in fluorescence over time was recorded using a BMG Labtech PHERAstar plate reader (excitation 485 nm, emission 520 nm). As a control, samples were taken in which 40 µL of a 600 µM and 6 µM inhibitor solution in buffer (1% DMSO) was added to 35 µL of a 69 nM HOIP solution. After 1 hour of incubation, 5 µL of a 16µM UbSRhodol solution was added, after which 15 µL of each solution was transferred to the same 384-well plate mentioned above, and the increase in fluorescence intensity was measured concomitantly. Fluorescent intensities were plotted against time using GraphPad Prism 9.3.1.

Cell lysate experiments with the activity based probes SCy5-UbVME and -UbPA, and bypass probe SCy5-UbSR

HEK293T cells were transiently transfected on 6 well or 10 cm dishes, or mock-treated, using PEI as transfection reagent according to the manufacturer's instructions. For ARIH1 overexpression pcDNA™FRT/TO-GFP-ARIH1 WT, CS, ARIH1OPEN and ARIH1OPEN-CS were used9,10. 24h after transfection, cells were washed with ice cold PBS and harvested by scraping in lysis buffer (50 mM Tris pH 7.5, 150 mM NaCl, 0.5% Triton X100, 2 mM TCEP and protease inhibitor tablet (Roche)), and lysate was clarified by centrifugation. Lysates were subsequently aliquoted and stored at -80. For activity based probe (ABP) assays 1 uM SCy5-labeled-ABP was added, lysates were incubated for 30 min at room temperature, reactions were stopped by boiling in 1x loading buffer containing βME,

proteins were separated by SDS-PAGE on 4-12% Bis-Tris NuPage gels (Invitrogen, NuPAGE) with MOPS-SDS running buffer (Novex, NuPAGE), imaged using a GE Typhoon FLA 9500, blotted on nitrocellulose, and after blocking, incubated o/n with rabbit anti-GFP serum11, washed, incubated 30min with LI-COR IRDye 800CW goat anti-rabbit secondary antibody, and imaged on LICOR Odyssey system v3.

Cell lysates were equalized for protein concentration by measuring A280 absorbance using a NanoDrop™ One/OneC Microvolume UV-Vis Spectrophotometer.

UbSRhodol transthiolation in cell lysates

Ub76 and UbPA were transferred from DMSO stocks (2 mM) , and appropriate volumes were transferred from these stocks to the empty plate 384-well plate (Corning3820) using a Labcyte Echo550 acoustic dispenser and accompanying dose–response software to obtain a 6-point serial dilution (4 replicates) of 0/0.5/1/2.5/5/10μM. A DMSO backfill was performed to obtain equal volumes of DMSO (37.5 nL, 0.25%) in each well. Cell lysates were equalized with their intrinsic absorbance at 280nm, diluted 150 fold with the assay buffer (50 mM HEPES, 150 mM NaCl at pH 7.5, 1.0 mM TCEP, 0.5 mg/mL 3-[(3-cholamidopropyl)dimethylammonio] propanesulfonic acid (CHAPS)), and 9μL were dispensed to the plate, and incubated for 30 minutes at room temperature. Then, 6uL of UbSRhodol (2.5X stock, 1μM final concentration) were added with a Biotek MultiFlowFX dispenser, the plate was centrifuged (1000 rpm, 1min), and ligase-mediated release of Rhodol was measured at the emission wavelength of 520 nm (±10 nm) after excitation at 485 nm (±10 nm) in a Pherastar plate reader (BMG LABTECH GmbH, Germany) in continuous mode for several timepoints. Gain (5 /10%) was set at the probe only well.

Chemical characterization compounds

Compound **3**: ^{1}H NMR (300 MHz, $CDCl_3$)

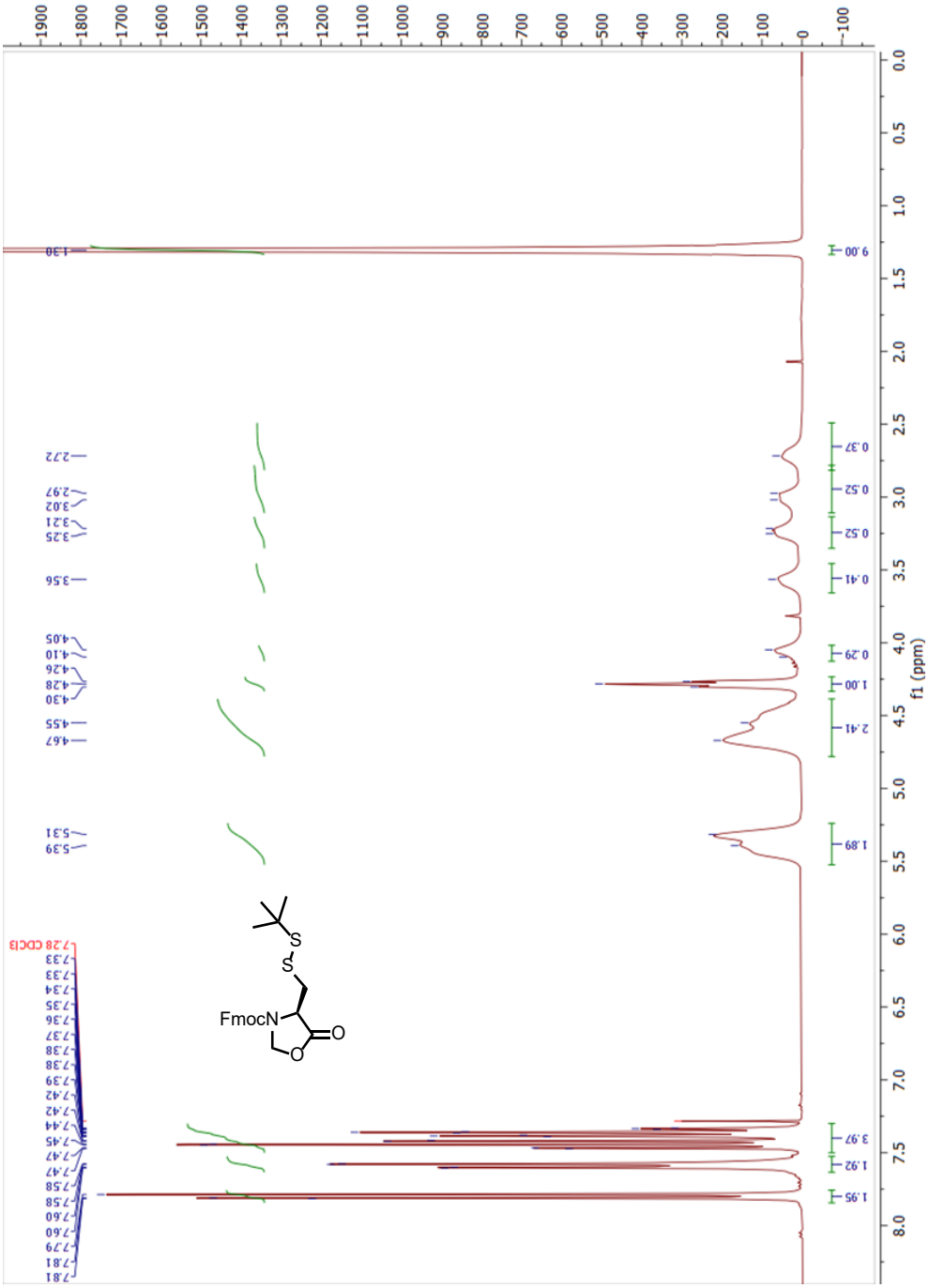

Compound **3**: ^{13}C NMR (75 MHz, $CDCl_3$)

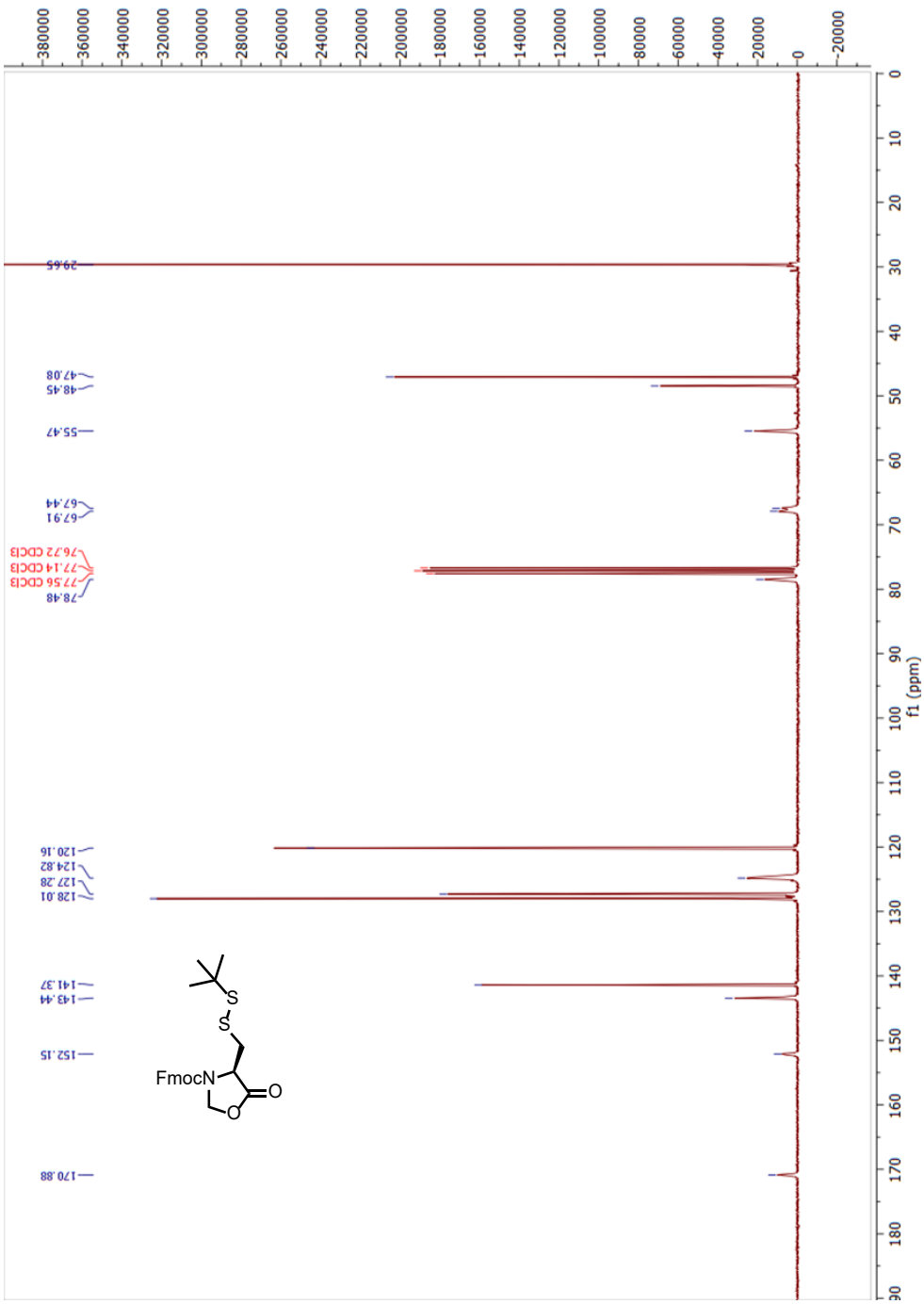

Compound **4**: ^{1}H NMR (300 MHz, $CDCl_3$)

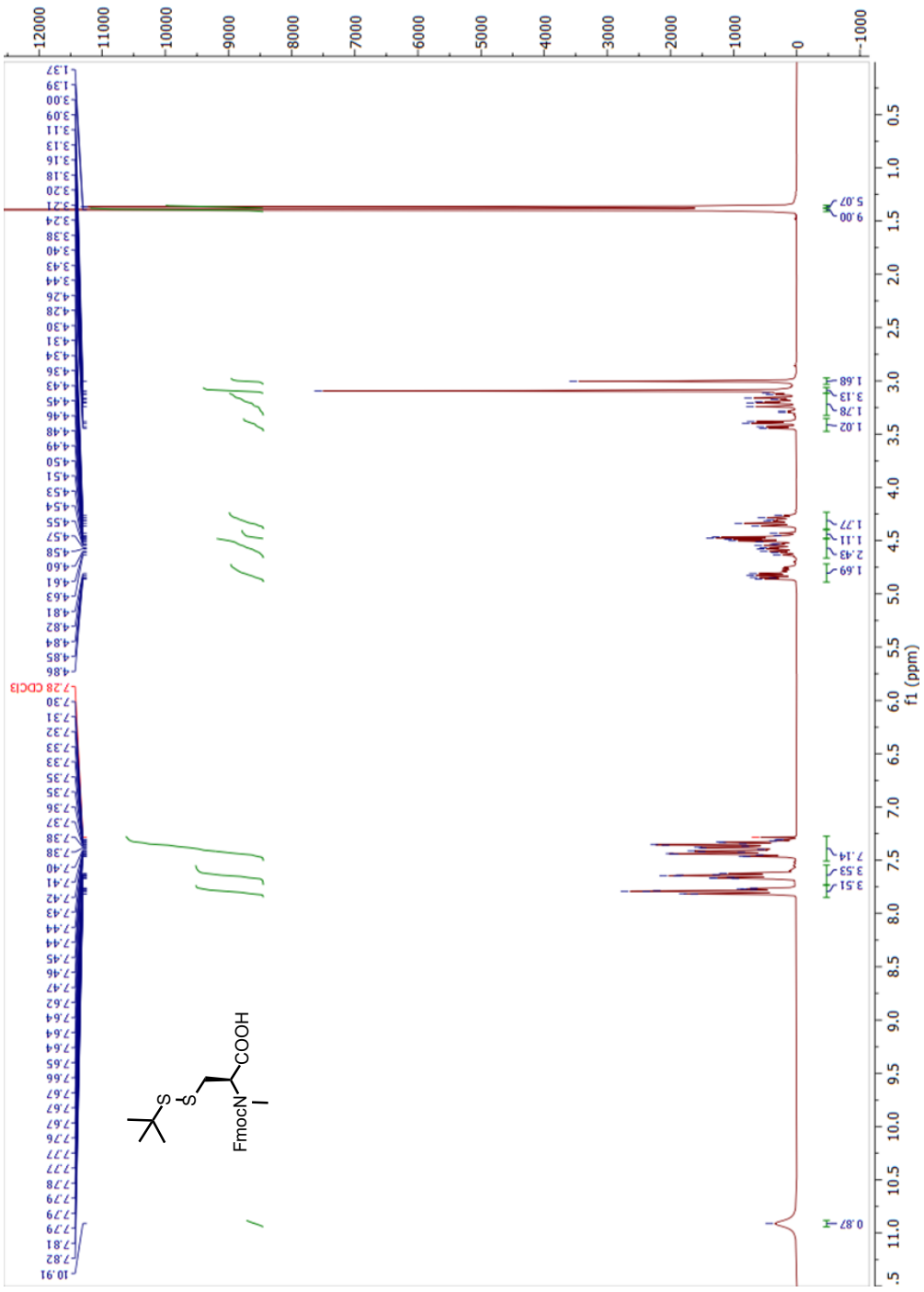

Compound **4**: ^{13}C NMR (75 MHz, $CDCl_3$)

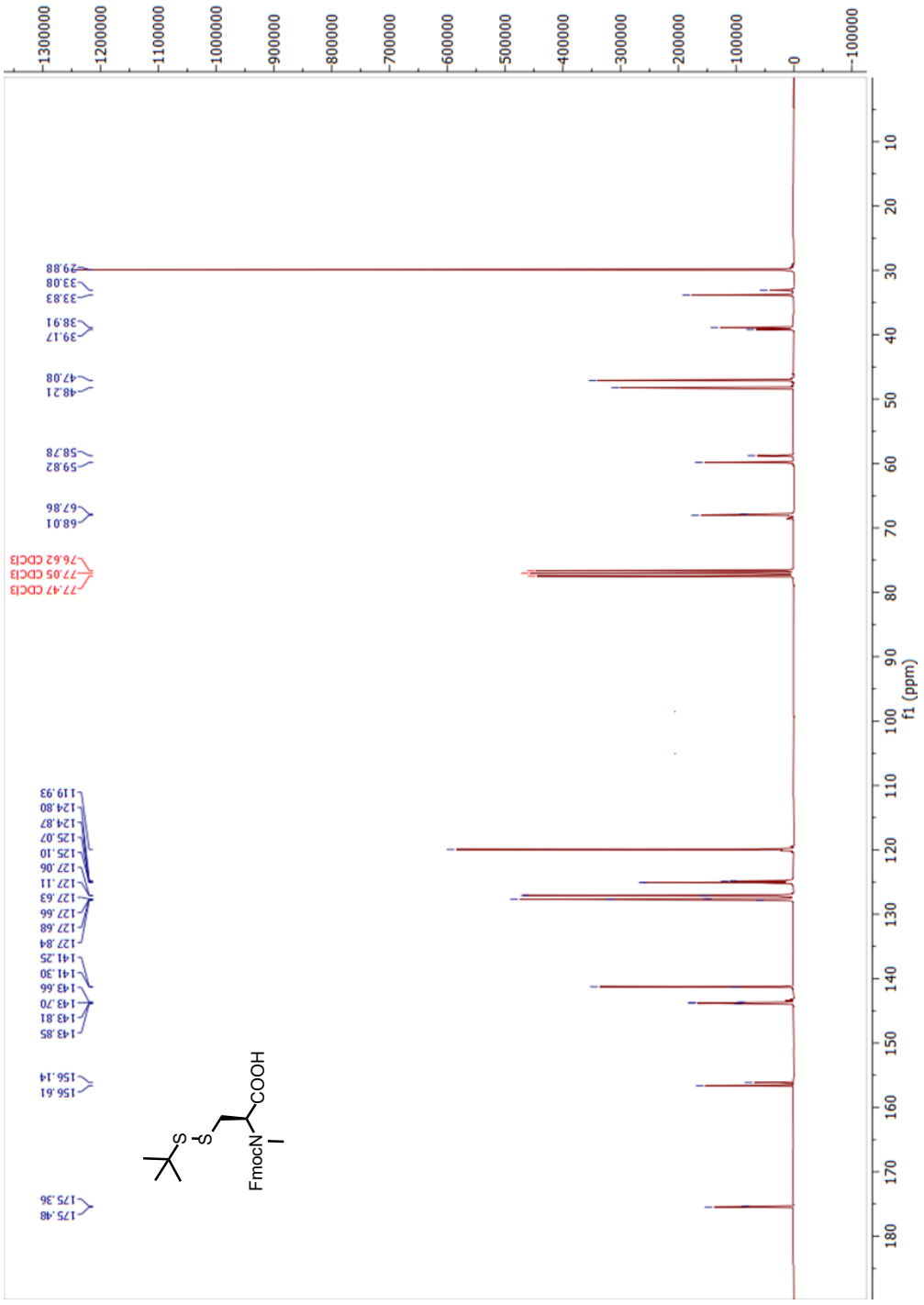

Compound **5**: ^{1}H NMR (300 MHz, $CDCl_3$)

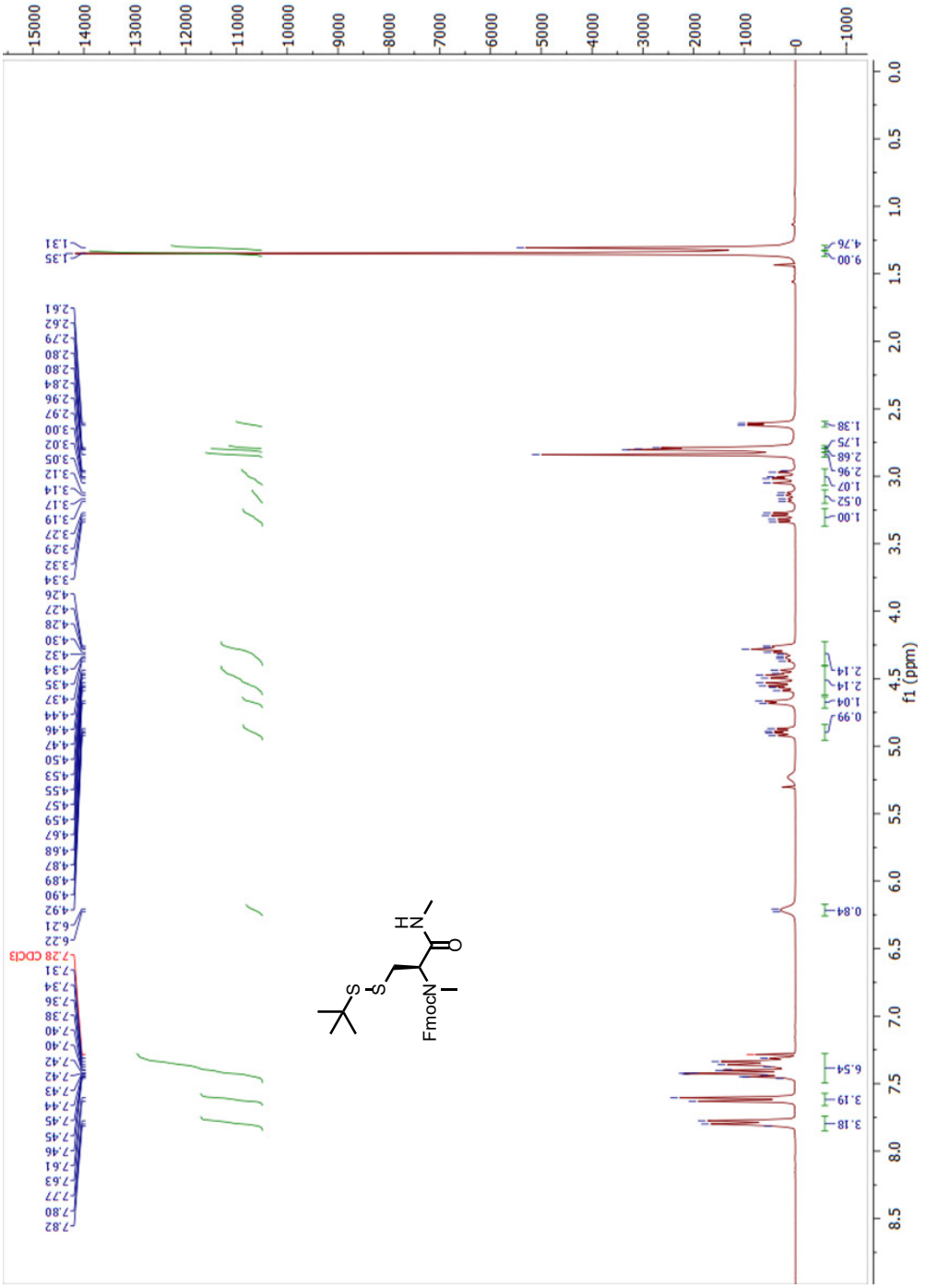

Compound **5**: ^{13}C NMR (75 MHz, $CDCl_3$)

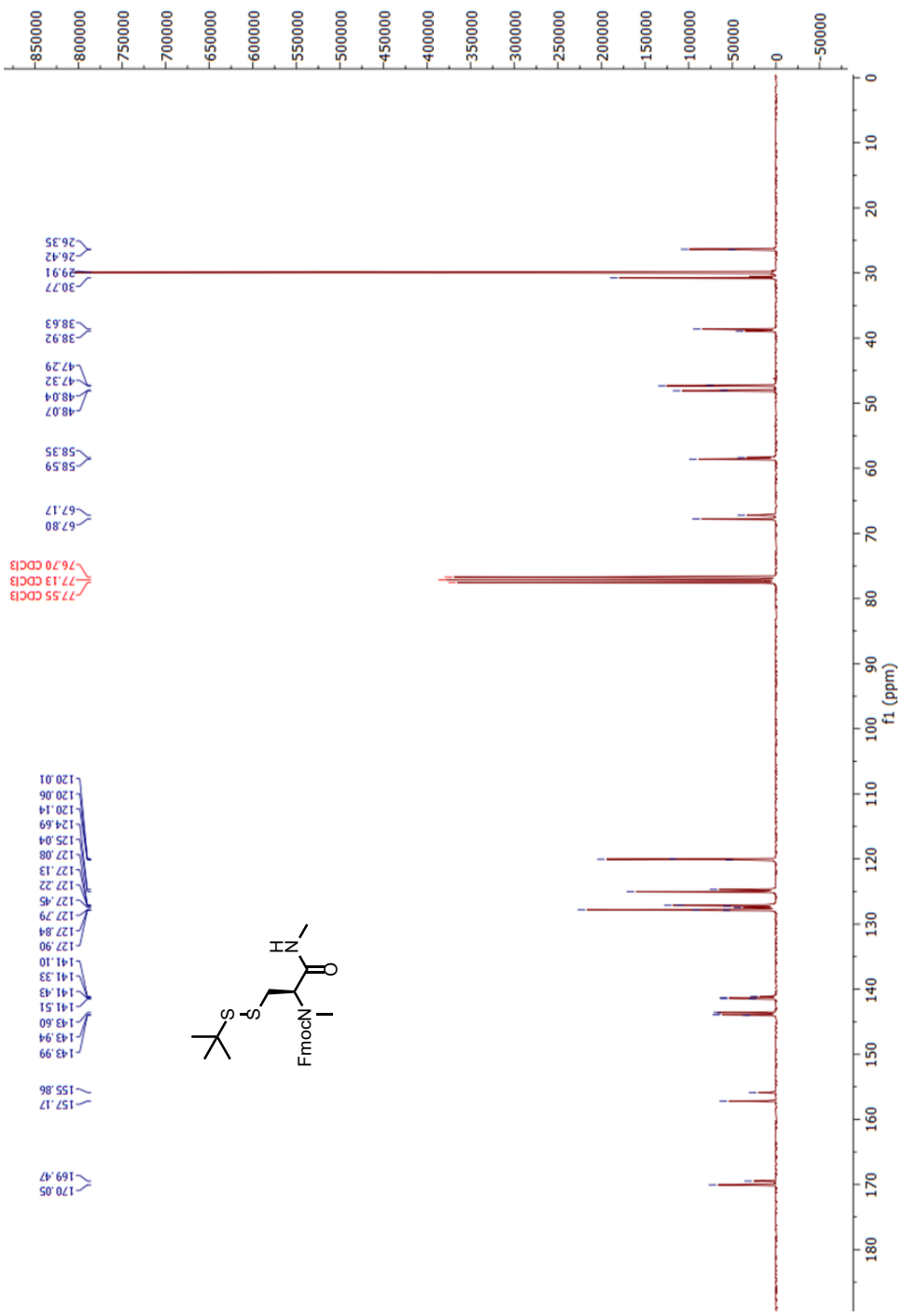

Compound **6**: ^{1}H NMR (300 MHz, $CDCl_3$)

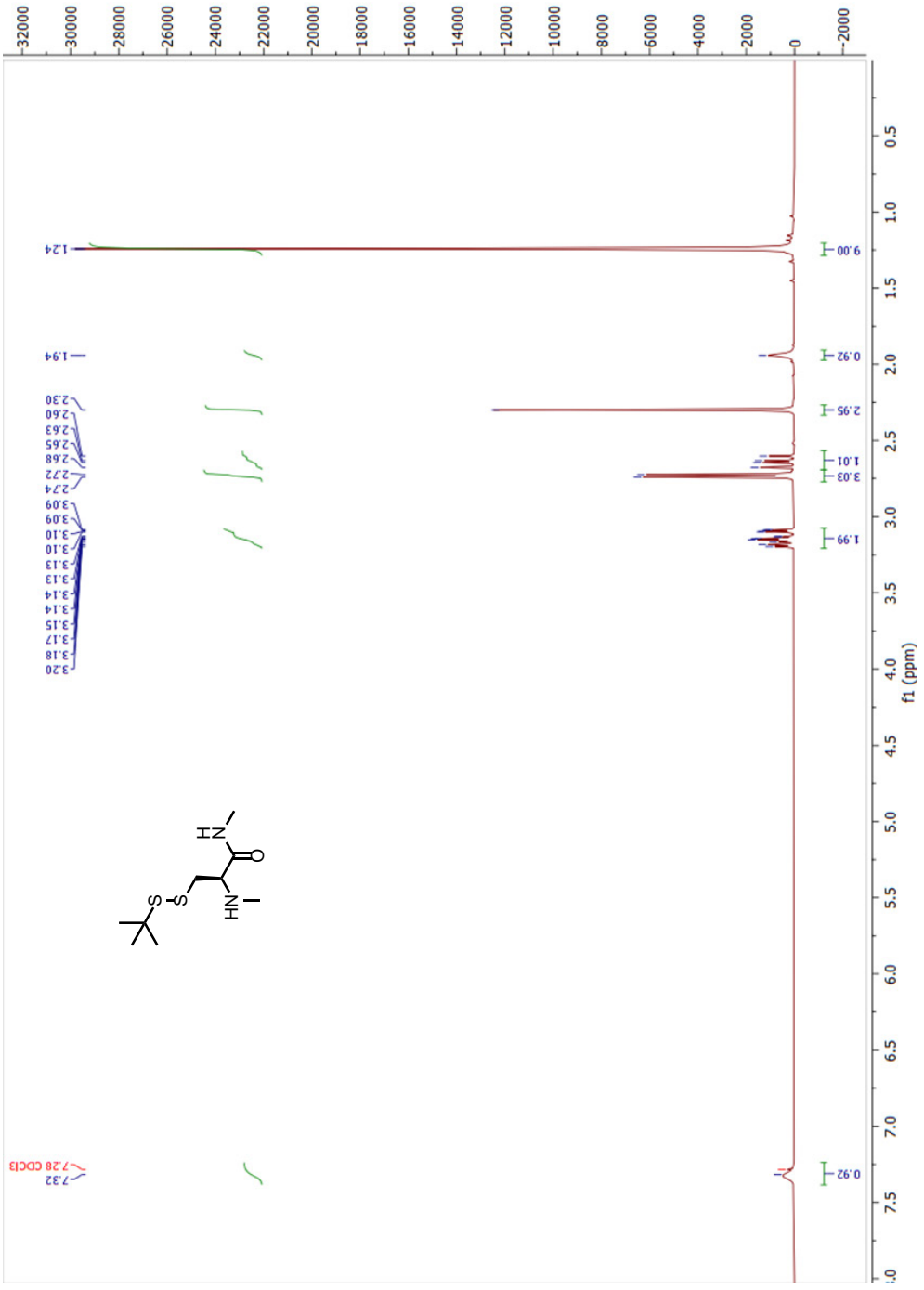

Compound **6**: ^{13}C NMR (75 MHz, $CDCl_3$)

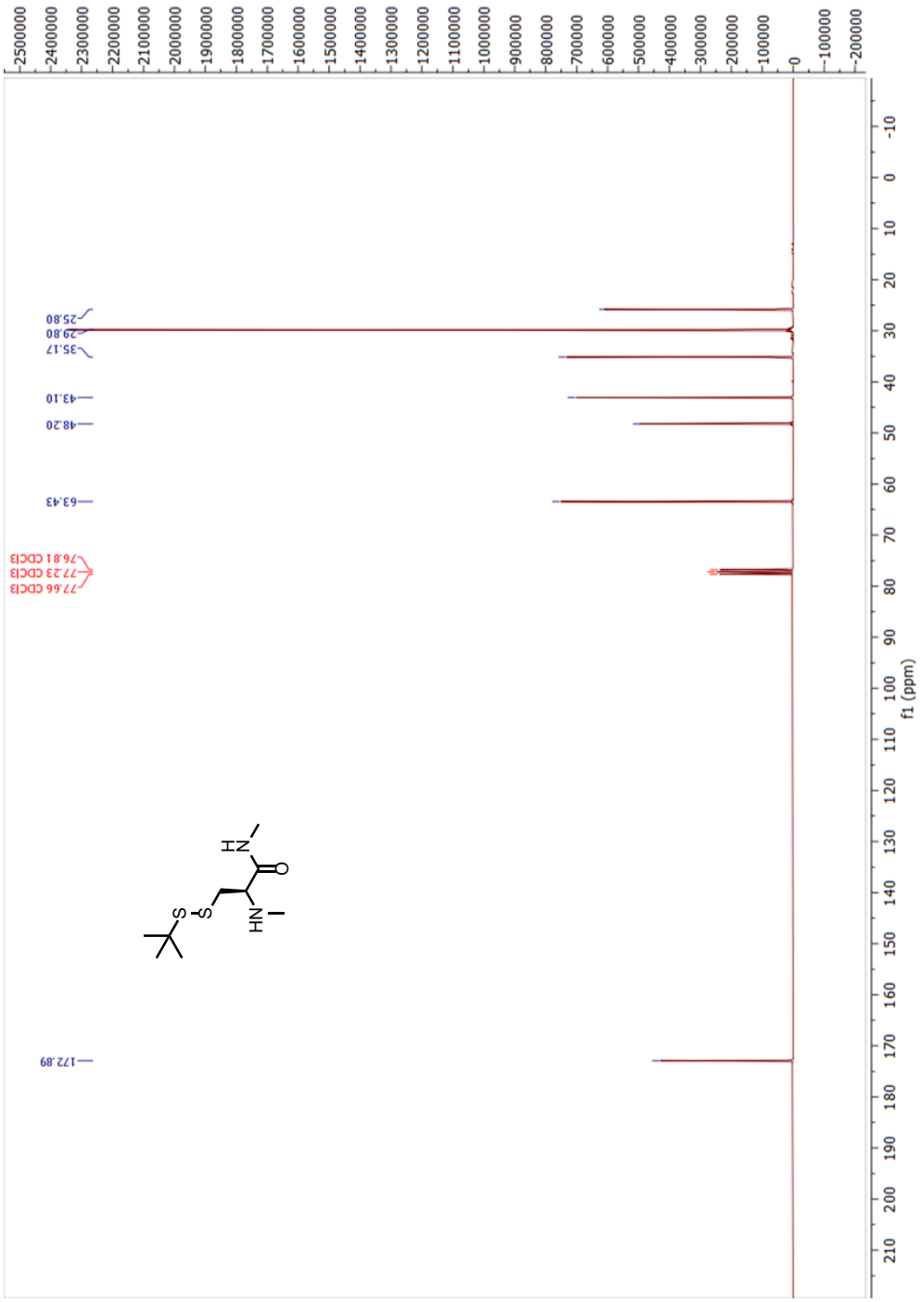

Compound **7**: ^{1}H NMR (300 MHz, DMSO-d_6)

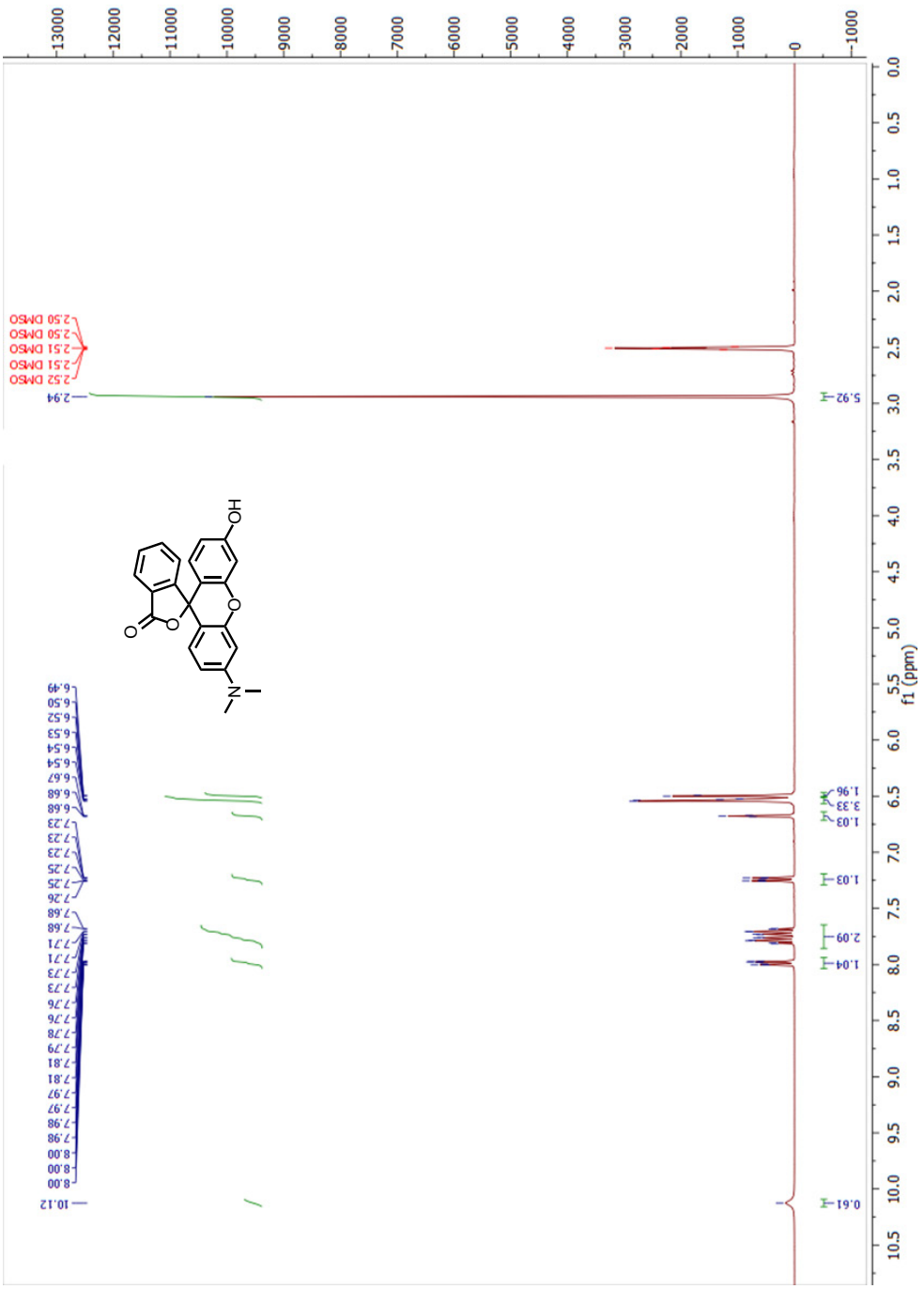

Compound **7**: ^{13}C NMR (75 MHz, DMSO-d_6)

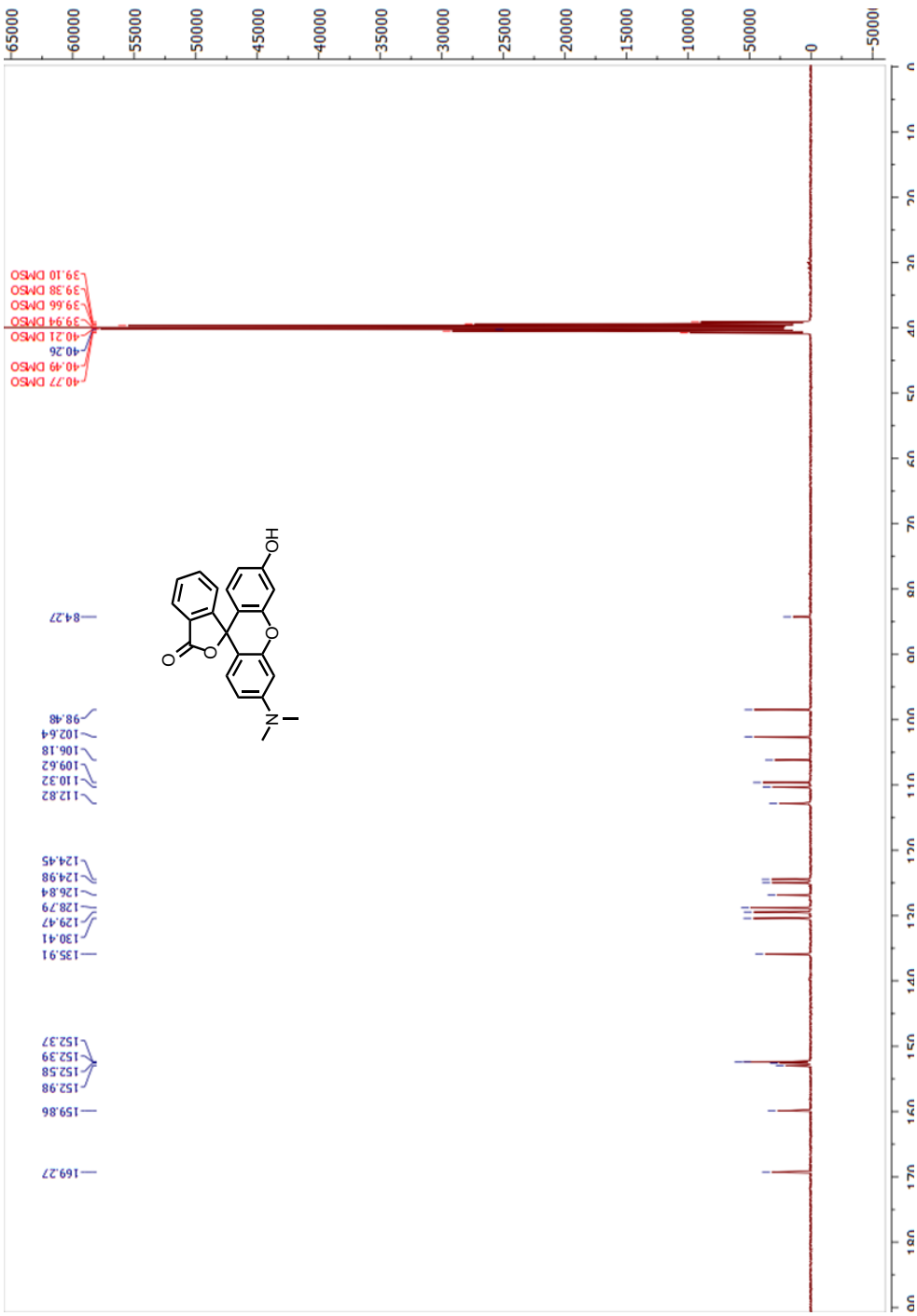

Compound **8**: ^{1}H NMR (300 MHz, $CDCl_3$)

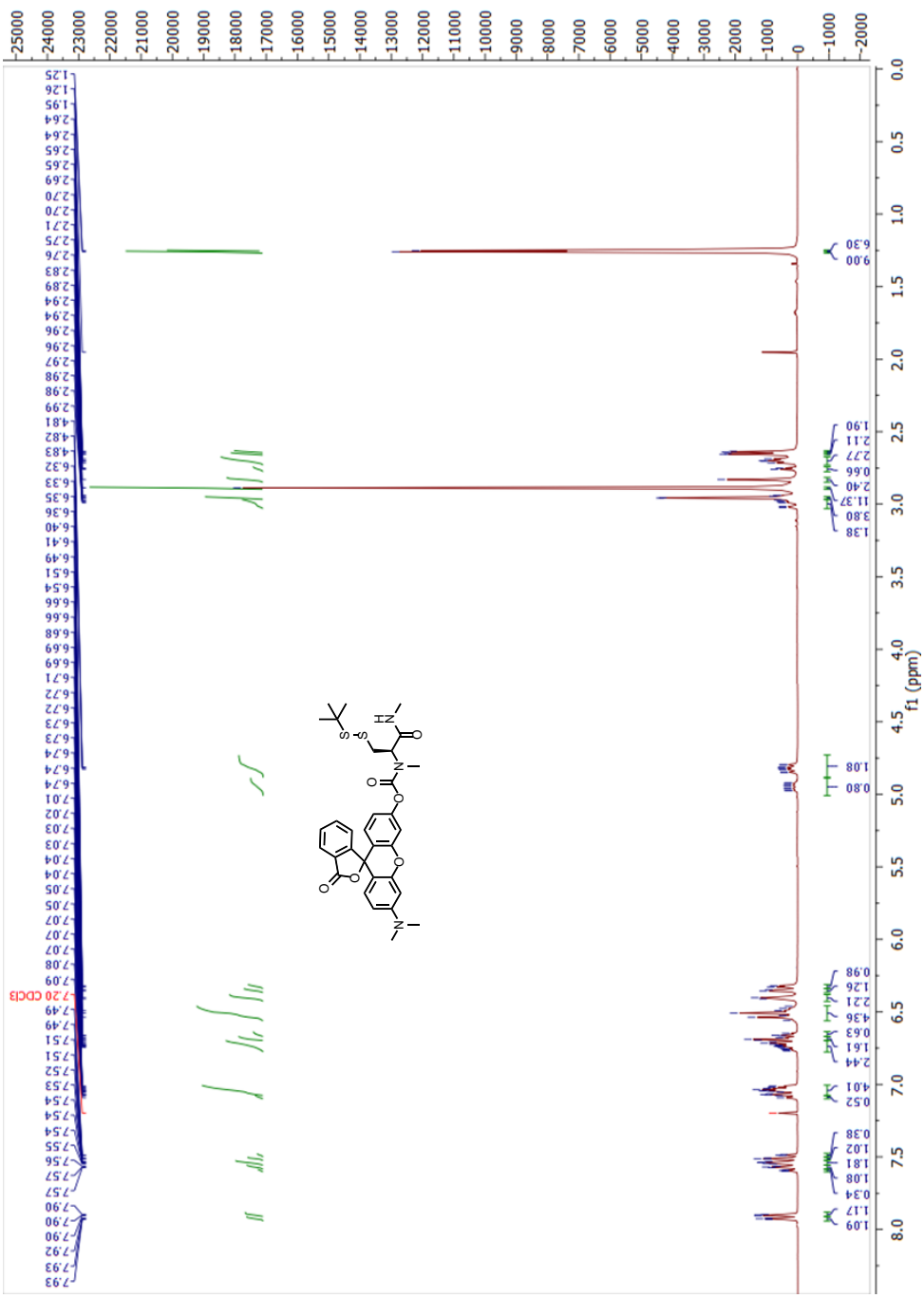

Compound **8**: ^{13}C NMR (75 MHz, $CDCl_3$)

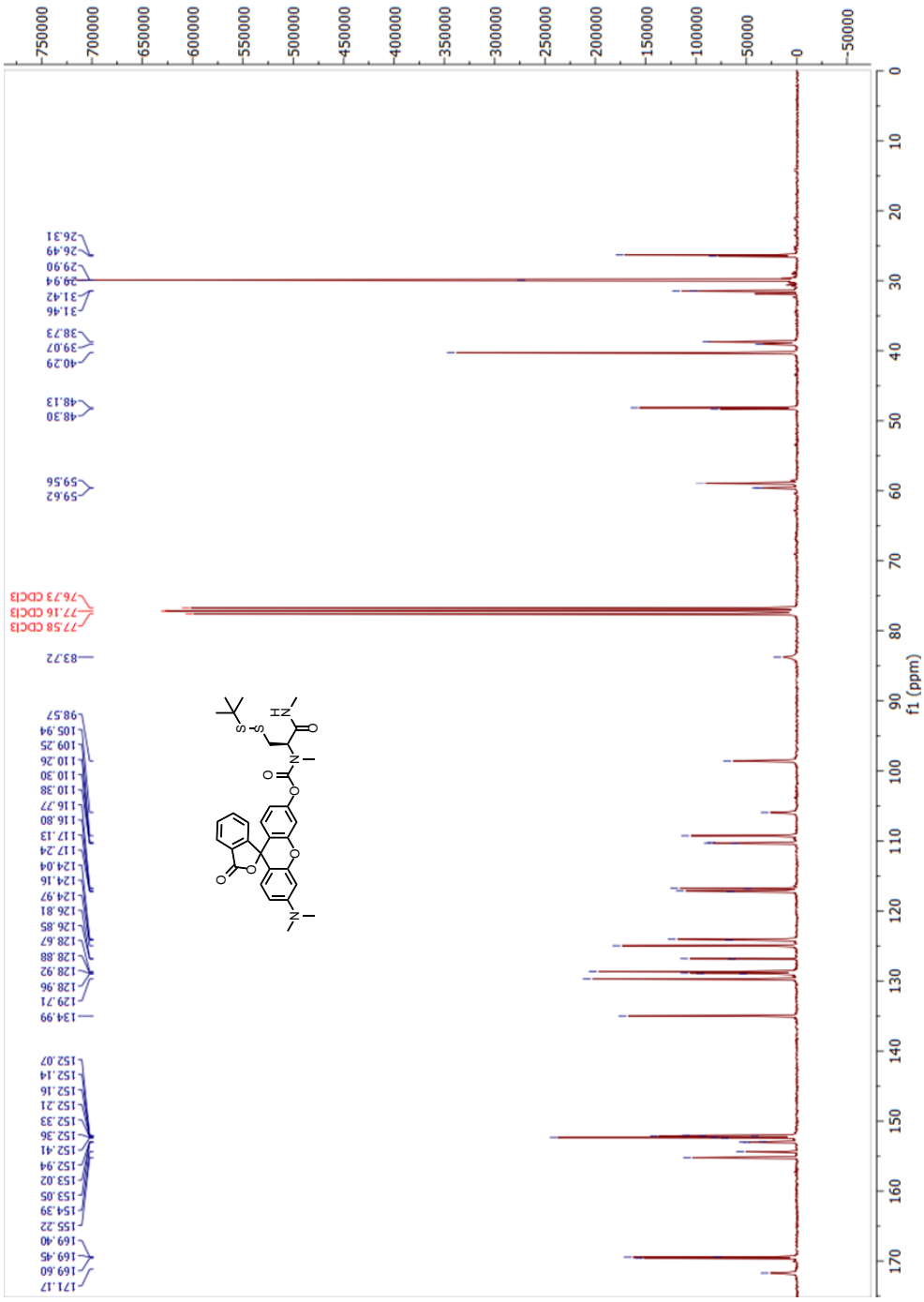

Compound **9**: ^{1}H NMR (300 MHz, $CDCl_3$)

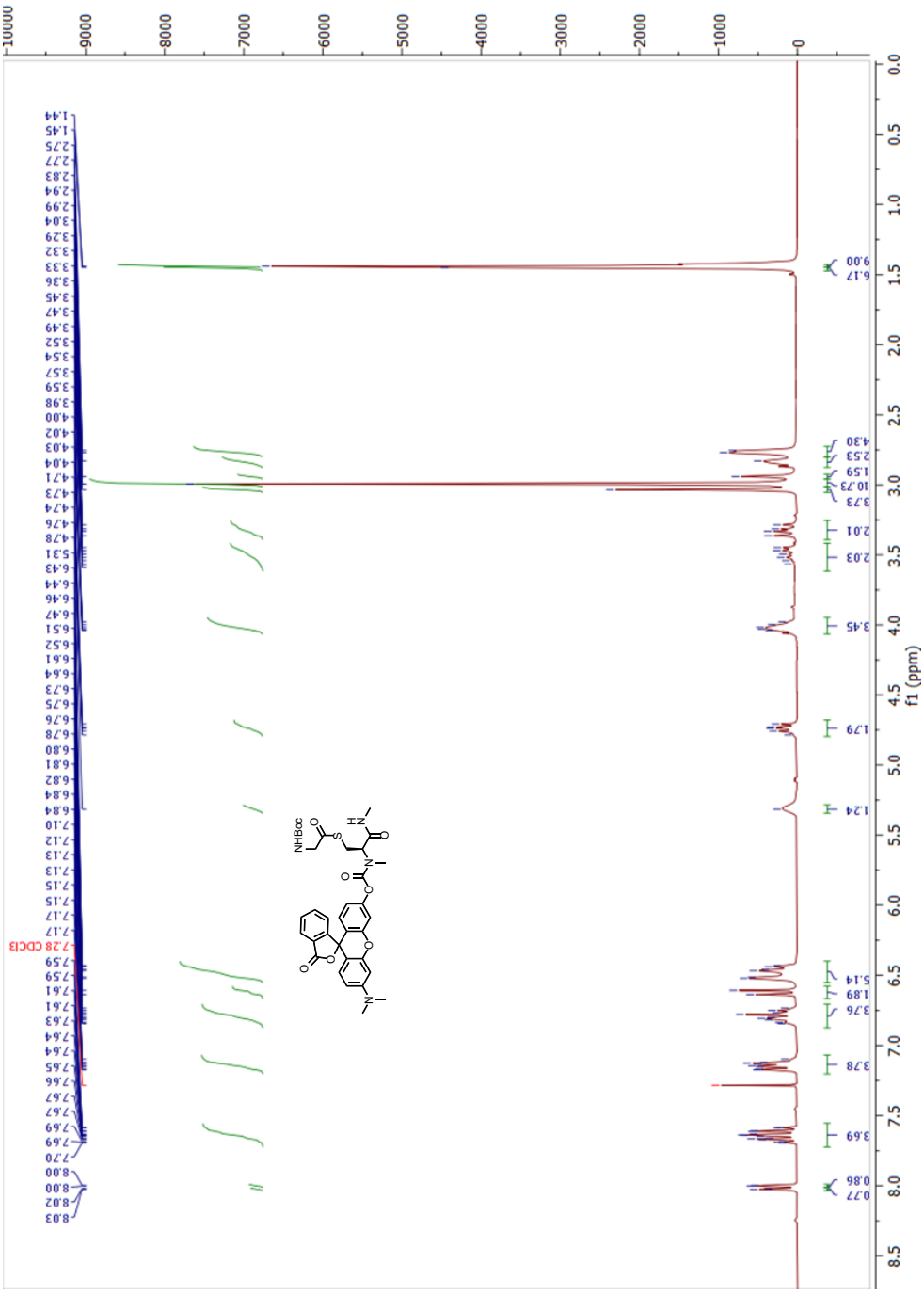

Compound **9**: ^{13}C NMR (75 MHz, $CDCl_3$)

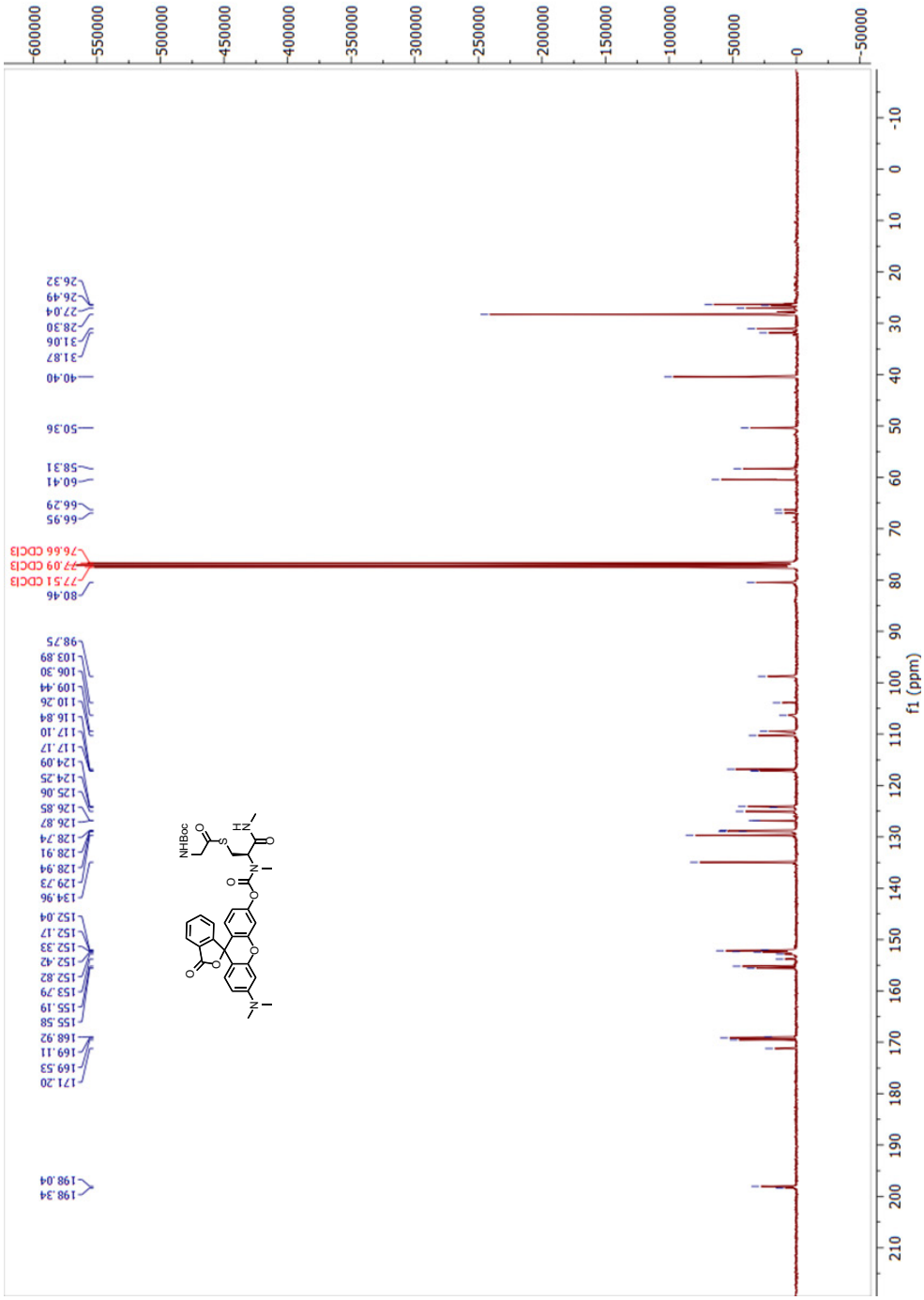

Compound **1**: ^{1}H NMR (300 MHz, DMSO-d_6)

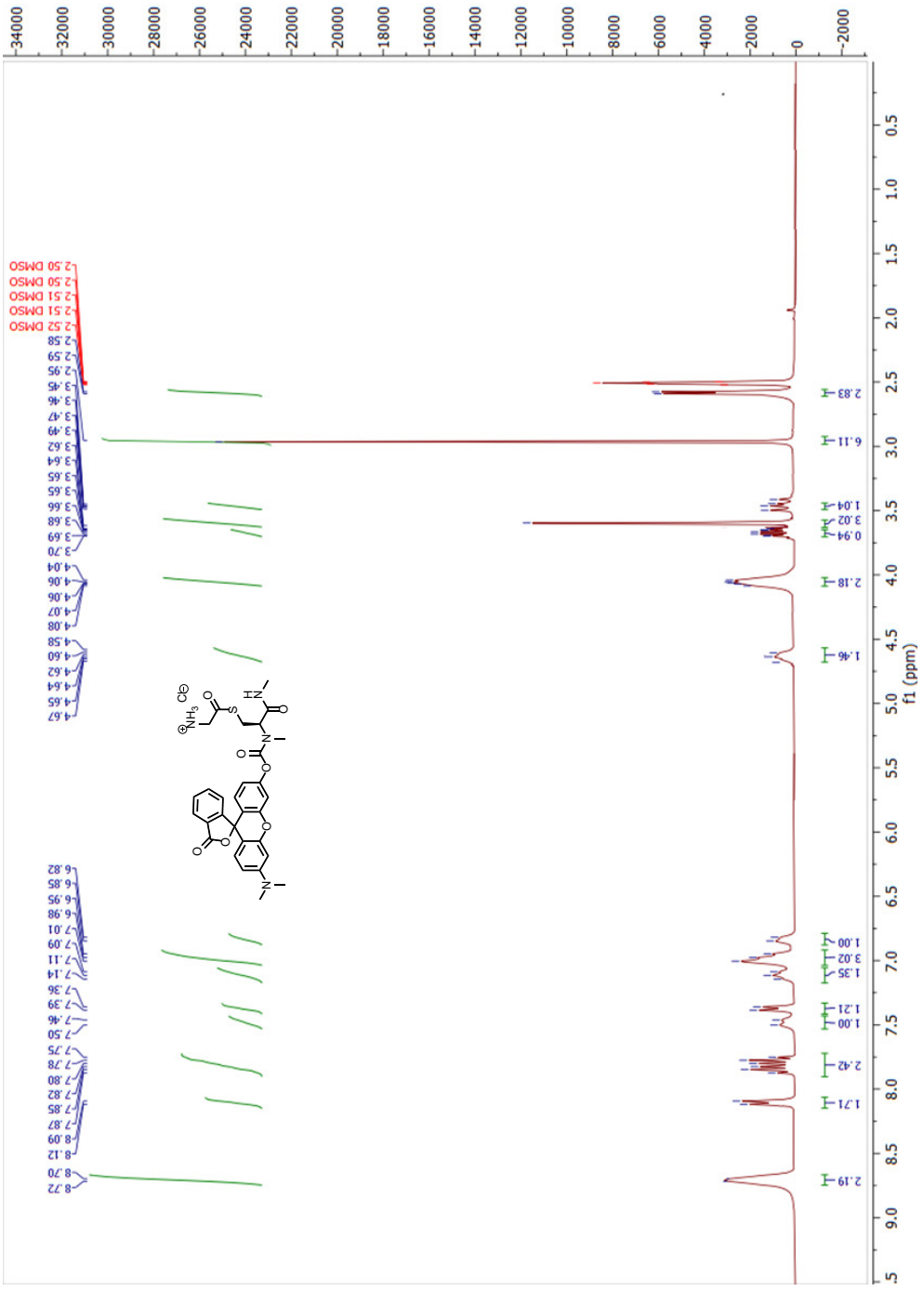

Compound **1**: ^{13}C NMR (75 MHz, DMSO-d_6)

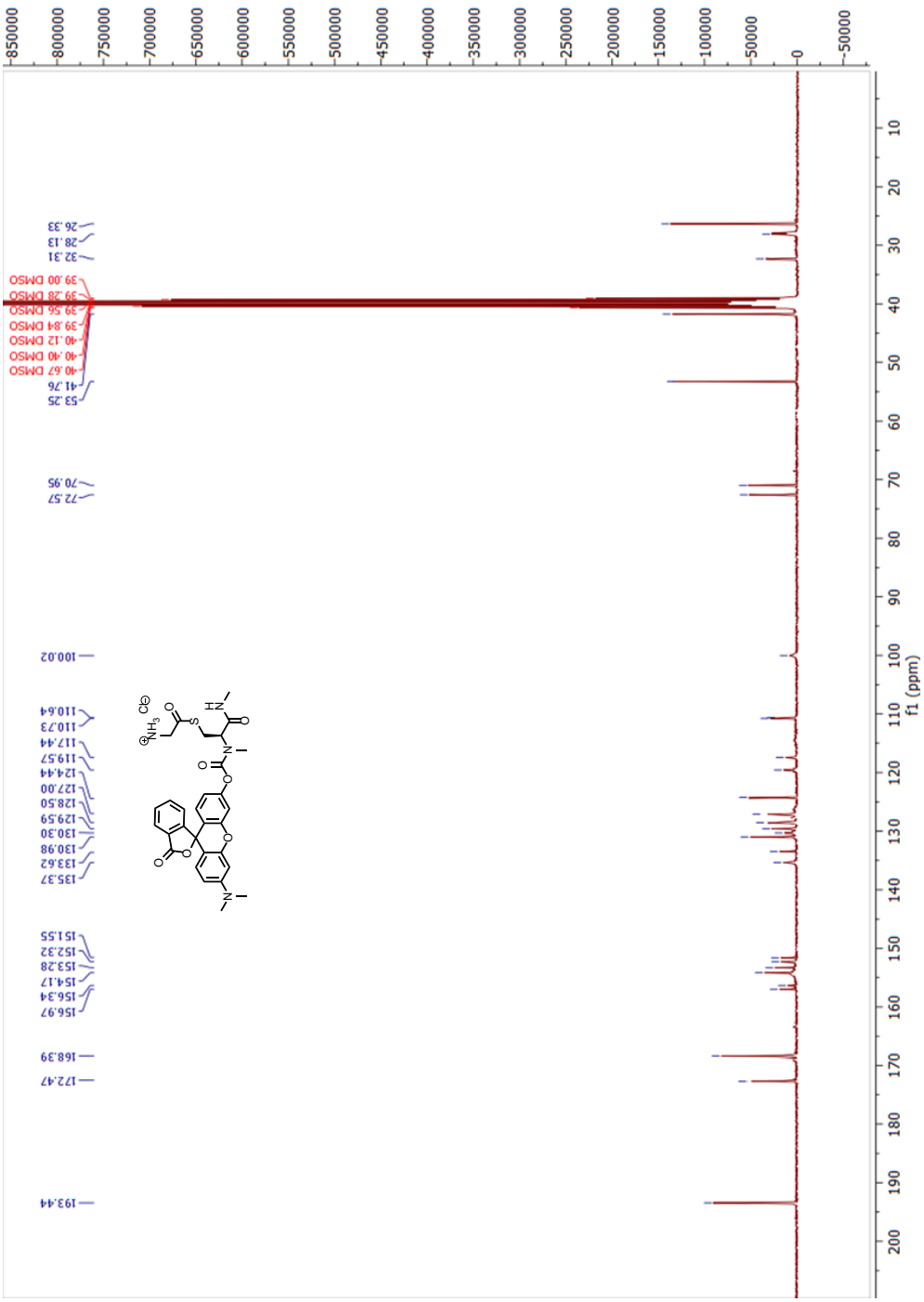

Supplementary references:

1 Ruggles, E. L., Flemer, S., Jr. & Hondal, R. J. A viable synthesis of N-methyl cysteine. Biopolymers 90, 61-68, doi:10.1002/bip.20889 (2008).
2 Sauers, R. R., Husain, S. N., Piechowski, A. P. & Bird, G. R. Shaping the absorption and fluorescence bands of a class of efficient, photoactive chromophores: synthesis and properties of some new 3H-xanthen-3. Dyes and Pigments 8, 35-53, doi:https://doi.org/10.1016/0143-7208(87)85004-0 (1987).
3 Xue, F. & Seto, C. T. Fluorogenic Peptide Substrates for Serine and Threonine Phosphatases. Organic Letters 12, 1936-1939, doi:10.1021/ol1003065 (2010).
4 Raz, R. & Rademann, J. Fmoc-Based Synthesis of Peptide Thioesters for Native Chemical Ligation Employing a tert-Butyl Thiol Linker. Organic Letters 13, 1606-1609, doi:10.1021/ol1029723 (2011).
5 El Oualid, F. et al. Chemical Synthesis of Ubiquitin, Ubiquitin-Based Probes, and Diubiquitin. Angewandte Chemie International Edition 49, 10149-10153, doi:https://doi.org/10.1002/anie.201005995 (2010).
6 García-Nafría, J., Watson, J. F. & Greger, I. H. IVA cloning: A single-tube universal cloning system exploiting bacterial In Vivo Assembly. Scientific Reports 6, 27459, doi:10.1038/srep27459 (2016).
7 Horn-Ghetko, D. et al. Ubiquitin ligation to F-box protein targets by SCF–RBR E3–E3 super-assembly. Nature 590, 671-676, doi:10.1038/s41586-021-03197-9 (2021).
8 Kostrhon, S. et al. CUL5-ARIH2 E3-E3 ubiquitin ligase structure reveals cullin-specific NEDD8 activation. Nature chemical biology 17, 1075-1083, doi:10.1038/s41589-021-00858-8 (2021).
9 Kelsall, I. R. et al. TRIAD1 and HHARI bind to and are activated by distinct neddylated Cullin-RING ligase complexes. The EMBO Journal 32, 2848-2860, doi:https://doi.org/10.1038/emboj.2013.209 (2013).
10 Scott, D. C. et al. Two Distinct Types of E3 Ligases Work in Unison to Regulate Substrate Ubiquitylation. Cell 166, 1198-1214.e1124, doi:10.1016/j.cell.2016.07.027 (2016).
11 van der Kant, R. et al. Late endosomal transport and tethering are coupled processes controlled by RILP and the cholesterol sensor ORP1L. Journal of Cell Science 126, 3462-3474, doi:10.1242/jcs.129270 (2013).